PALEOLIMNOLOGICAL ANALYSIS OF SEDIMENT CORES FROM GUANA ISLAND POND, GUANA ISLAND, THE BRITISH VIRGIN ISLANDS

A THESIS IN
Environmental and Urban Geosciences

Presented to the Faculty of the University
of Missouri-Kansas City in partial fulfillment of
the requirements for the degree

Master of Science

By
Theresa Lynne Goyette

B.S. Geology, University of Missouri – Kansas City, 2011
B.A. Political Science, University of Missouri – Kansas City, 2011

Kansas City, Missouri
May 2017

PALEOLIMNOLOGICAL ANALYSIS OF SEDIMENT CORES FROM GUANA ISLAND POND, GUANA ISLAND, THE BRITISH VIRGIN ISLANDS

Theresa Lynne Goyette, Candidate for the Master of Science Degree

University of Missouri – Kansas City, 2017

ABSTRACT

Shallow sediment cores extracted from three locations in Guana Island Pond were analyzed using multiple paleolimnological techniques, including sediment description, grain-size analyses, X-Ray Fluorescence, elemental analyses, scanning electron microscopy, and fossil identification. These data were used to define six depositional units (1-6) that mark the change in paleoenvironment of the lake. Two radiocarbon dates on organic material from 27 cm and 65 cm depth in the cores yielded calibrated ages of 720 ± 40 yr BP and 1307 ± 46 yr BP, respectively. Approximately 2200 yr BP, Guana Island Pond was likely a tidal estuary with sandy storm deposits. By 1500-900 yr BP, an abundance of *Chara fibrosa* oogonia (a freshwater algae) suggest the pond closed off from the sea and runoff exceeded evaporation in a regional wetter climate phase. At this time, the lake was possibly a viable source of potable fresh water for pre-Columbian native peoples and early European settlers. After about 900-700 yr BP, the lake alternated between marine to brackish to freshwater conditions. The uppermost layer of the lake sediment contains high levels of Fe, Ti, and Si indicating an increase in watershed erosion and soil runoff, likely from development of the island from the Quaker settlement period (18^{th} century) through the 20^{th} century.

The faculty listed below, appointed by the Dean of the College of Arts and Sciences have examined a thesis titled "Paleolimnological Analysis of Sediment Cores from Guana Island Pond, Guana Island, The British Virgin Islands," presented by Theresa Lynne Goyette, a candidate for the Master of Science degree, and certify that in their opinion it is worthy of acceptance.

Supervisory Committee

Tina M. Niemi, Ph.D., Committee Chair
Professor
Department of Geosciences

James B. Murowchick, Ph.D.
Associate Professor
Department of Geosciences

L. Mark Raab, Ph.D.
Adjunct Professor
Department of Geosciences

TABLE OF CONTENTS

LIST OF ILLUSTRATIONS

LIST OF TABLES

ACKNOWLEDGEMENTS

There are so many people who made the completion of this thesis possible. Many thanks go out to my family and friends, many of whom supported and believed in me, even when I didn't believe in myself. Completion of this has been a long time coming, and I couldn't have done it without the love and support of you all. Special thanks go out to my mom, dad, sister, and best friend, Nick. You guys really kept me going, while still making sure I managed to get some sleep throughout the process. Thank you to my coworkers, for listening to me go on about my thesis, even when you really weren't sure what I was talking about, and feigning interest in my research. Thank you to Anne Billingsley and Robyn Daniels for keeping me sane during coursework, and for giving me a place to bounce ideas off of. This thesis would not have been completed without your help. Thanks to Nancy Hoover for all of her help and answering my random questions, even well after business hours. Thank you to Dr. Tina Niemi for introducing me to sediment analysis using microfossils, Dr. James Murowchick for all of your assistance with the SEM, microscopes, and any other questions I had, and Dr. Mark Raab for always bringing a sense of humor to all of his courses.

Thank you to the team that helped with the 2012 fieldwork: Dr. Tina Niemi, John Rucker, Dr. Joe Andrew, and Amy Ameis. Your assistance in the field was invaluable. I would also like to thank the Jarecki family for hosting us for "science month", as well as the scientists and researchers present on Guana Island in 2012.

CHAPTER 1

INTRODUCTION

Islands are especially useful when studying past climates and environments, as they are inherently isolated from outside impact. In particular, inland lakes and ponds on islands are excellent sources of data for sediment analyses as the physical, chemical, mineralogical, and biological variations of the sediment trapped in the basin can be measured and used to study changes in the depositional environment over time. Lake and pond sediments can be proxies for changes in climatic conditions such as precipitation and evaporation. For example, high levels of rainfall may increase sediment runoff into the pond, or high temperatures and increased evaporation rates can cause changes in water chemistry. Preservation of lake sediments can be impacted by a number of factors that are especially pronounced in small shallow lakes, as they are subjective to desiccation, erosion by wind deflation, and anthropogenic influences.

This study focuses on Guana Island Pond located on the southwest portion of Guana Island in the British Virgin Islands (BVI). It is a eutrophic pond and covers an area of about 1.9 hectares. The lake is approximately triangular in shape and is currently saline. Guana Island Pond was historically a seasonally dry lake (Jarecki, 2003). The pond is surrounded on the west, north, and east by mountains that reach elevations from 226 m to 806 m. Guana Island Pond is separated from White Bay on the Caribbean Sea to the southwest by a 180-m-wide vegetated sand plain (Jarecki, 2003). The plain effectively prevents sea water inflow into the pond, except during extreme storm events.

The main objective of this study of Guana Island is to analyze sediment from cores collected from Guana Island Pond. It is hypothesized that the pond was once a tidal estuary and became an isolated lake in part due to a change in climate and land use. This study will also investigate whether Guana Island Pond was once a viable source of potable fresh water for pre-Columbian native peoples and early European settlers. Factors potentially influencing the paleoenvironment of the pond include the development and potential migration of the berms on the sand plain; whether the pond was once a tidal estuary, and if so, when it closed; the climate change on the scale of decades to centuries; and the size and recurrence of large storms over time.

Twelve soft sediment cores were collected from ten locations in Guana Island Pond in October 2012, along two approximately east-west transects perpendicular to the shoreline where the ruins of an 18^{th} century Quaker sugar mill are located. Analyses of the sediment from four core locations using techniques including sediment description, X-ray fluorescence (XRF), scanning electron microscopy (SEM), microfossil identification, grain-size analysis, and radiocarbon dating are used to define six depositional units and to interpret the changes in environment of Guana Island Pond over time.

CHAPTER 2

BACKGROUND

Study Area

The British Virgin Islands (BVI) are a British territory located in the Caribbean Sea, directly north and east of the United States Virgin Islands (USVI), and are composed of four large and numerous small islands. Guana Island is located in the BVI, just north of the largest island, Tortola (Figure 2.1). The island is approximately 850 acres in area. The only habitation on the island is the structures of the Guana Island Resort that lie along the west ridge between White Bay to the south and Muskmelon Bay to the north (Figure 2.2). The island and its resort are privately owned and boast of being a sanctuary for both the flora and fauna found naturally on the island. The occupational history of Guana Island will be discussed later in this chapter.

Figure 2.1 British Virgin Islands with the location of Guana Island outlined by a box (Encyclopædia Britannica, Inc.)

The pond was previously a seasonal pond that would fill with water during the rainy season, and evaporate until it was a dry pond bed during the dry season. In 1990, a desalination plant was built on the west side of the pond. Seawater is pumped into the reverse osmosis plant and the hypersaline brine outflow is pumped into Guana Island Pond, causing it to be inundated during both the rainy and dry seasons (Jarecki, 2003).

Figure 2.2 Google Earth Satellite Image of Guana Island with White Bay, Muskmelon Bay and North Bay visible. Red box outlines location of Guana Island Pond.

Further modifying the natural conditions of the pond is a round fountain on an island that was installed in the center of the pond. The purpose of the fountain is purported to aerate the water to lessen the stagnation. According to verbal reports from scientists and staff of the island, storm surges from large storms do occasionally breach the berm along the western side of the plain that separates the pond from White Bay. These overwash events cause ocean water to enter the pond and also bring fish and other marine organisms into the pond. These organisms are said to live for a short while until the water salinity increases by evaporation thus causing a massive fish die-off.

Figure 2.3 View of Guana Island Pond, looking to the southeast from the ridge where the Guana Island Resort housing units are located.

In October 2012, our water depth soundings show that Guana Island Pond (Figure 2.3) is very shallow and varies from 13 cm to 36 cm in depth. Influx of water into the pond comes from rainfall, seawater overflow during storm events, and hypersaline brine outflow from the desalination plant located on the northwest side of the pond.

Temperatures in the Caribbean are generally hot and humid. The climate of the BVI is no exception, and is considered subtropical. Temperatures average 25.6°C year round, with the dry season occurring from February to April and the rainy season occurring May to November; though it is not uncommon for year-round pop-up rainclouds to briefly pass over the island before departing. Guana Island Pond would fill during the rainy season, and evaporate during the dry season prior to the installation of the desalination plant on the island in 1990. Since the installation of the desalination plant, the pond no longer evaporates completely, but does decrease in overall size during the dry season. A shrinking of the surface area of the pond and a wider beach on the south shore of the pond can be seen during times of low rainfall, such as in August 2012 as compared to times of high rainfall, such as February 2014 using historical imagery in Google Earth (Figure 2.4).

Figure 2.4 August 29, 2012 aerial image (left) during the low rainfall and February 28, 2014 aerial image (right) during the high rainfall. A wider beach can be seen along the southern side of Guana Island Pond in the August 2012 image.

Tectonic Setting

The BVI are located on the Caribbean Tectonic Plate, which is situated between the North American Plate and South American Plates, and east of the Cocos, Nazca, and Panama Plates. Pindell and Barrett (1990) posit that during the Late Triassic to Early Jurassic, the North and South American plates separated, the Yucatan block migrated towards its present location in the Gulf of Mexico, and continental fragments near Florida migrated southeast and now underlie the south Florida shelf and western Bahamian platform (Figure 2.5a).

In the Early Cretaceous (Valanginian), 130 Ma, seafloor spreading in the Gulf of Mexico ceased and caused the Yucatan block to become part of the North American Plate (Pindell and Barrett, 1990). At this time, the basement of the Greater Antilles likely formed, and the Farallon Plate subducted to the southeast, beneath the South American Plate (Figure 2.5b).

At the beginning of the Late Cretaceous (Cenomanian), 95 Ma, seafloor spreading had created a wide proto-Caribbean seaway. A thick buoyant lithospheric block entered the north-dipping proto-Greater Antilles subduction zone with a flip in polarity. The south-dipping subduction began on the northern side of the Greater Antilles arc, allowing for the migration of the Greater Antilles into the proto-Caribbean area. The Farallon Plate continued to be subducted to the northeast towards the North American Plate (Figure 2.5c) (Pindell and Barrett, 1990). By the middle of the Late Cretaceous (80 Ma), seafloor spreading had ceased, with the Caribbean Plate migrating northeast into the gap between North and South America, led by the Greater Antilles subduction (Figure 2.5d).

In the Paleocene (59 Ma), the Caribbean Plate continued to migrate to the northeast, though the proto-Caribbean Sea was wider than the gap between Colombia and the southern Yucatan, likely causing two back-arc spreading events, which formed the Yucatan and Grenada basins. During this time, the collision between the Cuban frontal arc complex and the Bahamas margin begins (Figure 2.5e) (Pindell and Barrett, 1990).

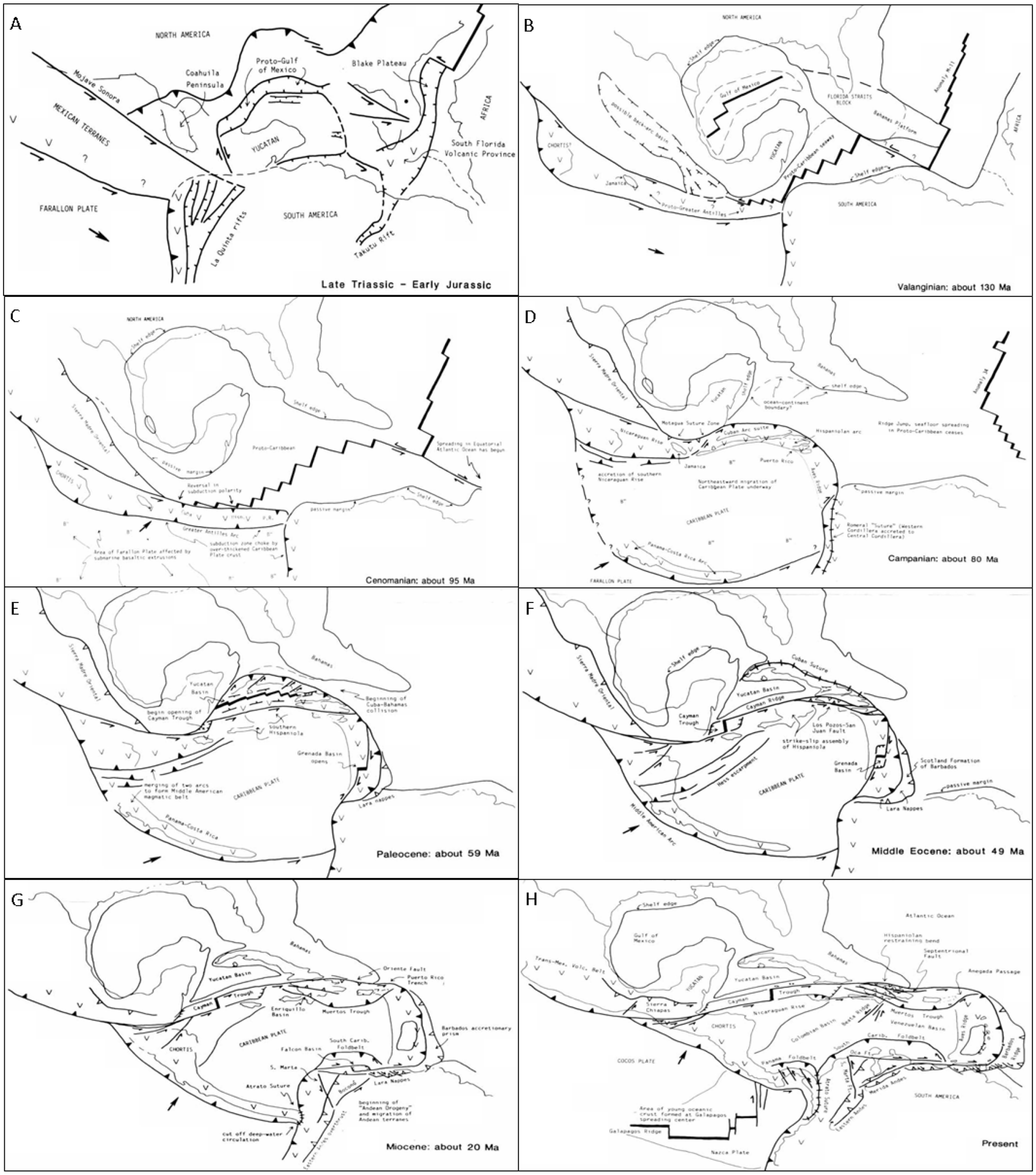

Figure 2.5 Tectonic evolution of the Caribbean Plate from the Late Triassic to present. A. Late Triassic to Early Jurassic; B. Valanginian; C. Cenomanian; D. Campanian; E. Paleocene; F. Middle Eocene; G. Miocene; H. Present. (Pindell and Barrett, 1990).

In the Middle Eocene (49 Ma), the Yucatan and Grenada basins were fully opened; the Cuba-Bahamas collision was complete, with the capture of Cuba to the North American

Plate. The northern Caribbean plate boundary zone is defined by the eastern movement along the Cayman Trough (Figure 2.5f).

By the Miocene (20 Ma), the Caribbean Plate had migrated approximately half the length of the Cayman Trough and Puerto Rico had separated from southeastern Hispaniola. Most strike-slip motion in the northern Caribbean occurred along the Oriente Fault and Puerto Rico Trench (Figure 2.5g) (Pindell and Barrett, 1990).

The BVI is located on the northern side of the Caribbean plate close to the boundary with the North American Plate. This tectonic boundary is marked by the Puerto Rico Trench which is also the geographical boundary between the Caribbean Sea and the Atlantic Ocean. The deepest part of the Puerto Rico Trench is located approximately 120 km north of San Juan, Puerto Rico. Geographically, the trench can be divided into two different areas at approximately the 65-66° longitude line. West of this point, the boundary is 10-15 km wide, water depths are deep (ca. 8 km), plate motion is oblique and accommodated on a transform fault. East of this point, the trench shallows to 7.6-7.7 km and the North American Plate is subducted beneath the Caribbean Plate (Brink et al., 2004).

The Puerto Rico Trench located between the American and Caribbean Plates is unique. Although called a trench, this plate boundary is largely a transform boundary with only a small area of subduction measured along the eastern boundary of the trench. Here the western edge of the North American Plate is being subducted under the eastern edge of the Caribbean Plate, along the Lesser Antilles.

Relative to the Caribbean Plate, the North American Plate is moving westward at a rate of approximately 2 cm/yr. Relative to the North American Plate, the Caribbean Plate is moving eastward (Figure 2.6) (Nealon and Dillon, 2001). The Puerto Rico Trench and the Anegada Trough are along the boundary between the Caribbean and North American Plates. The Anegada Trough is an area of deep ocean bathymetry to the southeast of the island of Anegada. The Virgin Islands Trough is located on the Caribbean Plate, and is an area of deep bathymetry, directly south of the USVI and BVI, but north of St. Croix, USVI. The Muertos Trough is located south of Puerto Rico, and north of the Venezuelan Basin and Plain on the Caribbean Plate. At the latitude of the BVI, the North American Plate is being subducted under the Caribbean Plate along the Antilles Arc.

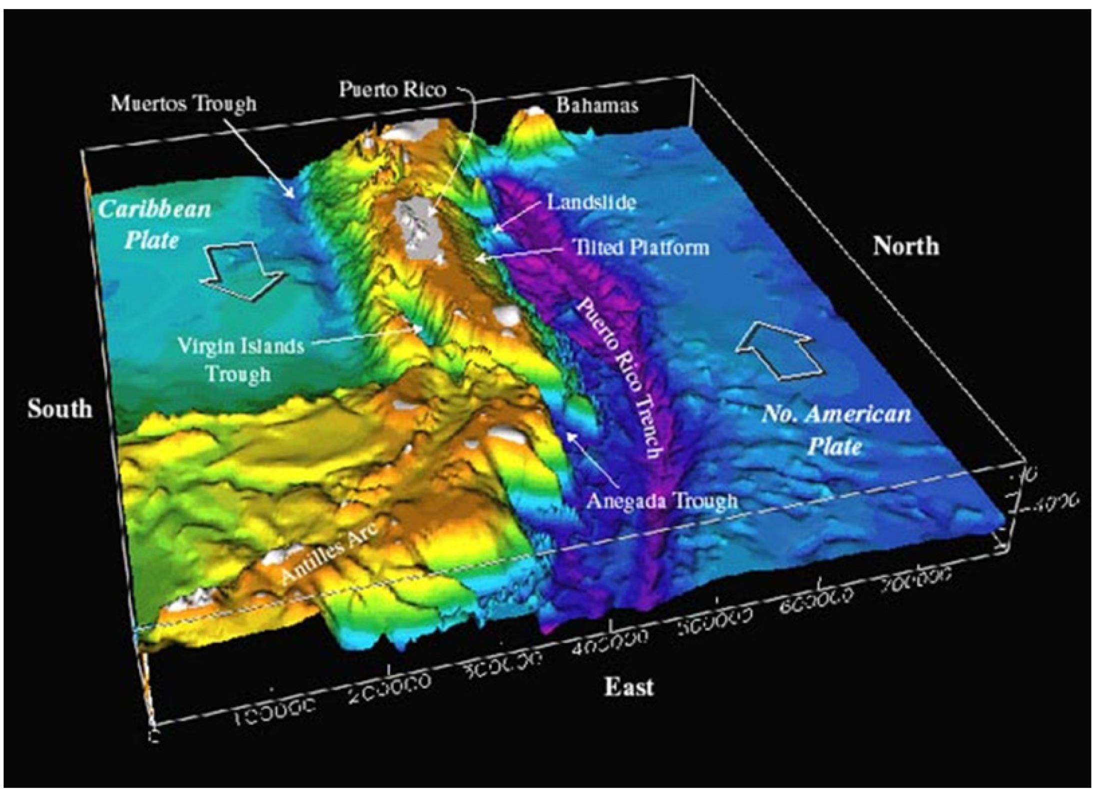

Figure 2.6 Bathymetry of the seafloor and relative plate motion along the Caribbean-North American Plate boundary. Magenta and deep blue colors indicate deep bathymetry and yellow and orange colors indicate shallow bathymetry. (Nealon and Dillon, 2001).

The Antilles Island Chain marks a western boundary of the North American Plate as it is being subducted beneath the Caribbean Plate. The Greater Antilles (Figure 2.7), generally classified as including Cuba, Hispaniola, Jamaica, and Puerto Rico are volcanic and metamorphic in their basement rocks, but are overlain with thick carbonate sedimentary rocks. The exposure of igneous basement rocks in the Greater Antilles indicates that the subduction volcanism that formed the Greater Antilles arc ended in the past.

The Lesser Antilles (Figure 2.7), generally classified as stretching from the U.S. Virgin Islands to Trinidad and Tobago to the south and Aruba to the west are volcanic in nature. Volcanism is ongoing along the eastern boundary between the North American and Caribbean Plates, which formed the Lesser Antilles Island Chain. As the Lesser Antilles Island Chain continues southward towards South America, there is a second area of subduction. At this point, the South American Plate is being subducted under the Caribbean Plate, continuing island growth in the Lesser Antilles.

As a result, most of the BVI are uplifted volcanic rocks, consisting of large fractured breccias and tuffs (Figure 2.9). One exception is Anegada which is predominantly a limestone island with a maximum elevation of only 8 m above sea level (Helsley, 1960). The Lesser Antilles Island chain is made up of two Cenozoic volcanic arcs, formed approximately during the early Eocene to mid-Oligocene and the Miocene to present (Bouysse, 1990).

During the late Pleistocene, sea levels were far lower than present day, and the Puerto Rican Plateau was a large land mass that encompassed the present-day island of Puerto Rico, as well as the entirety of the Virgin Islands, with the exception of St. Croix (Island Resources Foundation and Jost Van Dykes (BVI) Preservation Society, 2009). While geographically the British Virgin Islands belong to the Lesser Antilles, geologically they belong to the Greater Antilles, rising from the Puerto Rican Plateau, located 65 m below present day sea level, with basement plutonic rocks overlain with volcanic breccia tuffs.

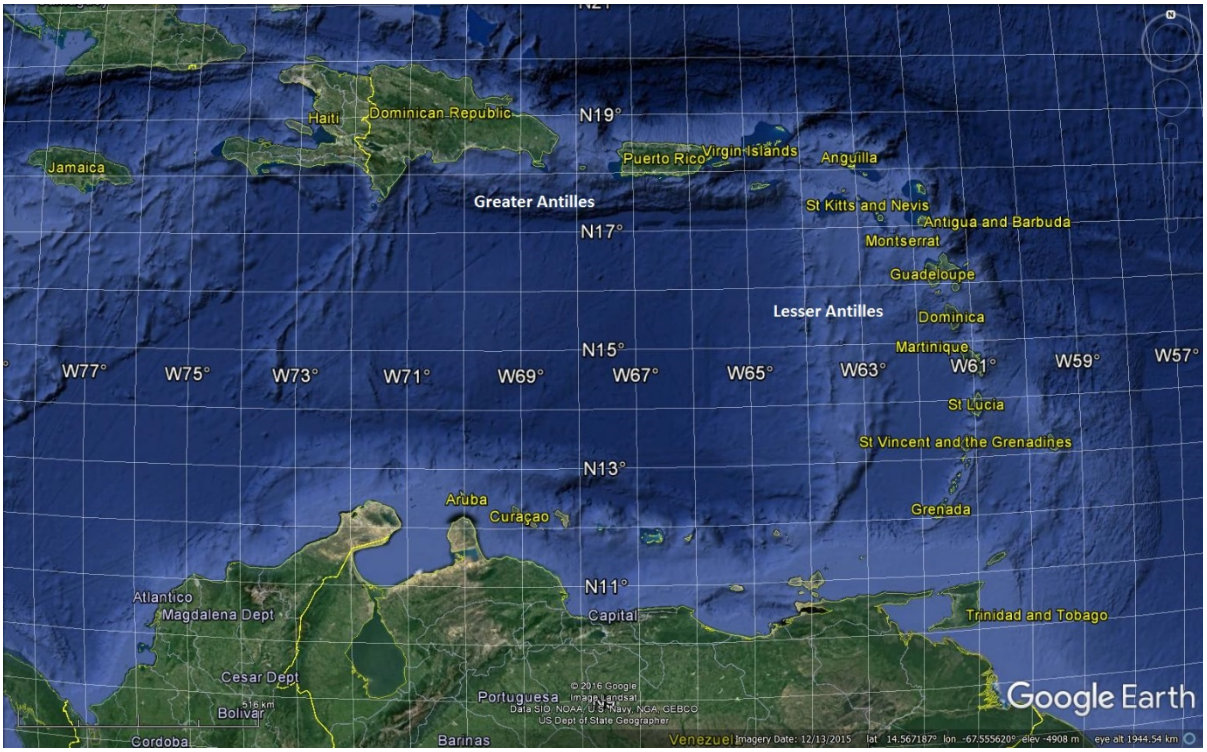

Figure 2.7 Map of Greater and Lesser Antilles islands. Image courtesy of Google Earth.

Helsley (1960) mapped the stratigraphy of the BVI. The oldest bed encountered was the Water Island Formation, with an unknown age. The Water Island, Louisenhoj, Outer Brass Limestone, Tutu, and Tortola Formations are described in general. The Water Island Formation consists of volcanic flows and breccias interbedded with altered basic to intermediate, volcanic or subvolcanic rocks. The Louisenhoj Formation consists of coarse breccias interbedded with finer tuffs. The Outer Brass Limestone Formation consists of dark grey carbonaceous limestone. The Tutu Formation consists of tuffaceous wacke sandstone interbedded with coarser clastic rocks. The Tortola Formation is composed of breccias, tuffs, and volcanic sandstones.

Above the Tortola Formation is the intrusion of the Virgin Gorda Batholith. Above the batholith is the Necker Formation (Helsley, 1960). Helsley (1960) states that the Necker Formation is present on Mosquito, Prickly Pear, Eustatia, Little Saba, Necker, Guana, and Great Camanoe Islands, the Seal Dogs, Cockroach Dog, and George Dog.

North of Virgin Gorda, the Necker Formation is pyroclastic in nature, with fine tuffs that are less deformed than those in the Tortola Formation. The basal tuffs are light blue green to green, very fine tuffs with poor bedding, and are interbedded with a few moderately well sorted green lithic coarse tuffs (Helsley, 1960). Helsley (1960) posits that the Necker Formation was likely deposited as subaerial ash that was later mildly altered or metamorphosed. Above the basal tuffs are lithic coarse tuffs and lithic lapilli tuffs, which range in color from whitish green to dark green and contain dark green chloritic fragments that were likely originally glass.

On Guana Island, Helsley (1960) records a wide variety of rock types which were deposited subaerially with the exception of one thinly bedded very fine porcellaneous tuff, which may be a subaqueous deposit (Figure 2.8). All breccias and tuffs were weathered shortly after deposition without reworking, and some are cut with later porphyritic basalt dikes and sills. The entire section has undergone alteration, with the original rock being replaced with a metaconglomerate of quartz, chlorite, and calcite. The southern units show overturned bedding with steep dips, while the northern units show gentle folding and dips of 10°-20° (Helsley, 1960). Helsley (1960) approximates the unit to be approximately 2,000’ thick and include welded tuffs interbedded with lithic lapilli and coarse tuffs, with the unit being highly altered and weathered. In thin section, the welded tuffs contain oriented and highly altered plagioclase phenocrysts in an aphanitic matrix, which has been replaced by calcite and silica.

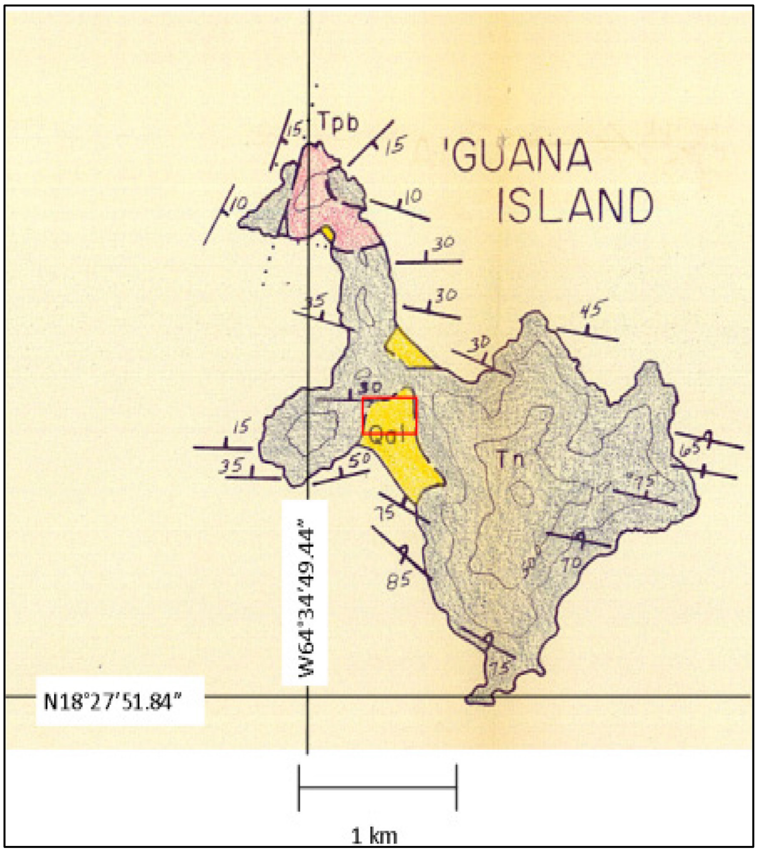

Figure 2.8 Helsley's 1960 Geologic Map of Guana Island. Tbp is porphyritic basalt, Tn is the Necker Formation, and Qal is unconsolidated alluvium. Legend present in Appendix A. Box indicates location of Guana Island Pond.

Above the welded tuffs, Helsley (1960) notes an approximately 3,000' thick sequence of volcanic breccias and tuffs containing several welded tuff units. These breccias vary in color from green to brown to purple, consist of large blocks imbedded mostly in a coarse tuff and seldom a lapilli tuff. This unit is also present on Great Camanoe Island. The third unit consists of tuffs, both coarse and fine, lapilli tuffs, and a few breccias, with exposures being present along the north and western shores of Guana Island (Helsley, 1960). Helsley (1960) interprets that this unit was deposited as subaerial ashes, because tuffaceous mudballs are present. No fossils were found in the Necker Formation. The Necker Formation is assigned a middle to late Eocene age because it overlies the Shark Bay Member of the Tortola Formation (Helsley, 1960).

The Rogue's Bay Calcarenite sits above the Necker Formation and Helsley (1960) describes it as being named after its source location, at the eastern edge of Rogue's Bay on the north shore of Tortola. The calcarenite is exposed over an area of approximately 10,000 square yards and has a total thickness of 30'-40', and is composed of well sorted pelecepod, gastropod, and peneroplid shell fragments (Helsley, 1960). Helsley (1960) states the calcarenite is cemented with calcite to form a limestone with approximately 10% porosity, with very few silicates with plagioclase and epidote being the only ones present at less than 1% of the total rock. The age of the unit is late Miocene to present, and the unit dips away from the Virgin Gorda Batholith, indicating the area of the unit has risen approximately 15° since the late Miocene (Helsley, 1960).

The youngest layer encountered by Helsley (1960) is Quaternary Alluvium, which has a maximum thickness of 150', and is comprised of valley fill, beach, and mangrove deposits.

While performing the study of the BVI, Helsley (1960) took particular note of the geology of Guana Island. The bedrock of the island consists mostly of the Necker Formation (Figure 2.9), with the area on the northwestern portion of the island, between North Bay and Muskmelon Bay being composed of porphyritic basalt, and the area of Guana Island Pond being classified as Quaternary Alluvium.

Figure 2.9 Igneous rock outcrop along the shoreline of Guana Island showing the Necker Formation. Image taken from White Bay (Figure 2.2) looking west.

Within the Necker Formation, Helsley (1960) hypothesized that a major fracture or fault set exists; creating the northwest-southeast trend of shorelines and ridges which are not controlled by stratigraphic variations, as the strikes of these potential faults is nearly east-west. He describes the coves on many of the islands consisting of mainly gravel or boulder size rocks, with the exception of locations where offshore reefs create a slight barrier to prevent storm waves from removing the sand. Helsley's geologic map of Guana Island can also be found in Appendix A.

Cultural History

Pre-Columbian Occupation

The Caribbean has a long history of occupation. The first historical documentation is from the Spanish, led by Christopher Columbus, arriving on what is now San Salvador Island in the Bahamas in 1492. The Spanish found three major indigenous groups of people occupying the Caribbean – the Ciboney, the Arawak, and the Carib (Rogoziński, 1999). These native people are thought to have originated from South America. The Ciboney were found on the northwestern parts of Cuba and Hispaniola, while the Arawak (sometimes known as the Lucayans) dominated the Bahamian archipelago, and the Carib occupied the Virgin Islands, much of the Lesser Antilles, and the northern portion of Trinidad. According to reports of the Spanish, the Arawak followed after the Ciboney and were being chased by the Carib (Rogoziński, 1999). Other scholars posit that the Taíno, a subclass of the Arawak, occupied Puerto Rico, and shared a war-torn existence with the Carib of the Virgin Islands (Figueredo, 2006).

According to the National Park Service, occupation in the Caribbean can be divided into three major units: Paleoindian Period (9500-5000 B.C.), Mesoindian Period (5000 B.C.-A.D. 1), and the Neoindian Period (A.D. 1-A.D. 1500). The Paleoindian Period is identified at the El Jobo site in Venezuela, but no Paleoindian Period sites have been identified in the Caribbean Islands. These people are believed to be big game hunters. The Mesoindian Period people are the peoples that the early Spanish explorers described as the Ciboney, who were a hunter gatherer people. Their sites tended to be coastal shell middens found on or near the coast, and have evidence of stone tools, such as flake points and knives. Within the Mesoindian Period are two ceramic subcultures: the Casimiroid Culture and the Ortoiroid Culture. The Ortioiroid Culture is further broken down into the Krum Bay Subseries and Coroso Subseries (Prehistory of the Caribbean Culture Area, U.S. National Park Service). The youngest unit is the Neoindian Period, the peoples of which came after the Mesoindian groups, and eventually pushed the Mesoindians into western Cuba. Part of this group was the Ostionoid agricultural culture, which migrated out of the Orinoco area of Columbia and Venezuela into the Antilles. Part of this culture is the Elenan-Ostionoid subseries, which has been dated from A.D. 600-1200, and pottery has been found on the eastern half of Puerto Rico. These Elenan-Ostionoid culture sites such as Tibes, Collores, and El Bronce in Puerto Rico, have multiple plazas and ball courts (Prehistory of the Caribbean Culture Area, U.S. National Park Service).

Pottery excavated from a site on Guana Island suggest habitation as far back as 600-1500 A.D. These early people are identified as the Ostionoids, an evolutionary predecessor to the Taíno (Saunders, 2005). The Ostionoids were a culture built upon pottery and villages, including large settlements. They also had well established cultural customs and beliefs, many of which were later incorporated into the Taíno culture. Davis (2011) proposed that Guana Island was used by the pre-Columbian natives as a ceremonial or religious location, without being a location that was permanently occupied.

The discovery of pottery from differing times and native groups goes to further support the idea of repeated occupation of Guana Island before European arrival, though evidence for continual occupation is still being investigated. In 2008, while performing a shovel test on Guana Island, Joshua Kehrburg discovered an almost entirely intact bowl dating back to the Elenan-Ostionoid style (Figure 2.10), which was dated to approximately 1100-1400 A.D. by Elizabeth Righter during the excavation (Righter, 2008).

Figure 2.10 Nearly intact Elenan-Ostionoid style bowl. From Righter, 2008. No scale present.

The arrival of Europeans in the Caribbean in the 15th Century brought diseases that decimated the population of the native peoples. Many islanders also succumbed to these diseases, ultimately leading to the eventual eradication of the native peoples. The diseases brought to the Americas by European explorers include smallpox, hepatitis, measles, encephalitis, typhus, tuberculosis, diphtheria, whooping cough, mumps, and influenza (Mann, 2011). Africans coming to the Caribbean had some immunity to European diseases, but brought diseases of their own, such as malaria and yellow fever, neither of which Europeans or pre-Columbian peoples had immunity to. Rogoziński (1999) suggests that when Columbus landed in 1492, the Caribbean was home to at least a quarter of a million Arawaks and Caribs. Some archaeological estimates have that population closer to 6 million natives (Rogoziński, 1999). Within 20 years of European contact, almost all native Americans had perished or had been enslaved (Rogoziński, 1999).

European Occupation

After the discovery of the islands, Europeans quickly conquered the region. Columbus landed in the Bahamas and then sailed south to Cuba, under the guide of several Lucayans, and from Cuba he ventured to what is now known as Hispaniola (Rogoziński, 1999). Since the early 16^{th} century, the Virgin Islands were under European control and have suffered conflict associated with the islands changing hands from one controlling country to another; as fights and battles often occurred during changes in power. European wars often determined who controlled the islands. In the 1620s, Europeans outside of Spain were able to establish colonies in the Eastern Caribbean, before eventually moving west into the Greater Antilles (Figure 2.7). All new colonies depended on the goods transported by Dutch traders, and the Dutch West India Company was born (Rogoziński, 1999). In 1648, Dutch pirates settled on Tortola, which was attacked and overtaken by the British in both 1665 and 1672. The British Virgin Islands have remained in British control ever since (Peffer, 2001; Rogoziński, 1999).

According to the surviving records of the Tortola Society of Friends, in the early-1700s, two Quaker families, the Lake and Parke families (Jenkins, 1923), settled on Guana Island as part of "the Quaker Experiment", also known as the Religious Society of Friends, which lasted for almost 50 years. The goal of "the Quaker Experiment" was to spread equality, simplicity, and peace, but these ideals were difficult to encourage in a region of slavery (Chenoweth, 2014). The Lake and Parke families grew sugarcane and used African slaves to work the fields. The sugarcane was processed at a mill whose ruins mark the eastern side of Guana Island Pond on the island (Figure 2.11).

The British used Tortola and other islands for sugarcane production. While initially highly profitable on other islands, it failed to take off in the Virgin Islands due in large part to the aridity of the islands. Sugar production in the Virgin Islands declined and eventually ended in the 1830s, following the end of British slave trade in 1808 and the abolition of slavery in 1833 (Rogoziński, 1999), though the islands remained a British territory.

Figure 2.11 Ruins of late 18th Century Quaker Sugar Mill on the east side of Guana Island Pond. No scale present.

Current Occupation

There is a marked hiatus in the history of the island from the 18th Century Quakers until the 20th Century ownership of the island. After European occupation and ownership for close to 450 years, Guana Island was purchased by Beth and Louis Bigelow of Massachusetts in 1925. The Bigelow's guests were travelers, intellectuals, and professionals, and came to stay on the island for months at a time (www.guana.com). In 1975, Henry and Gloria Jarecki purchased Guana Island from the Bigelow's, and immediately began improving and updating the accommodations and facilities on the island. The Jarecki's were believers in preserving the natural, undeveloped beauty of Guana Island, and began a program to preserve and reintroduce many of the flora and fauna of Guana Island (www.guana.com). The Jarecki's also updated the structures on the island, as well as installing a desalination plant in 1990, fulfilling the freshwater needs of the island's resort, as well as sprawling gardens and orchard.

Guana Island is still owned by the Jarecki family today. Guana Island is prized to this day as a piece of paradise essentially untouched by the development and construction associated with large scale resorts, such as those on Tortola and many of the islands in the United States Virgin Islands. And by being one of the few islands in the Caribbean that is both privately owned and open to the public, the Jarecki's plan to share their piece of paradise with generations to come.

Climate

With the exception of the northernmost Bahamian Islands, the Caribbean lies entirely south of the Tropic of Cancer. This allows the region to have a warm and humid climate. The temperatures rise to peak around noon and decrease as the afternoon progresses. Humidity is highest, sometimes 90%, at dawn, before tapering off during late afternoon. Humidity can drop to as low as 50%, but is generally not any lower than 70% (Rogoziński, 1999). The tropical climate of the Caribbean, caused by average temperatures not differing by more than a few degrees throughout the entire year, is due in large part to the Trade Winds. The British Virgin Islands (BVIs) lie within the northeast trade winds, with winds coming from east-northeast from December to February, from the east from March to May, from the east-southeast from June to August, and from the south-southeast from September through November. Jarecki (2003) writes that this climate is subtropical with a long dry season, with average temperatures ranging from 26° to 31°C in the summer and 22° to 28°C in the winter months. The northeast trade winds, which originate in the Bermuda-Azores high-pressure cell, are the main meteorological cause of weather in the Caribbean and Gulf of Mexico. These winds blow at a constant 15 to 25 knots, with very little change in direction noted from day to day. They begin at the latitude of Bermuda and then shift clockwise to the northeast, eventually becoming the mid-latitude westerlies that travel back across the Atlantic towards England, France, and northern Europe (Rogoziński, 1999). The combination of the trade winds and the ocean currents that follow them in the Caribbean lend themselves to the formation and locomotion of many tropical hurricanes.

Islands in the Caribbean usually experience both a “rainy season”, which occurs from May to November, and a “dry season”, which occurs from February to April (Rogoziński, 1999). Mean rainfall from 1991 through 2001 was 104 cm/yr, and ranged from 69 cm in 1994 to 157 cm in 1998 (Jarecki, 2003). Reports from local BVI islanders state that 40 to 50 years ago the climate was rainier than present, and this idea is corroborated by a 1959 report stating an average of 135 cm/yr, ranging from 76 cm and 250 cm between 1901 and the time of publication. Additionally, due to orographic effects (i.e. mountains), rainfall can vary greatly across and between islands, such as Tortola and Guana Island. It is said that rainfall on Tortola can be up to 25% higher than on Guana Island, with its large surface area and high peak at Mount Sage, than on smaller, flatter, neighboring islands (Jarecki, 2003).

CHAPTER 3

METHODOLOGY

Field Procedures

Twelve soft-sediment cores were collected from ten locations from Guana Island Pond. Fieldwork was conducted on Guana Island during October 2-12, 2012. The cores were collected using a Bolivia-type, drive-rod piston corer purchased from LacCore at The University of Minnesota (www. http://lrc.geo.umn.edu/laccore/). With this coring system, a piston attached to a cable is placed inside a clear 1.25-m-long polycarbonate tube, i.e. the core barrel. The core barrel is then attached to a housing and a rod. Two or three people push the piston corer into the sediment while an additional person keeps tension on the piston cable. As the corer is pushed into the sediment, the piston moves up the tube and the sediment moves into the core barrel and the core is collected.

Cores were labeled for “GI” for Guana Island, “12” for the year 2012, “FP” for Flamingo Pond (the pond’s nickname), followed by the core number, and letter A, B, C, if deeper sediment was recovered from the same core location.

Cores GI12FP6A/B/C, GI12FP7, GI12FP8, and GI12FP10 (i.e. cores 6, 7, 8, and 10) form a roughly east-west transect across the northern portion of the pond, while cores GI12FP1, GI12FP2, GI12FP3, GI12FP4, GI12FP5, and GI12FP9 (i.e. cores 1, 2, 3, 4, 5, and 9) create a second east-west transect across the southern portion of the pond (Figure 3.1). Core collection data for locations 6, 7, 8, and 10, including UTM coordinates, initial core barrel length, percent recovery, and distance from benchmark core GI12FP6A/B/C can be found in Table 3.1. Additional data on all cores can be found in Appendix B.

During core collection, cores 6A, 6B, and 6C were all collected from the same boring in an attempt to recover sediment of the deeper stratigraphic layers. Upon visual observation, it was determined that the lowest core, 6C, correlated with the bottom sediment in core 6B rather than the base of core 6B.

Compaction of sediment is common during piston coring. Therefore, the core tube length and core recovery are important to document. By dividing the length of the core recovered by the initial core barrel length pushed into the substrate, the percent of the core recovered can be calculated. The percent recovery defines both potential compaction of sediment and loss of sediment during the coring process, and is a quantifiable value. Additional information on core collection can be found in Appendix B.

Table 3.1: Core location, barrel length, core recovered, percent recovered, and distance from core GI12FP6ABC. Information on other cores can be found in Appendix B.

Core	UTM	Barrel Length	Recovered	Percent Recovered	Distance from GI12FP6
GI12FP6A	20Q 0333705 2043798 (+\- 5m)	125 cm	17 cm	13%	0
GI12FP6B	20Q 0333705 2043798 (+\- 5m)	108 cm	88 cm	81%	0
GI12FP6C	20Q 0333705 2043798 (+\- 5m)	52 cm	32 cm	61%	0
GI12FP7	20Q 0333659 2043778 (+/- 5m)	125 cm	89 cm	71%	51 m to the SW
GI12FP8	20Q 0333606 2043767 (+/- 5m)	88 cm	80 cm	91%	103 m to the SW
GI12FP10	20Q 0333563 2043724 (+/- 4m)	63 cm	38 cm	60%	160 m to the SW

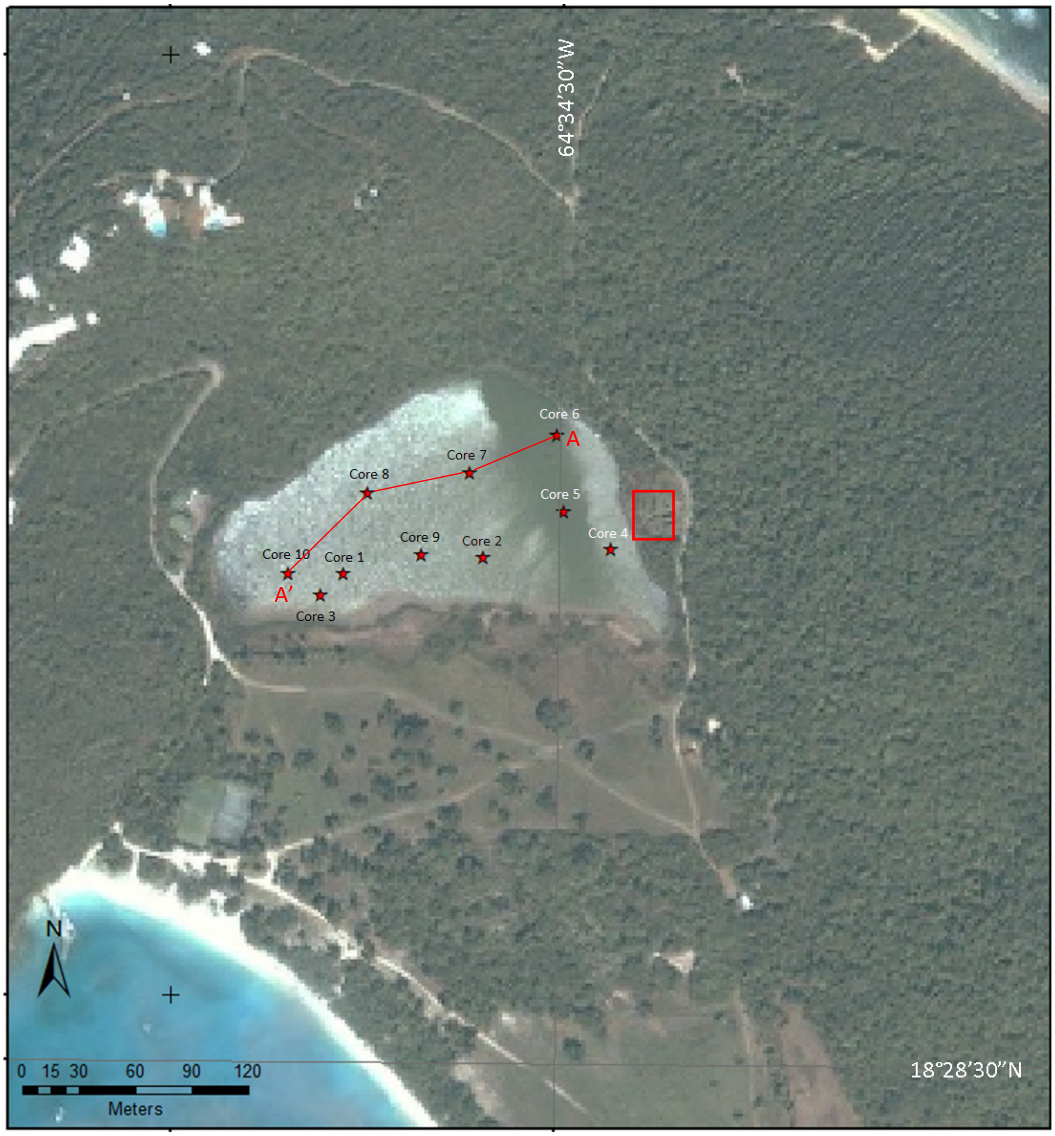

Figure 3.1 ArcGIS Image of Guana Island Pond core locations. Satellite image date: pre-2005. Line of section A-A' shown in red, and location of Quaker Sugar Mill Ruins boxed.

Bathymetric and sediment bottom type data were collected across Guana Island Pond. From a canoe, water depth was measured at points using a pole marked in 2 cm increments. GPS coordinates were recorded on a Panasonic Toughbook CF-19. Bathymetric measurements were made in conjunction with sediment bottom type observations. When inserting the measurement pole to measure water depth, an evaluation of the bottom sediment composition was recorded. Sediments were classified by texture as sand, clay (firm, medium firm, soft), or sandy clay.

Water depth and GPS location data were input into the ESRI company ArcGIS software program and a bathymetric map was generated using the topography, hillshade, and contour tools (Figure 3.2). Water salinity, pH, and temperature data were also taken at bathymetric points in Guana Island Pond, and can be found in Appendix C.

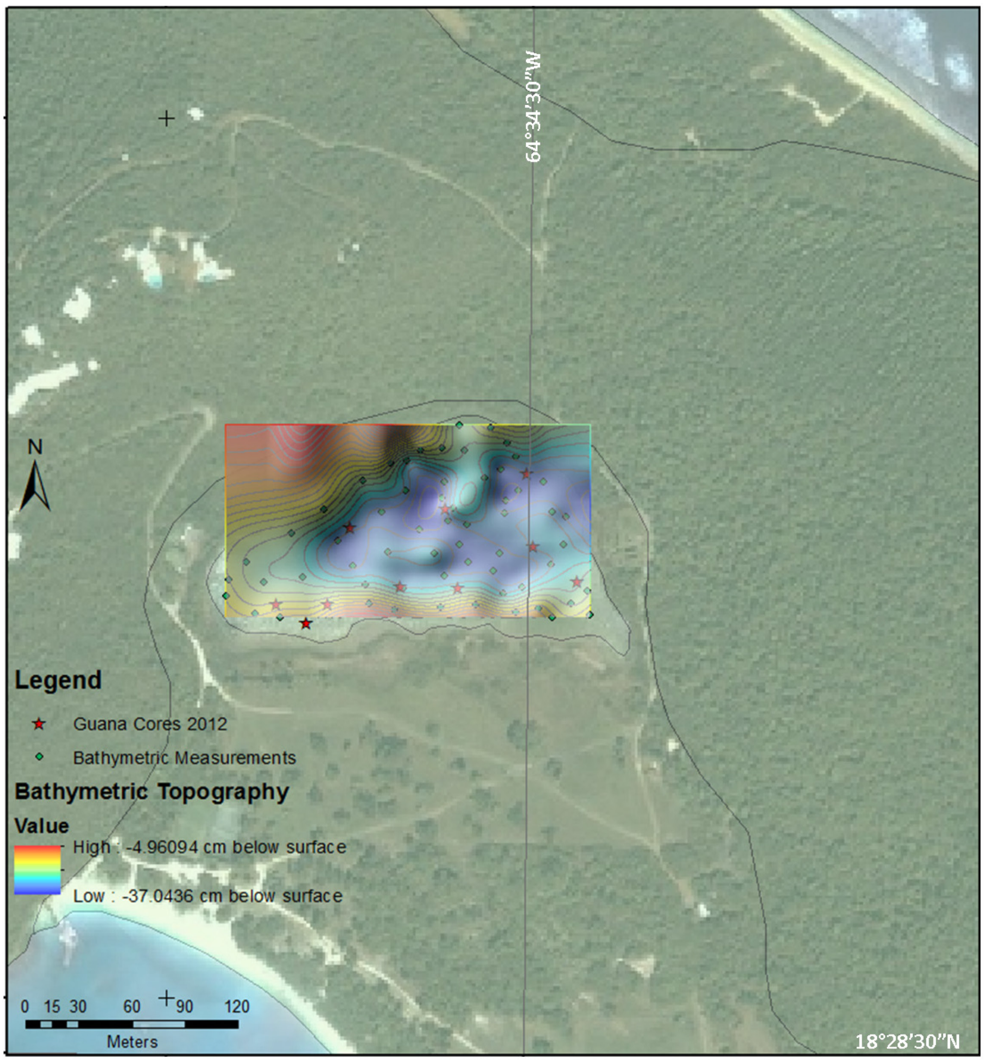

Figure 3.2 ArcGIS map of bathymetry of Guana Island Pond. GIS digitization by Andrew (2012).

Laboratory Procedures

The Guana Island Pond cores were transported from the British Virgin Islands to the University of Missouri-Kansas City (UMKC) as checked luggage. They are stored in a walk-in cooler at 4°C for preservation. In January 2014, core 6A, 6B, 6C, 7, 8, and 10 were shipped to the National Lacustrine Core Facility (LacCore) located at the University of Minnesota-Minneapolis. Analyses conducted at LacCore on the Guana Island Pond cores are described below.

The cores were run through the LacCore Multi-Sensor Logger. This equipment allows for photographs to be taken before the core is split, as well as after it is split. The Multi-Sensor Logger also allows for the viewing of internal stratigraphic structures before splitting and cleaning of the cores, as well as testing for magnetic susceptibility. After the cores are split and cleaned, smear slides were made. Smear slides contain a thin layer of unconsolidated sediment spread on a glass slide for petrographic microscopic analysis. Smear slides are useful for sediment classification and identification of any microfossils that are present in the core. In addition to the smear slides prepared by LacCore, three smear slides were made at UMKC, without optical cement or cover slide to allow scanning electron microscope (SEM) images to be taken to help identify diatoms present in multiple smear slides and diatoms smaller than visible under 10x magnification.

Visual descriptions of the cores include the location of sediment boundaries based on color change using the Munsell Soil Color Chart and description of sediment grain size and composition. Color and sediment descriptions were recorded every centimeter. These descriptions can be found in Appendix D. Cores are photographed to allow for correlation between units (Appendix E).

A 3.5 cm^3 subsample was taken every 5 cm along the length of the cores for grain-size analysis. Samples were weighed before and after drying 24 hours in an oven set at 105°C. The samples are then placed in 125 mL Nalgene bottles with a 1% Calgon solution and left for at least 24 hours to disperse the sediment into individual grains. Samples were then wet sieved through a sieve stack of 250 µm (≥ medium sand), 125 µm (fine sand), and 63 µm (very fine sand) mesh, and when dried, the sand-size fractions were weighed. Sediment below very fine sand (63 µm) was not retained, but the weight percent of this size fraction was calculated. The average grain-size weight percent values used in the unit descriptions were calculated by adding the weight percent values of all grain-size data together and then dividing the sum by the total number of samples in the unit. The grain-size data can be found in Appendix F.

X-Ray Fluorescence

X-ray fluorescence (XRF) was performed at the Large Lakes Observatory at the University of Minnesota-Duluth. The split cores were scanned at 1 cm increments for 60 seconds using the Cox Analytical Itrax XRF Core Scanner. The principle behind XRF is that a surface is saturated with X-rays, which then emit a secondary X-ray, characteristic of the element which emitted them. This secondary X-ray allows for the trends of elements to be plotted, permitting an approximate unitless concentration to be calculated and plotted (Marshall et al., 2012). XRF data are plotted in Excel and used to measure the elemental trends down the length of the cores. All XRF data was normalized by dividing each sample by the highest value/trend of each element in each core. Each core then had a scale from 0.0-1.0 for each element.

The elements focused on for this study include: aluminum (Al), silicon (Si), titanium (Ti), iron (Fe), and zirconium (Zr) that represent proxies for terrestrial sediment input; and sulfur (S), chlorine (Cl), calcium (Ca), bromine (Br), and strontium (Sr) that are derived from a marine source.

Terrestrial proxies act as indicators of land input into the sediments, such as large precipitation events that can lead to increased erosion and soil runoff from bedrock sources into the pond (e.g. Nearing et al., 2005). Changes in the watershed due to deforestation or other land use practices caused by humans may also increase terrestrial runoff (e.g. Brenner and Binford, 1988). Marine proxies act as indicators of seawater influx into the pond, such as storm surges that could breach the berm during large storm events, or may indicate a lagoonal environment.

For XRF terrestrial proxies into Guana Island Pond, aluminum and silicon were selected due to their abundance in igneous rocks. The bedrock of the island of Guana is part of the Necker Formation, and contains quartz-andesite tuffs and breccias with minor welded tuffs. There is also porphyritic basalt on the north end of the island, but it is not part of the Guana Island Pond watershed (Helsley, 1960). Titanium and zirconium were selected due to their high density, relative immobility, and concentration during transport via water or wind (e.g. Marshall et al., 2012), and the tendency of titanium to settle into clays and zirconium into silt to fine sands (Oldfield et al., 2003). Dellwig et al. (2001) indicate iron is an indicator of terrestrial runoff as opposed to seawater influence.

For XRF marine proxies, sulfur was selected due to seawater sulfate ion being the main source of sulfur (Dellwig et al., 2001). Chlorine was selected due to seawater, and subsequent evaporites, being the only source of chloride (Whitaker and Smart, 2007). A decrease in chlorine would indicate marine influence, as it would dilute the hypersaline chlorine concentrations normally found in the pond. Calcium was selected due to its increased presence in carbonate environments (Shamberger and Foos, 2004), such as the coral reefs in White Bay and North Bay, and its ability to act as a proxy for storm deposits. Bromine was selected due to its relatively high concentrations in seawater and saline lakes (approximately 65mg/l) and its extremely low concentrations in freshwater (Song and Müller, 1993), and strontium was selected due to the fact that concentrations are higher in seawater than freshwater (Reinhardt et al., 1998). Core GI12FP8 XRF data can be seen in Figures 3.3 and 3.4 as an example of elemental trends in Guana Island Pond. XRF data for each core analyzed can be found in Appendix G.

Shells and Microfossils

Sediment samples from wet sieving were viewed under 3x stereo microscope magnification. Visible microfossils from the 250 µm samples were picked and placed on microfossil microscope slides. Sediment samples from other wet-sieved size fractions were not analyzed. The percent of carbonate sediment and percent siliclastic sediment were

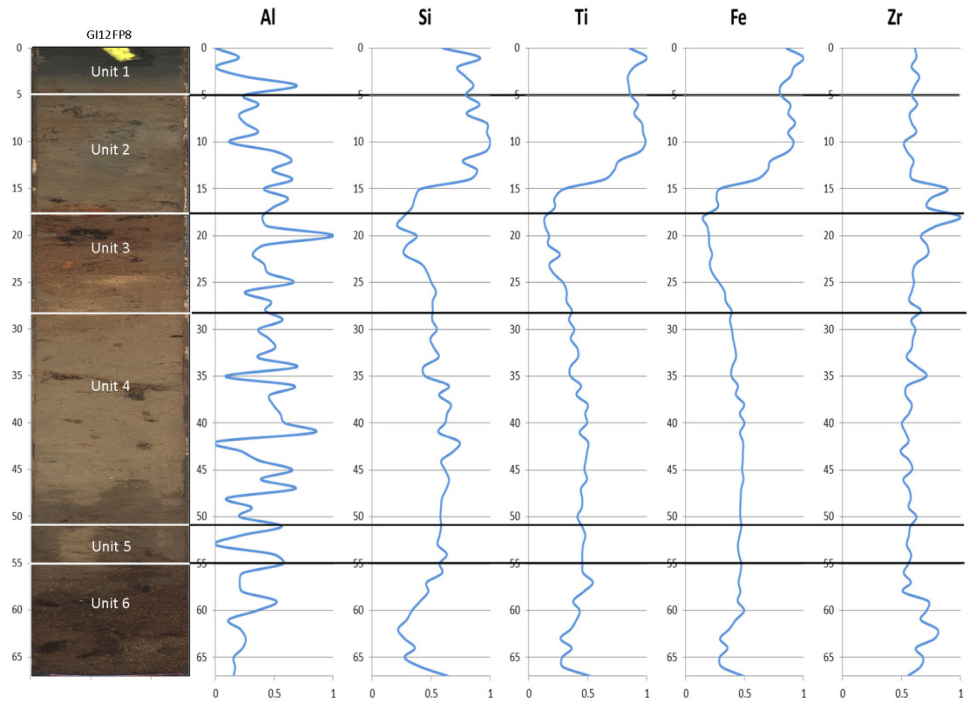

Figure 3.3 Core 8 Terrestrial XRF Graphs with depositional units marked.

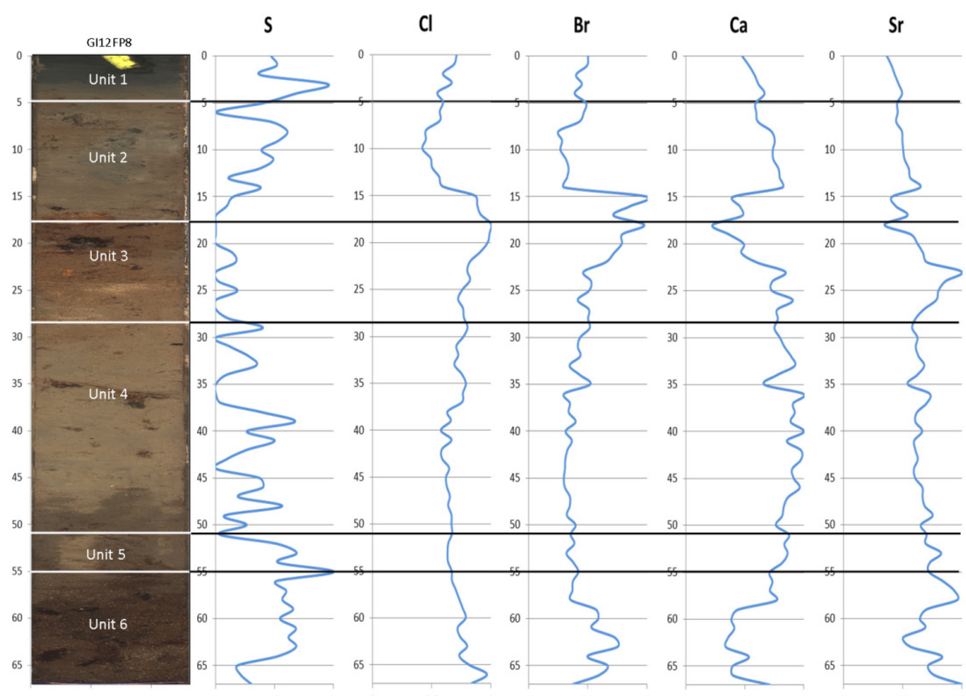

Figure 3.4 Core 8 Marine XRF Graphs with depositional units marked.

estimated visually under magnification. Matte grey sediment was classified as carbonate and and reflective/glossy sediment was classified as siliclastic based on a 5% HCl solution test and visual observations.

Microfossils from Guana Island Pond sediment were imaged using UMKC's Vega3 LM Tescan Scanning Electron Microscope. SEM irradiates the area to be analyzed with a beam of finely focused electrons in order to create data that can be interpreted as an image with visible depth of field (Goldstein et al., 2003). Images were taken using the secondary detector, rather than the primary detector, as contrast by topography was desired, as opposed to contrast by composition. SEM images can be found in Appendix H. Dr. Jeffery Stone from the Indiana State University Paleolimnology Laboratory was consulted to assist in diatom identification. The microfossil assemblages and photo plates can be found in Appendix I, and select microfossil SEM images can be found in Appendix H.

Smear slides were created by LacCore during the initial core splitting, cleaning, and imaging. Smear slides were remade for three samples containing an unidentified diatom, without using optical cement or cover slides. These smear slides were then viewed using a Nikon Optiphot-Pol microscope with a Lumenera camera, and areas with the unidentified diatom were circled directly on the slide. The slides were then examined using Tescan Vega 3 LMU scanning electron microscope, which allowed the diatom to be viewed with great depth of field. By using the secondary electron detector rather than the back-scattered electron detector, images with great depth of field were created. Two diatoms were located and photographed.

Microfossil Analysis

Micro fossils and shells are divided up into three groups: freshwater, brackish water, and marine species.

Freshwater species identified include *Chara fibrosa* oogonia (Figure 3.5), the diatom *Campylodiscus clypeus* (Figure 3.6), and the gastropod *Pyrgophorus platyrachis* (Figure 3.7). *Chara fibrosa* is a species of freshwater green algae (AlgaeBase), *Campylodiscus clypeus* is a species of diatom found in Units 3-5 that can live in both freshwater and marine environments (AlgaeBase), and *Pyrgophorus platyrachis* is a species of gastropod, closely related to the *Pyrgophorus parvulus,* which can live in fresh or brackish water (WoRMS).

The only exclusively brackish species identified during the study is the gastropod *Cerithideopsis costata* (Figure 3.8), which only one specimen was found (WoRMS).

Marine species identified include the diatom *Tryblionella compressa* (Figure 3.9), the gastropods *Pyrgophorus parvulus* (Figure 3.10) and *Cerithium lutosum* (Figure 3.11), and ostracods interpreted to be part of the *Cyprideis* sp., possibly *Cyprideis Americana and Cyprideis torosa* (Figure 3.12). *Tryblionella compressa* is a marine diatom found only in Unit 5/6 (AlgaeBase), *Pyrgophorus parvulus* is a gastropod found only in marine environments, *Cerithium lutosum* is an exclusively marine gastropod identified in only two specimens, *Cyprideis* sp. is a genus and *Cyprideis Americana* is a species of ostracods that can live in brackish to marine waters, and *Cyprideis torosa* is a species of ostracod that live in marine waters (WoRMS).

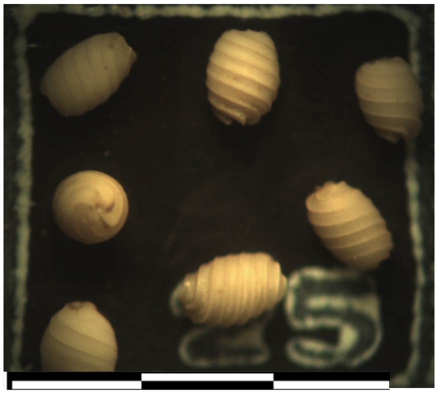

Figure 3.5 Freshwater algae *Chara fibrosa* oogonia. Scale = 3.0 mm.

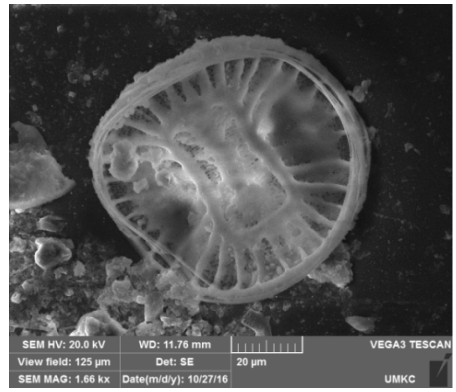

Figure 3.6 Marine or freshwater *Campylodiscus clypeus* diatom.

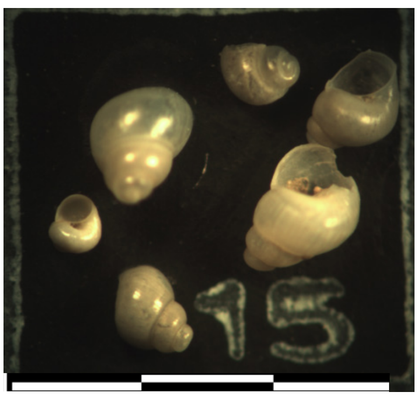

Figure 3.7 Brackish to freshwater *Pyrgophorus platyrachis* gastropod. Scale = 3.0 mm.

Figure 3.8 Brackish *Cerithideopsis costata* gastropod. Scale = 3.0 mm.

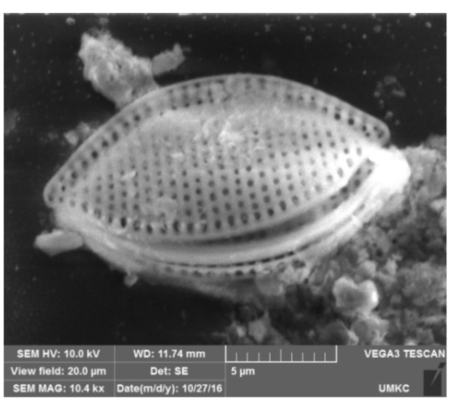

Figure 3.9 Marine *Tryblionella compressa* diatom.

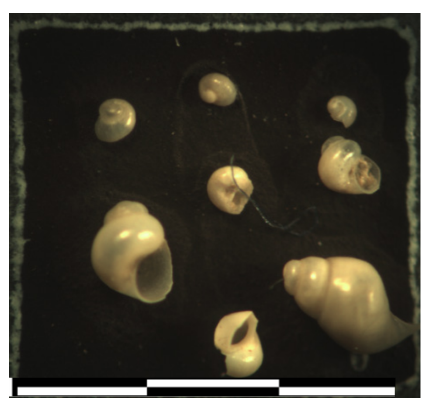

Figure 3.10 Marine *Pyrgophorus parvulus* gastropod. Scale = 3.0 mm.

Figure 3.11 Marine *Cerithium lutosum* gastropod. Scale = 3.0 mm

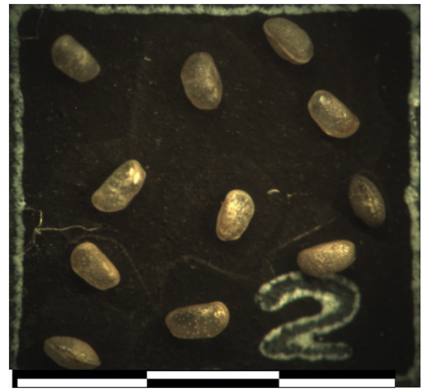

Figure 3.12 *Cyprideis* sp. ostracod. Scale = 3.0 mm.

Radiocarbon Analysis

Wood and peat fragments were collected for radiocarbon dating and sent to Lawrence Livermore National Laboratory for dating using Accelerator Mass Spectrometry (AMS). The age of the sample is based on ^{14}C having a half-life of 5,730 years. After the ^{14}C data was received, the data was calibratd. Calibration is necessary because atmospheric ^{14}C has not been constant over time. The CALIB software converts data from radiocarbon age to calibrated years by calculating the probability distribution of the sample's true age. By measuring the radiocarbon age of tree rings of known independently dated samples, calibrated ^{14}C values are obtained (Reimer et al., 2004). The calibration dataset used for the Guana Island Pond ^{14}C samples was the IntCal13 database. This was selected due to the Guana Island Pond samples being non-marine. For the Guana Island Pond samples, the calibration was based on tree-ring ^{14}C measurements (Stuiver and Reimer, 1993). This data can be found in Table 3.2 and Appendix J.

A sedimentation rate was calculated by plotting the median probability age of the two radiocarbon dates at depths of 28 cm and 63 cm, respectively. A least squares regression line was plotted to the data (Figure 3.13). The data show a 0.5 mm/yr average sediment accumulation rate. Core 6 extends an additional 45 cm below the radiocarbon date of 1307 ± 46 yr BP in core 7. Using a sedimentation rate of 0.5 mm/yr and a core thickness of 450 mm, the age at the base of the deepest core, core 6, at 110 cm, is approximately 900 yr older than the radiocarbon date at ~63 cm in core 7. Thus, the age of the oldest sediment recovered in this study is likely 2200 yr BP.

Table 3.2: Radiocarbon sample number, type, depth, and age. Additional information can be found in Appendix J. *There was an error in the ^{14}C reporting. The updated age is in the table below.

Sample No.	Sample Type	Depth (cm)	^{14}C Age	Calibrated Age ± 2σ	Calendar Age AD ± 2σ
GI12FP8	wood	27-28.5	805 ± 25*	720 ± 40 yr BP	1230 ± 40
GI12FP7	wood	62-65	1380 ± 35	1307 ± 46 yr BP	643 ± 46

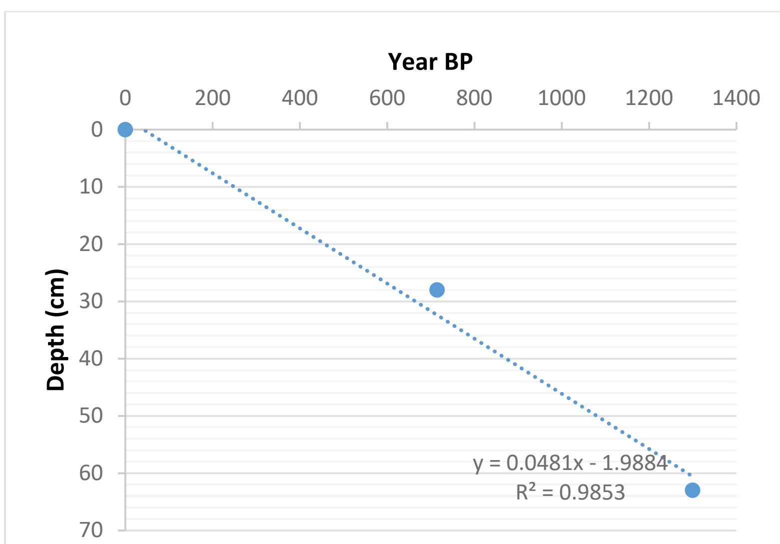

Figure 3.13 Sedimentation rate plot for samples GI12FP8 and GI12FP7.

CHAPTER 4

RESULTS

Six depositional units were defined in the core stratigraphy based on sediment composition, color, grain-size weight percent, age, elemental analyses, and shell and microfossil identification (Table 4.1). Cores 6, 7, 8, and 10 are aligned along an approximately east-west transect (see Figure 3.1 for location), perpendicular to the shoreline of the abandoned sugar mill on the east side of Guana Island Pond (Figure 2.11).

<u>Unit Descriptions</u>

Unit 6

Unit 6 is a very dark grey to black, medium to fine sand unit with organics. The maximum thickness of Unit 6 is 28 cm in Core 10. The unit was encountered at the base of cores 7, 8, and 10, and is believed to be interbedded with Unit 4 in core 8 (Figure 4.1). The average grain-size weight percent for Unit 6 is 30% silt/clay, 6.3% very fine sand, 31% fine sand, and 33% coarse to medium sand (Table 4.1). Unit 6 is interpreted as a shallow marine storm deposit based on the uniform coarseness and broken fossils found in the unit. XRF of Unit 6 shows low levels of Si, Ti, and Fe and high levels of Cl, Ca, Sr, and Br that suggest a marine water input; and high levels of zirconium are potentially due to Unit 6 being predominantly sand. Shells found in Unit 6 include *Cerithium lutosum,* a marine gastropod identified in Unit 6 of Core 10.

Table 4.1 The six depositional units of Guana Island Pond with defining features and associated radiocarbon ages.

Radiocarbon Age (yr BP)	Unit	Thickness (cm)	Description	Grain Size (average wt %)	Elemental Analysis	Depositional Environment
	1	4 cm to 9 cm	Very dark grey to dark greyish brown firm clay to silty clay to silt, coarsening with depth.	93% silt/clay, 1.9% very fine sand, 2.9% fine sand, 1.9% medium sand	High Sr, Ti, Fe	Fresh/marine mixed shallow water
	2	8 cm to 13 cm	Very dark grey to dark grey clay to silty clay to silt with fine angular sand, coarsening with depth.	93% silt/clay, 2.9% very fine sand, 2.3% fine sand, 2.0% medium sand	High Sr, Ti, Fe, Ca; low Cl, Br	Fresh/ Brackish shallow water
720 ± 40 yr BP	3	2 cm to 7 cm	Dark grey to very dark greyish brown sandy silt with organics, coarsening with depth.	78% silt/clay, 7.2% very fine sand, 3.7% fine sand, 10% medium sand	Zr decreases with depth; high Cl, Br; low Ca, Sr but increases with depth	Marine shallow water
	4	20 cm to 40 cm	Dark grey to dark olive grey clayey silt to silt with interbedded carbonate facies and organics.	91% silt/clay, 3.8% very fine sand, 3.1% fine sand, 2.4% medium sand	Low Cl, Br; High Ca, Sr, Si	Fresh shallow water; carbonate facies
1307 ± 46 yr BP	5	4 cm to 44 cm	Dark grey to black organic sandy silt, coarsening and increased organics with depth. Oldest unit in Cores 6B and 6C.	85% silt/clay, 3.8% very fine sand, 5.1% fine sand, 5.4% medium sand	Low Fe; mid-level Zr; pulses in Cl, Ca, Br, Sr, Si, Ti; high S	Marine shallow water
	6	8 cm to 28 cm	Very dark grey to black medium sand with organics. Oldest unit in Cores 7, 8, and 10.	30% silt/clay, 6.3% very fine sand, 31% fine sand, 33% medium sand	Low Si, Ti, Fe; High Cl, Zr, Ca, Sr, Br	Marine shallow water/ storm deposit

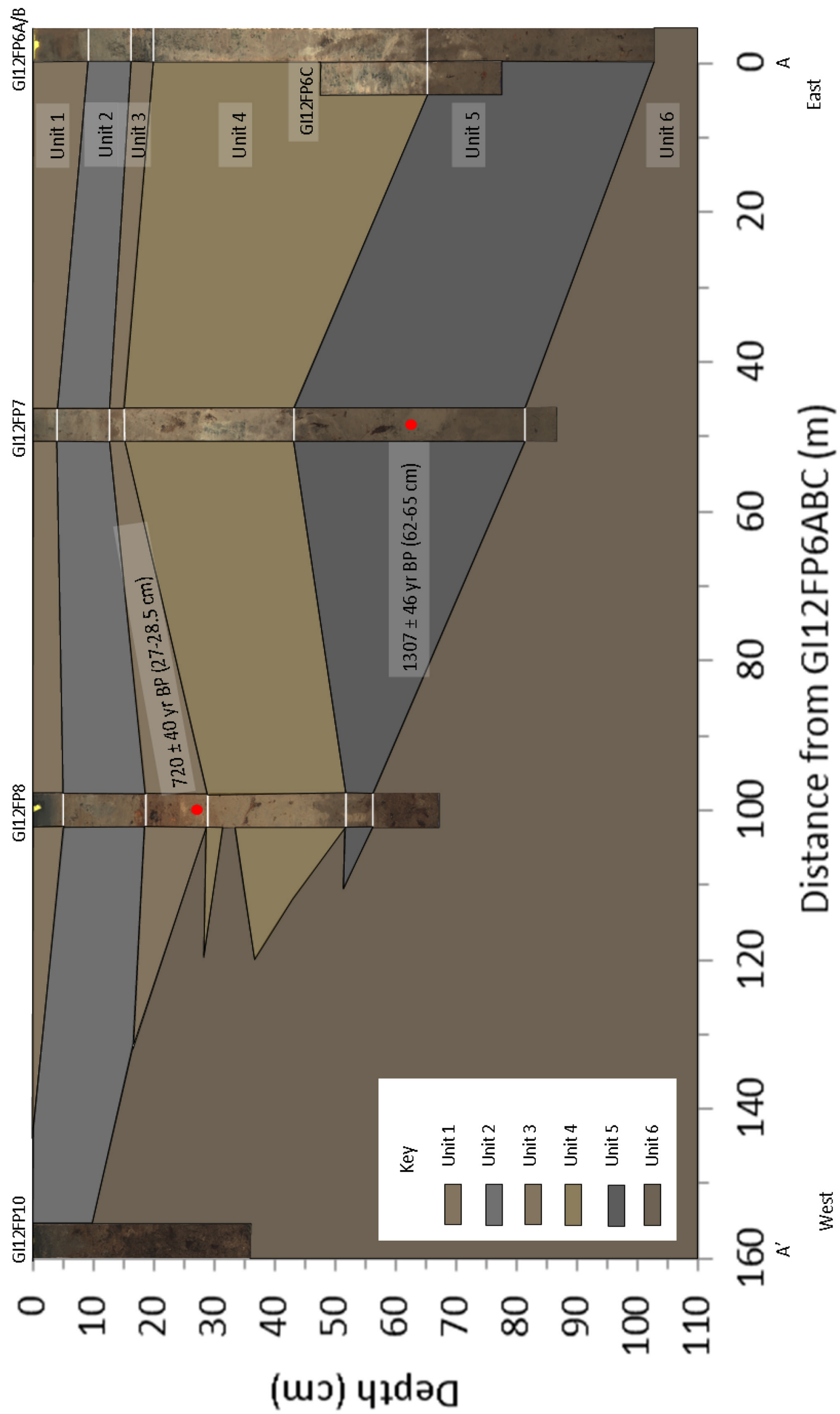

Figure 4.1 Cross section of east-west transect of cores 6A, 6B, 6C, 7, 8, and 10 with vertical exaggeration of approximately 10x. The cross section reflects the correct placement of core GI12FP6C adjacent to core GI12FP6B rather than below it. Red dots mark ^{14}C locations.

Unit 5

Unit 5 is a dark grey to black, carbonate silty clay with approximately 10% to 25% sand. The maximum thickness of the unit is 44 cm and the unit thins westward from 6B/C. Unit 5 is approximately 90% carbonate sand and 10% siliclastic sand, and a spot test using 5% HCl solution confirmed the presence of calcium carbonate in the sand. The average grain-size weight percent for Unit 5 is 85% silt/clay, 3.8% very fine sand, 5.1% fine sand, and 5.4% coarse to medium sand.

Microfossils found in Unit 5 include diatoms identified as likely being *Campylodiscus clypeus* and *Tryblionella compessa* (Dr. Jeffery Stone, Indiana State University, pers. comm.); 142 intact and 228 half ostracods identified as likely being in the *Cyprideis* sp., possibly *Cyprideis americana* (Dr. Andrew Cohen, University of Arizona, pers. comm.) or *Cyprideis torosa*; and ten charophyte oogonia identified as likely being *Chara fibrosa* (AlgaeBase), an exclusively freshwater species. Macrofossils found in Unit 5 include 52 gastropods identified as likely being *Pyrgophorus platyrachis* or *Pyrgophorus parvulus* [World Register of Marine Species (WoRMS)].

XRF of Unit 5 shows high levels of Ca, Sr, and S and low levels of the terrestrial elements. Unit 5 is interpreted as shallow marine water due to the presence of the diatom *Tryblionella compressa,* which can only live in a marine environment. In addition, low levels of Fe combined with high levels of S further indicate a marine environment. Unit 5 has a wood age of 1307 ± 46 yr BP. It is likely that the gastropods found in Unit 5 belong to *Pyrgophorus parvulus,* a marine species, rather than *Pyrgophorus platyrachis,* a fresh to brackish water species. Additionally, the presence of *Chara fibrosa* oogonia suggests some mixing of freshwater.

Unit 4

Unit 4 is a dark grey to dark olive grey, carbonate mud with interbeds of fine-to-medium-grained sand layers and organic material. The maximum thickness of the unit is 40 cm. Sand is predominantly carbonate sediment (85%) with 15% siliclastic sand. The average grain-size weight percent for Unit 4 is 91% silt/clay, 3.8% very fine sand, 3.1% fine sand, and 2.4% coarse to medium sand.

Microfossils found in Unit 4 include the diatom identified as likely being the fresh or marine water diatom *Campylodiscus clypeus*; 77 intact and 200 half ostracods identified as likely being in the *Cyprideis* sp., possibly *Cyprideis americana* or *Cyprideis torosa*; and 125 freshwater charophyte oogonia identified as likely being *Chara fibrosa* (AlgaeBase). Macrofossils found in Unit 4 include 124 gastropods identified as likely being *Pyrgophorus platyrachis* or *Pyrgophorus parvulus* (WoRMS).

XRF of Unit 4 shows low levels of Cl and Br, suggesting low input of saline water. High levels of Ca and Sr indicate the presence of carbonate mud and microfossils. Si present throughout the unit may indicate the presence of diatoms or siliclastic sand.

Unit 4 is interpreted as shallow fresh water due to the presence of 125 *Chara fibrosa* oogonia, indicating a freshwater environment, as *Chara fibrosa* is an exclusively freshwater species. The diatom *Tryblionella compressa*, which can live only in a marine environment, was absent in Unit 4, and the diatom *Campylodiscus clypeus* was present in Unit 4, and can live in either fresh or marine waters. The 124 gastropods were found in Unit 4 and are likely *Pyrgophorus platyrachis,* a fresh to brackish species, rather than the marine *Pyrgophorus parvulus*. XRF of Unit 4 shows low levels of chlorine and bromine combined with the relatively high levels of silicon indicate a freshwater environment for Unit 4, indicating a period of high precipitation and subsequent terrestrial erosion.

Unit 3

Unit 3 is a thin (2-10 cm) dark grey, silt to sandy silt, and is approximately 90% carbonate sand and 10% siliclastic sand. The average grain-size weight percent for Unit 3 is 78% silt/clay, 7.2% very fine sand, 3.7% fine sand, and 10% coarse to medium sand.

Microfossils found in Unit 3 include the diatom identified as likely being the fresh or marine water diatom *Campylodiscus clypeus*; six intact and ten half ostracods identified as likely being in the *Cyprideis* sp., possibly *Cyprideis americana* or *Cyprideis torosa*; and two freshwater charophyte oogonia identified as likely being *Chara fibrosa* (AlgaeBase). Macrofossils found in Unit 3 include 13 gastropods identified as likely being *Pyrgophorus platyrachis* or *Pyrgophorus parvulus* (WoRMS).

XRF of Unit 3 shows high levels of Cl and Br, initially high levels of Zr and low levels of Ca and Sr. Zr decreases with depth, potentially indicating a high level of sand in the upper portion of Unit. Ca and Sr increase with depth towards the Unit 4 boundary.

Unit 3 is interpreted as shallow marine water due to the presence of only two *Chara fibrosa* oogonia and only 13 gastropods, likely *Pyrgophorus platyrachis* or *Pyrgophorus parvulus. P. platyrachis* lives in fresh to brackish water, and *P. parvulus* lives in marine water, making it likely that the gastropods found in Unit 3 belong to *Pyrgophorus parvulus* rather than *Pyrgophorus platyrachis*. The diatom *Campylodiscus clypeus* was present in Unit 3, and can live in either fresh or marine waters. The limited number of *Chara fibrosa* oogonia and gastropods suggest a subtidal to intertidal marine environment for Unit 3, with a wood age of 720 ± 40 yr BP.

Unit 2

Unit 2 is a thin (8-13 cm) dark grey silty clay with fine angular sand, coarsening with depth, and is approximately 85% carbonate sand and 15% siliclastic sand. The average grain-size weight percent for Unit 2 is 93% silt/clay, 2.9% very fine sand, 2.3% fine sand, and 2.0% coarse to medium sand.

Microfossils found in Unit 2 include 29 intact and 60 half ostracods identified as likely being in the *Cyprideis* sp., possibly *Cyprideis americana* or *Cyprideis torosa* and 61 charophyte oogonia identified as likely being *Chara fibrosa* (AlgaeBase). Macrofossils found in Unit 2 include 112 gastropods identified as likely being *Pyrgophorus platyrachis* or *Pyrgophorus parvulus* (WoRMS) and one gastropod identified as likely being *Cerithideopsis costata* (WoRMS).

XRF of Unit 2 shows high Ca and Sr from carbonate sand and mud, high Si, Ti, and Fe from terrestrial runoff, and low levels of Cl and Br indicate limited saltwater input.

Unit 2 is interpreted as shallow fresh to brackish water due to the presence of 61 *Chara fibrosa* oogonia and 112 gastropods, likely *Pyrgophorus platyrachis* rather than the marine *Pyrgophorus parvulus.* There was also one gastropod identified as likely being

Cerithideopsis costata in Unit 2, which lives exclusively in a brackish environment. Minimal marine proxies and elevated terrestrial proxies further support the fresh to brackish water interpretation of Unit 2.

Unit 1

Unit 1 is the upper 4-9 cm in cores GI12FP6A, GI12FP7, and GI12FP8 and is a dark greyish brown, firm silty clay, and is approximately 85% carbonate sand and 15% siliclastic sand. The average grain-size weight percent for Unit 1 is 93% silt/clay, 1.9% very fine sand, 2.9% fine sand, and 1.9% coarse to medium sand.

Microfossils found in Unit 1 include 7 intact and 25 half ostracods identified as likely being in the *Cyprideis* sp., possibly *Cyprideis americana* or *Cyprideis torosa* and ten charophyte oogonia identified as likely being *Chara fibrosa* (AlgaeBase). Macrofossils found in Unit 1 include 34 gastropods identified as likely being *Pyrgophorus platyrachis* or *Pyrgophorus parvulus* (WoRMS).

XRF of Unit 1 shows high levels of Sr, Ti, Fe, Zr, Si, and Ca; and mid-range levels of Cl. High levels of marine proxies indicate carbonates, and high levels of terrestrial proxies indicate terrestrial runoff from precipitation. The prevalence of both terrestrial and marine XRF proxies indicate a unit of mixed freshwater and marine deposition, and is therefore interpreted as a shallow fresh/marine mixed unit. Unit 1 was classified as mixed due to the presence of 34 gastropods, likely *Pyrgophorus platyrachis* or *Pyrgophorus parvulus. P. platyrachis* lives in fresh to brackish water, and *P. parvulus* lives in marine water, making it equally likely that the gastropods found in Unit 1 could belong to either species. There were also 10 *Chara fibrosa* oogonia in Unit 1, indicating a more freshwater environment.

CHAPTER 5

DISCUSSION

Six depositional units interpreted from the sediment core data are used to investigate and define the change in climate and land use on Guana Island over time. All units coarsen westward, with core 6 containing the smallest weight percent of coarse to medium sand, and core 10 containing the highest weight percent of coarse to medium sand. The coarsening westward is likely due to berm-breaching storm events.

During the early to mid-Holocene locations at mid latitudes appear to have been warmer in the past 5,000 years, while at lower latitude locations, temperature averages were cooler (Rimbu et al., 2003). In the Caribbean, wet conditions persisted through the mid-Holocene (Hodell et al., 1991) and were replaced by drier conditions in the late Holocene (Haug et al., 2001), due to a shift in the position of the Inter-Tropical Convergence Zone (ITCZ). When the ITCZ is in the northward position, it causes Belize, Saint-Martin, Barbados, and the Cariaco Basin to be humid and Haiti to be dry. This is reversed when the ITCZ is in the southward position; when Haiti is humid and Belize, Saint-Martin, Barbados, and the Cariaco Basin are dry (Figure 5.1, Malaizé et al., 2011).

Tedesco and Thunell (2003) present data on increases in planktonic foraminifera $\delta^{18}O$ isotopes leads to an increase in salinity and decreases in sea surface temperature. These increases are centered at 5,500 yr BP, and coincide with development of arid conditions in the Caribbean region and the end of the "African humid period", which indicates a global drying of the northern tropics at the time.

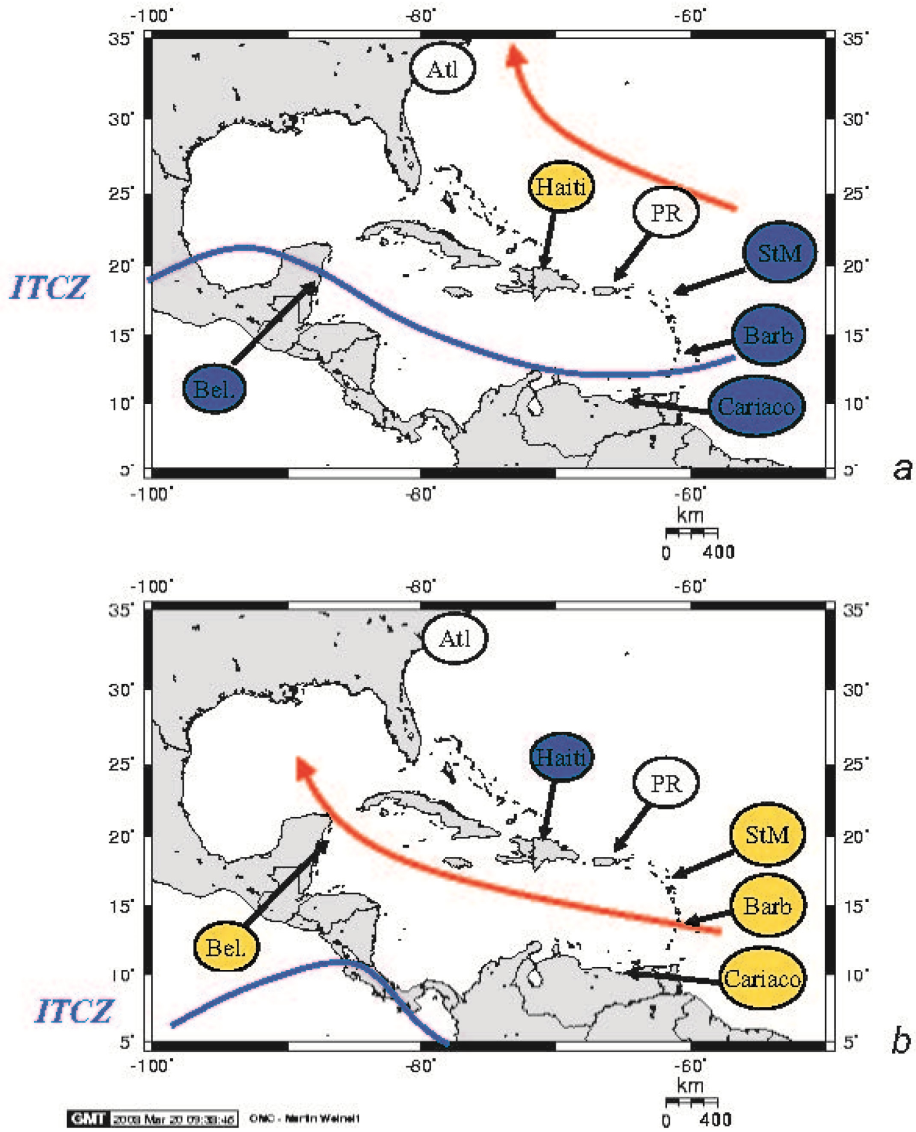

Figure 5.1 Northward (a) and southward (b) positions of the Inter-tropical Convergence Zone (ITCZ). Dark grey/blue indicates humid conditions and light grey/yellow indicates dry conditions. Belize (Bel.), US Atlantic Coast (Atl), Puerto Rico (PR), Saint-Martin (StM), Barbados (Barb). (Malaizé et al., 2011).

During the drying of the northern tropics, wetter conditions were occurring in the Altiplano of Bolivia/Peru, which are attributed to the southern positioning of the ITCZ. This placement would have resulted in decreased precipitation and increased strength of the trade winds in the Caribbean while increasing rainfall over the Altiplano (Tedesco and Thunell, 2003).

During boreal winter and spring, the ITCZ is in its most southerly position; rainfall is at a minimum and strong easterly winds cause intense upwelling of deep, nutrient rich, cold seawater along the Venezuela coast. When the ITCZ moves north during the boreal summer, the trade winds diminish, upwelling ceases, and precipitation increases. Therefore, when the Cariaco Basin region or northern tropics are dry, the southern tropical region of South America is wet, and vice versa (Tedesco and Thunell, 2003).

In their study of the planktonic foraminifera $\delta^{18}O$ isotope record, Tedesco and Thunell (2003) determined the highest salinities and coolest ocean temperatures are recorded from 6,000 to 5,000 yr BP, followed by a long term warming and freshening. The largest increase in $\delta^{18}O$ planktonic foraminifera that they found occurred from 3,500 to 3,000 yr BP, which coincides with the aridity of the Caribbean (Hodell et al., 1991; Haug et al., 2001). In the Cariaco basin and northern Amazon the climate became progressively drier since the mid-Holocene due to a southward migration of the ITCZ (Haug et al., 2001). Decreased metal concentrations in the Cariaco Basin sediments correlate to less runoff from precipitation and drier conditions. Cooler and drier conditions developed in the Cariaco Basin from 3,800 to 3,500 yr BP. In the Kilimanjaro ice core $\delta^{18}O$ record at a latitude of 3°05’S suggests a period of most severe drought in tropical Africa during historical/human times (Thompson et al., 2002). Pollen records from Lake Miragoane, in Haiti indicate the lake filled in the early Holocene and remained high until the development of arid conditions at approximately 3,400 yr BP (Hodell et al., 1991).

Tedesco and Thunell (2003) interpreted that an increase in seasonality and a southward displacement of the ITCZ combined with an intensification of the South

American summer monsoon would have changed the moisture balance of the Caribbean region.

Malaizé et al. (2011) studied cores from the Grand-Case Pond, a shallow ~1.5-m-deep pond isolated from the sea by sand berm in Saint-Martin (Malaizé et al., 2011), making it very similar to Guana Island Pond. Preliminary sedimentological study on the latest Grand-Case core showed three different phases: a dry period from 4,500 to 2,350 yr BP, indicated by carbonate mud deposition and gypsum layers; a wet phase from 2,350 to 1,100 yr BP, indicated by pyrite-rich organic mud in connection with high lake levels; and an overall dry phase from 1,100 yr BP to present, indicated by carbonates and detrital inputs due to human activities (Malaizé et al., 2011).

Malaizé et al. (2011) compiled regional data from multiple sites in the Caribbean in order to create a model for the paleoclimate pattern in the eastern Caribbean islands. On a regional scale, there are parallels between the Grand-Case Pond data and those found elsewhere in the Caribbean, such as Barbados, the Cariaco Basin, Belize, and Haiti. In the Cariaco Basin, bulk titanium content is linked with increased rainfall and consequent increase in erosion. Low Ti values are thus correlated to droughts. In the Cariaco Basin, periods of increased precipitation occurred between 3,800 to 2,600 yr BP following droughts between 2,600-1,250 yr BP and a wetter climate from 1,250 yr BP to present (Haug et al., 2003). Tedesco and Thunell's (2003) data on planktonic foraminifera $\delta^{18}O$ isotope values show high frequency of arid conditions between 3,800 to 3,200, 3,000 to 2,800, and 1,200 to 800 yr BP. High Ti levels in the Cariaco basin coincide with the drier evaporite layers found in the Grand-Case sediments (Malaizé et al., 2011).

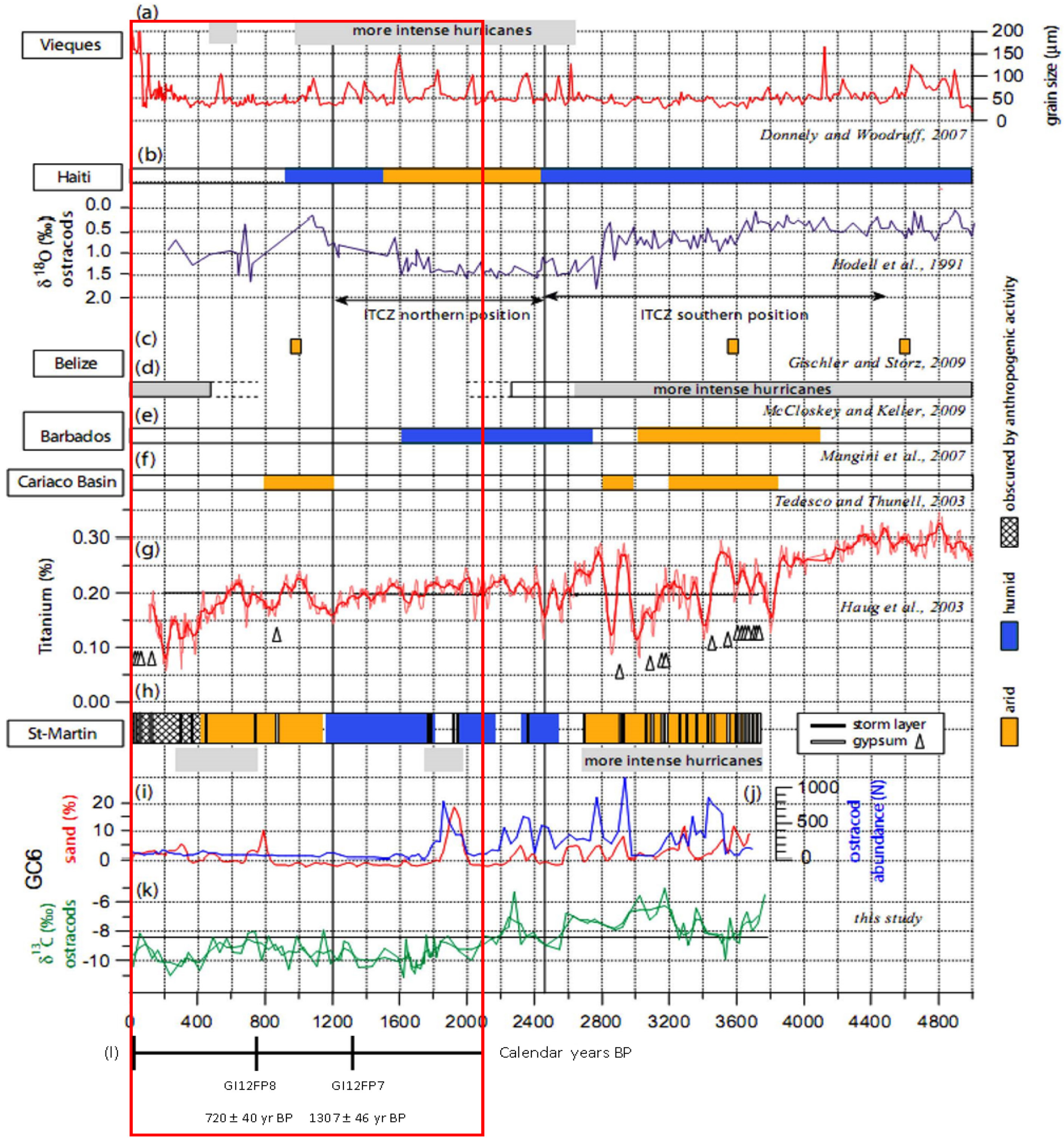

Figure 5.2 Compilation of Caribbean climate studies (Malaizé et al., 2011). (a) shows grain size data from Puerto Rico (Donnelly and Woodruff, 2007), (b) shows ostracod isotope composition from Lake Miragoane, Haiti (Hodell et al., 1991), (c) shows climate data from fossil corals in Belize (Gischler and Storz, 2009), (d) shows hurricane strike records from Belize (McCloskey and Keller, 2009), (e) shows stalagmite data from Barbados (Mangini et al., 2007), (f) shows Cariaco Basin climate records (Tedesco and Thunell, 2003), (g) shows Cariaco Basin Ti levels (Haug et al., 2003), (h) shows hydrological balance and hurricane history of Saint-Martin (Malaizé et al., 2011), (i) shows grain size in core GC6 from Saint-Martin (Malaizé et al., 2011), (j) shows ostracod abundance in core GC6 from Saint-Martin (Malaizé et al., 2011), and (k) shows carbon isotope composition of ostracods from GC6 from Saint-Martin (Malaizé et al., 2011). From Malaizé et al., 2011. (l) shows Guana Island Pond study data. Box indicates dates present in Guana Island Pond samples and radiocarbon ages.

Pollen data and fossil coral reefs from the Turneffe Islands in Belize and speleothems in Barbados also indicate a drier climate between 3,900 and approximately 3,200 yrs B.P. (Wooller et al., 2009; Gischler and Storz, 2009; Mangini et al., 2007). Ostracod data from Lake Miragoane, Haiti suggests the opposite climate as those determined for Barbados. In Lake Miragoane, ostracod data shows the lowest $\delta^{18}O$ levels between 7,000 and 5,300 yr BP (Hodell et al., 1991), while the Barbados speleothem data shows the highest $\delta^{18}O$ levels (Mangini et al., 2007). Low $\delta^{18}O$ levels relative to $\delta^{16}O$ levels indicate warm climates, whereas high $\delta^{18}O$ levels relative to $\delta^{16}O$ levels indicate cold climates. This contrast can be explained by the seasonal shifts in the ITCZ. A more stable northern position of the ITCZ from 2,400 to 1,250 yr BP could have maintained a long-lasting humid climate in the southern Caribbean, but not in Haiti (Malaizé et al., 2011). This compiled data can be seen in Figure 5.2.

The storm deposit interpreted in Guana Island Pond Unit 6 predates Unit 5's age of 1307 ± 46 yr BP. Using a sedimentation rate of 0.5 mm/yr, the base of Unit 6 likely date to 2200 to 1300 yr BP. This unit may correlate to the hurricane sand layers referenced by Malaizé et al. (2011) from the Saint-Martin Island core data. These authors identify hurricane landfalls via sand layers within the lake mud, which are interpreted as coastal sand barrier over wash. Unit 6 in Guana Island Pond appears to correlate with a warmer wetter climate, interpreted on Saint-Marten, approximately 2,000 yr BP. It is also possible that during the time of deposition of Unit 6, Guana Island Pond was still a tidal estuary partially open to White Bay.

Shallow marine or intertidal lagoonal conditions are interpreted for Guana Island Pond Unit 5, which were deposited ca. 1300 yr BP. These data suggest a cooler, drier climactic time period with possible hypersaline lake conditions that are supported by high levels of elemental bromine, strontium, and chlorine, and low levels of iron, titanium, and silicon. Guana Island Pond Unit 5 does not appear to have a high input of terrestrial elements, which suggest minimal runoff and minimal anthropogenic disturbance of the watershed.

Shallow freshwater lacustrine conditions prevailed in Guana Island Pond sometime between 1200 at 800 yr BP based on low levels of elemental chlorine and bromine and an abundance of freshwater algae. Relatively high levels of silicon also suggest an increase in watershed erosion (Figures 3.3 and 3.4). Precipitation rates were likely higher than evaporation rates, thus enabling a freshwater environment. Based on $\delta^{18}O$ ostracod levels from Lake Miragoane, Haiti, Hodell et al. (1991) interpret a brief period of wetter conditions, from 1500 to 900 yr BP, which correlates to the age of Unit 4 on Guana Island Pond. Brenner and Binford (1988), in discussing Lake Miragoane, suggest that the pre-history of the region is poorly known, but ceramic evidence indicates the presence of Arawak settlements as early as 600 CE (1350 yr BP), with two additional episodes of Arawak occupation that date to between 900 (1050 yr BP) and 1500 CE (450 yr BP). If Arawak occupation was occurring in the Caribbean as early as 600 CE (1350 yr BP), it is likely that Guana Island Pond was used as a viable source of potable water for the pre-Columbian native peoples.

By about 800 yr BP, Guana Island Pond appears to have been dominated by shallow marine water conditions based on increases in calcium, strontium, chlorine, and bromine, and low levels of titanium, zirconium, and lead. Data from Lake Miragoane indicate that following a brief wet period that occurred from approximately 1500 to 900 yr BP, there was a progressive increase in the ratio of evaporation to precipitation, indicating a cooler drier climate for Unit 3.

Since about 700 yr BP or later, Guana Island Pond has been a fresh to brackish water lake environment. Elemental data from Unit 2 shows high levels of chlorine and calcium which would normally indicate a marine environment. However, the repeatedly high levels of silicon, titanium, and iron indicate high inputs of terrestrial runoff. The presence of plentiful freshwater *Chara fibrosa* oogonia supports a freshwater environment for Unit 2. It is likely that during this time, there was marginally more precipitation than evaporation. These lacustrine sediments correlate to the arrival or Europeans (ca. 500 yr BP) to the Caribbean region. High levels of terrestrial derived elements to the lake suggest an increase in erosion and soil runoff that was likely caused by extensive land clearing beginning with the Quaker settlement around 300 yr BP.

The uppermost layer in Guana Island Pond, represented by Unit 1, is influenced by constant marine water inflow into Guana Island Pond from the reverse osmosis plant and local runoff. High levels of terrestrial elemental proxies in sediments of Unit 1 are likely from 20th century land clearing and development. The depositional environment of Unit 1 has nearly an equal ratio of evaporation to precipitation, thus maintaining marine to brackish water conditions as measured in October 2012.

CHAPTER 6

CONCLUSION

This study focused on interpreting the sedimentary record of cores extracted from Guana Island Pond located on the southwest portion of Guana Island in the British Virgin Islands (BVI). The lake is a eutrophic pond covering an area of about 1.9 hectares. Itis surrounded on the west, north, and east by mountains that present a viable source for terrestrial runoff into the pond. The main objective of this study of cores from Guana Island Pond is to determine how the environment has changed on the island over the past. From the sediment analyses of sediment from four shallow (15-100 cm) cores from the lake, six stratigraphic units were defined based on the grain-size, elemental concentration, and micro- and macrofossil identifications. A sedimentation rate of 0.5 mm/yr was calculated for the Guana Island Pond cores within a tidal estuary.

The oldest sediment from this study (Unit 6), deposited ca 2200 yr BP suggests that the island was dominated by storm deposit. The climate was warmer and wetter, as evident at other paleoclimate sites at this latitude in the Caribbean.

Overlying the storm deposits are shallow marine sediments (Unit 5), deposited ca 1307 ± 46 yr BP. These data correlate to a regional cooler and drier time period with more evaporation than precipitation.

Analysis of Unit 4 sediment from Guana Island Pond support a shallow freshwater environment of the lake during 1200 to 800 yr BP. This interpretation is supported by low levels of chlorine and bromine combined with relatively high levels of silicon, indicating the rate of precipitation exceeds evaporation. The timing of migration of pre-Columbian native peoples into the Caribbean islands is unknown. Various lines of evidence suggest that by 600 CE (1350 yr BP), native peoples were in the Lesser Antilles and possibly utilizing Guana Island Pond as a viable source of potable water. These data correlate to a brief (1500 to 900 yr BP) wet period documented at Lake Miragoane in Haiti.

Around 800 yr BP, Guana Island Pond reverted to shallow marine conditions for the deposition of Unit 3. These data correlate to a progressive increase in the ratio of evaporation to precipitation in Haiti after 900 yr BP.

By 800 yr BP (Unit 2) the lake becomes fresh to brackish. The repeatedly high levels of silicon, titanium, and iron indicate a freshwater environment. It is likely that during the time of deposition, there was marginally more precipitation than evaporation. It is possible that Unit 2 dates back to European arrival and conquest of the Caribbean, which could account for the high levels of terrestrial derived elements, due to land clearing and soil erosion.

The uppermost layer (Unit 1) represents mixed fresh, brackish, and marine conditions. Sedimentation is currently controlled by constant marine water inflow into Guana Island Pond from the reverse osmosis plant that was installed on the island in 1990. Storm overwash also occurs. It is likely that the depositional environment of Unit 1 has a nearly equal ratio of evaporation to precipitation.

Based on the depositional environments defined in Units 1-6 in Guana Island Pond, the lake was once a tidal estuary before becoming isolated from White Bay. It could have been a viable source of potable fresh water for pre-Columbian native peoples and early European settlers ca 1300 to 800 yr BP. Paleolimnological analyses of soft sediment cores from Guana Island Pond show the paleoenvironmental changes the pond has undergone throughout six depositional units; from a tidal estuary to an inland pond.

APPENDIX A

GEOLOGIC MAP OF GUANA ISLAND (HELSLEY, 1960)

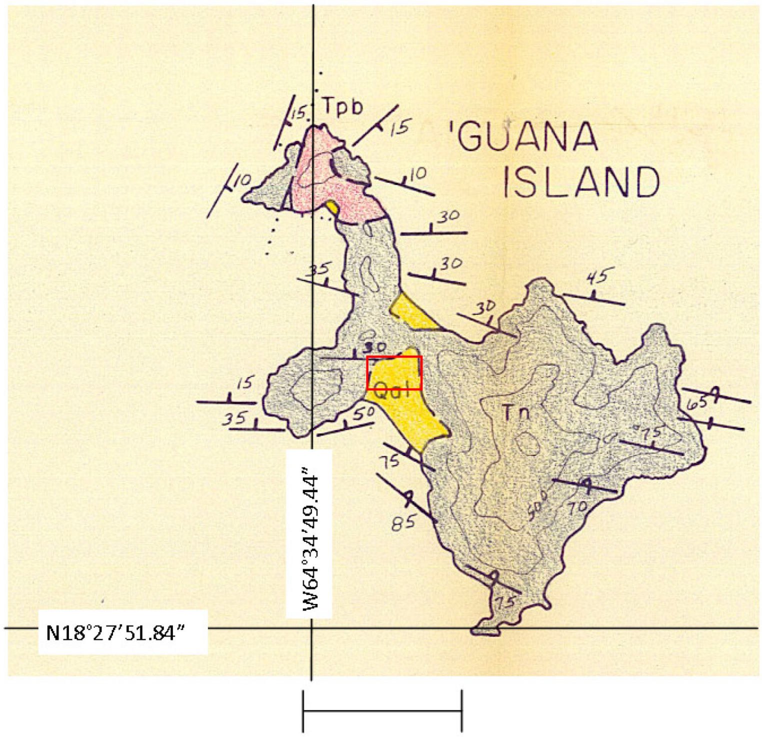

1 km
(box marts approximate location of Guana Island Pond)

Geologic Map

British Virgin Islands

Geology by C.E. Helsley (1960)

Qal: Alluvium: Valley fill, Beach rock, and Mangrove Deposits (recent)

Tn: Necker Formation: Quartz-andesite tuffs and Breccias with minor Welded Tuffs (Late Eocene)

Tpb: Porphyritic Basalt (Middle Eocene)

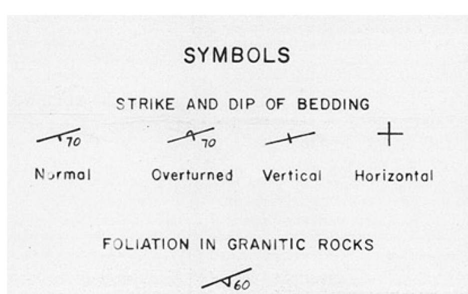

APPENDIX B
FIELD NOTES ON CORE COLLECTION

Core	UTM	Barrell Length	Recovered	Percent Recovered	Distance from GI12FP6	Notes
GI12FP1	20Q 0333592 2043724	not recorded	not recorded	not recorded	135 m to the WSW	
GI12FP2	20Q 0333667 2043733	not recorded	not recorded	not recorded	75 m to the SW	core was compressed
GI12FP3	20Q 0333580 2043713	not recorded	not recorded	not recorded	150 m to the WSW	
GI12FP4	20Q 0333734 2043737	125cm	73cm	58%	67 m to the SE	bent upper tube when pushing in
GI12FP5	20Q 0333709 2043757	125cm	57cm	45%	43 m to the SSE	piston slipped. First 15m from bank, 20cm deep layer of organics; under organics roughly 5cm sandy gravel with some larger rocks, starts at 20cm depth. 15-30m from bank black organics layer thins to roughly 10cm, sand layer gets less gravelly and firmer, water depth shallows. 30-45m from bank, black organic layer thickens and deepens.
GI12FP6A	20Q 0333705 2043798 (+\-5m)	125cm	17cm	13%	0	top layer is black; beneath it is a stiff hard cohesive grey clay that is preventing further penetration
GI12FP6B	20Q 0333705 2043798 (+\-5m)	108cm	88cm	81%	0	
GI12FP6C	20Q 0333705 2043798 (+\-5m)	52cm	32cm	61%	0	tension of the piston was lost. Possible slough from top of hole at the top of 6C
GI12FP7	20Q 0333659 2043778 (+/-5m)	125cm	89cm	71%	50 m to the WSW	
GI12FP8	20Q 0333606 2043767 (+/-5m)	88cm	80cm	91%	104 m to the WSW	
GI12FP9	20Q 0333633 2043734 (+/-5m)	not recorded	73cm	not recorded	96 m to the SW	shore at this location has signs of previous mangroves growing farther to the North-submerged. Also on shore is a piece of historic rock and mortar from an old structure; appears to be isolated. Today west of flamingo feeding area was a large dead fish and a dead rat on the shore
GI12FP10	20Q 0333563 2043724 (+/-4m)	63cm	38cm	60%	160 m to the SW	water between piston and core top

APPENDIX C
SEDIMENT BOUNDARY AND WATER CHEMISTRY DATA

Site #	UTM	GIS UTM	pH	Temp (C)	Salinity µS/cm[c]	Sediment description	Notes
1	20Q 0333722 2043628	20N 333722 2043628	7.73	30.70	121750	medium firm clay 32cm below surface	6cm black organic mat
2	20Q 0333709 2043644	20N 333709 2043644	7.77	30.80	122094	medium firm clay 36cm below surface	5cm black organic mat
3	20Q 0333694 2043647	20N 333694 2043647	7.82	31.54	122340	medium firm clay 38cm below surface	6cm black organic mat
4	20Q 0333647 2043645	20N 333647 2043645	7.75	31.29	122070	medium firm clay 34cm below surface	7cm black organic mat
5	20Q 0333634 2043646	20N 333634 2043646	7.80	31.21	122020	medium firm clay 35cm below surface	7cm black organic mat
6	20Q 0333604 2043643	20N 333604 2043643	7.85	31.49	121588	medium firm clay 33cm below surface	6cm black organic mat
7	20Q 0333585 2043633	20N 333585 2043633	7.82	32.03	120700	medium firm clay 30cm below surface	9cm black organic mat
8	20Q 0333586 2043631	20N 333586 2043631	7.79	32.56	119400	medium firm clay 30cm below surface	9cm black organic mat
9	20Q 0333547 2043629	20N 333547 2043629	7.70	31.65	114200	medium firm clay 25cm below surface	7cm black organic mat
10	20Q 0333547 2043630	20N 333547 2043630	7.82	32.82	115673	clay/sand boundary 20cm below surface	5cm black organic mat
11	20Q 0333551 2043595	20N 333551 2043595	7.94	33.51	115437	sand 15cm below surface	<1cm black organic mat
12	20Q 0333548 2043601	20N 333548 2043601	8.14	34.13	118370	sand 18cm below surface	2-3cm black organic mat in pockets - footprints from previous days?
13	20Q 0333563 2043732	20N 333563 2043732	7.99	32.65	120167	medium firm clay 27cm below surface	8cm black organic mat
14	20Q 0333730 2043775	20N 333730 2043775	8.13	34.71	122280	firm clay 36cm below surface	6cm black organic mat
15	20Q 0333710 2043802	20N 333710 2043802	8.10	34.34	122318	firm clay 33cm below surface	5cm black organic mat
16	20Q 0333675 2043821	20N 333675 2043821	7.95	35.33	123334	firm clay 28cm below surface, sand on top of clay	7cm black organic mat

17	20Q 0333652 2043804	20N 333652 2043804	8.06	34.96	123617	firm clay 31cm below surface	7cm black organic mat
18	20Q 0333663 2043756	20N 333663 2043756	8.09	34.67	123097	soft clay 35cm below surface	6cm black organic mat
19	20Q 0333637 2043773	20N 333637 2043773	8.14	34.68	123258	firm/soft clay boundary 31cm below surface	5cm black organic mat
20	20Q 0333595 2043778	20N 333595 2043778	8.17	35.58	121987	firm clay 29cm below surface	5cm black organic mat
21	20Q 0333584 2043748	20N 333584 2043748	8.09	35.31	122075	firm clay 30cm below surface	7cm black organic mat
22	20Q 0333532 2043773	20N 333532 2043773	8.23	37.91	110967	sandy clay 12cm below surface	1cm black organic mat
23	20Q 0333747 2043711	20N 333747 2043711	7.79	35.56	122969	sand 14cm below surface	<1cm black organic mat

BATHYMETRIC DATA

Site #	UTM	Water Depth (cm below surface)
1	20Q 0333802 2073742	32
2	20Q 0333680 2043794	28
3	20Q 0333668 2043811	25
4	20Q 0333658 2043811	21
5	20Q 0333646 2043809	20
6	20Q 0333637 2043805	28
7	20Q 0333627 2043804	20
8	20Q 0333612 2043793	23
9	20Q 0333589 2043777	20
10	20Q 0333570 2043763	23
11	20Q 0333545 2043747	23
12	20Q 0333536 2043736	20
13	20Q 0333533 2043728	18
14	20Q 0333550 2043717	18
15	20Q 0333564 2043716	15
16	20Q 0333555 2043735	24
17	20Q 0333579 2043738	26
18	20Q 0333598 2043759	33
19	20Q 0333606 2043745	33
20	20Q 0333613 2043734	26
21	20Q 0333615 2043724	14
22	20Q 0333629 2043719	13
23	20Q 0333633 2043732	29
24	20Q 0333626 2043753	30
25	20Q 0333621 2043776	33
26	20Q 0333634 2043789	31
27	20Q 0333643 2043764	35
28	20Q 0333652 2043752	29
29	20Q 0333658 2043739	32
30	20Q 0333656 2043721	18
31	20Q 0333676 2043722	16
32	20Q 0333672 2043747	34
33	20Q 0333667 2043756	34
34	20Q 0333660 2043770	33
35	20Q 0333656 2043783	36
36	20Q 0333658 2043792	33
37	20Q 0333663 2043777	28
38	20Q 0333671 2043769	31
39	20Q 0333686 2043742	33
40	20Q 0333691 2043729	29
41	20Q 0333699 2043719	16
42	20Q 0333689 2043752	33
43	20Q 0333702 2043733	30

44	20Q 0333711	2043721	16
45	20Q 0333719	2043716	17
46	20Q 0333730	2043723	23
47	20Q 0333741	2043717	17
48	20Q 0333739	2043731	23
49	20Q 0333726	2043758	29
50	20Q 0333727	2043772	33
51	20Q 0333719	2073775	31
52	20Q 0333714	2043793	34
53	20Q 0333698	2043807	29
54	20Q 0333693	2043815	24
55	20Q 0333684	2043823	19
56	20Q 0333666	2043825	24
57	20Q 0333689	2043800	33
58	20Q 0333700	2043788	35
59	20Q 0333693	2043782	35
60	20Q 0333718	2043746	30

APPENDIX D
CORE LOGS

GI12FP6A				Described 2/16/2015
Depth in Core (cm)	Texture	Munsell	Color	Features
1	firm clay	5Y 3/1	very dark grey	
2	firm clay	5Y 3/1	very dark grey	
3	firm clay	5Y 3/1	very dark grey	
4	firm clay	5Y 3/1	very dark grey	4.5 cm - smear slide
5	firm clay	5Y 3/1	very dark grey	
6	clay - not as firm	5Y 3/1	very dark grey	
7	clay	5Y 3/1	very dark grey	
8	firm clay	5Y 3/1	very dark grey	8.5 cm - boundary? Gets lighter.
9	clay - silty clay?	2.5Y 4/1	dary grey	
10	clay	2.5Y 4/1	dary grey	
11	clay	2.5Y 4/1	dary grey	
12	firm clay	2.5Y 4/1	dary grey	
13	firm clay	2.5Y 4/1	dary grey	
14	clay	2.5Y 4/1	dary grey	14.5 cm - smear slide
15	silty clay	2.5Y 4/1	dary grey	
16	silty clay	2.5Y 4/1	dary grey	
17	silty clay	2.5Y 4/1	dary grey	

GI12FP6B				Described 3/25/2015
Depth in Core (cm)	Texture	Munsell	Color	Features
1	silt	2.5Y 4/1	dark grey	
2	silt	2.5Y 4/1	dark grey	
3	silty clay	2.5Y 4/1	dark grey	
4	silty clay	2.5Y 4/1	dark grey	
5	silty clay	2.5Y 4/1	dark grey	
6	silty clay	2.5Y 4/1	dark grey	
7	silty clay	2.5Y 4/1	dark grey	
8	clay	2.5Y 4/1	dark grey	

9	clay	2.5Y 4/1	dark grey	9 cm - smear slide
10	clayey silt	2.5Y 4/1	dark grey	
11	clay	2.5Y 4/1	dark grey	
12	clay	2.5Y 4/1	dark grey	
13	clay	2.5Y 4/1	dark grey	
14	silty clay	2.5Y 4/1	dark grey	
15	silty clay	2.5Y 4/1	dark grey	
16	silty clay	2.5Y 4/1	dark grey	
17	clayey silt	2.5Y 4/1	dark grey	17.0cm - clay inclusions
18	silt with fine sand	2.5Y 4/1	dark grey	
19	silt with fine sand	2.5Y 4/1	dark grey	
20	silt with fine sand	2.5Y 4/1	dark grey	
21	silt with fine sand	2.5Y 4/1	dark grey	21.0 cm - clay inclusions at depth
22	silt with fine sand	2.5Y 4/1	dark grey	
23	silt with fine sand	2.5Y 4/1	dark grey	23.0 cm - clay inclusions at depth
24	silt with fine sand	2.5Y 4/1	dark grey	
25	silt	2.5Y 4/1	dark grey	
26	silt	2.5Y 4/1	dark grey	
27	clayey silt	2.5Y 4/1	dark grey	27.0 cm - clay inclusions at depth
28	clayey silt	2.5Y 4/1	dark grey	
29	silt	2.5Y 4/1	dark grey	
30	silt	2.5Y 4/1	dark grey	
31	silt with fine sand	2.5Y 4/1	dark grey	
32	clayey silt	2.5Y 4/1	dark grey	32.5 cm - smear slide
33	silt with fine sand	5Y 4/1	dark grey	33.0-39.0 cm - Varves?
34	silt with fine sand	5Y 4/1	dark grey	
35	silt with fine sand	5Y 4/1	dark grey	
36	silt with fine sand	5Y 4/1	dark grey	
37	silt with fine sand	5Y 4/1	dark grey	
38	clayey silt	5Y 4/1	dark grey	
39	silt with fine sand	5Y 4/1	dark grey	
40	silt with fine sand	5Y 4/1	dark grey	
41	silt with fine sand	5Y 4/1	dark grey	

42	silt with fine sand	5Y 4/1	dark grey	
43	silt with fine sand	5Y 4/1	dark grey	
44	silt with fine sand	5Y 4/1	dark grey	
45	silt with fine sand	5Y 4/1	dark grey	45.5-46.0 cm - boundary
46	silt with very fine sand	5Y 4/1	dark grey	
47	silt with fine sand	5Y 4/1	dark grey	
48	silt with fine sand	5Y 3/1	very dark grey	
49	silt with very fine sand	5Y 3/1	very dark grey	
50	silt with fine sand	5Y 3/1	very dark grey	
51	silt with very fine sand	5Y 3/1	very dark grey	
52	silt with very fine sand	5Y 3/1	very dark grey	52.0 cm - smear slide
53	silt with fine sand	5Y 3/1	very dark grey	
54	silt with fine sand	5Y 3/1	very dark grey	
55	silt with fine sand	5Y 3/1	very dark grey	
56	silt with fine sand and organics	5Y 3/1	very dark grey	
57	silt with fine sand and organics	5Y 3/1	very dark grey	
58	silt with fine sand and organics	5Y 3/1	very dark grey	
59	clayey silt with very fine sand and organics	5Y 3/1	very dark grey	
60	silt with fine sand	5Y 3/1	very dark grey	
61	silt with fine sand	5Y 3/1	very dark grey	
62	silt with fine sand	5Y 3/1	very dark grey	
63	silt with fine sand and organics	5Y 3/1	very dark grey	
64	silt with fine sand and organics	5Y 2/1	black	
65	silt with fine sand and organics	5Y 2/1	black	
66	silt with fine sand and organics	5Y 2/1	black	
67	silt with fine sand and organics	5Y 2/1	black	
68	silt with fine sand and organics	5Y 2/1	black	
69	silt with fine sand and organics	5Y 2/1	black	
70	silt with fine sand and organics	5Y 2/1	black	
71	silt with fine sand and organics	5Y 2/1	black	
72	silt with fine sand and organics	5Y 2/1	black	
73	silt with very fine sand and small organics	5Y 2/1	black	
74	silt with fine sand and small organics	5Y 2/1	black	

75	clayey silt with fine sand and small organics	5Y 2/1	black	
76	silty clay	5Y 2/1	black	
77	silt with fine sand and small organics	5Y 2/1	black	
78	silt with fine sand and small organics	5Y 2/1	black	
79	silt with fine sand and small organics	5Y 2/1	black	
80	silt with fine sand and small organics	5Y 2/1	black	
81	clayey silt with small organics	5Y 2/1	black	
82	silt with fine sand and small organics	5Y 2/1	black	
83	silt with fine sand and small organics	5Y 2/1	black	83.0 cm - smear slide
84	silt with fine sand and small organics	5Y 2/1	black	
85	silt with fine sand and small organics	5Y 2/1	black	
86	silt with fine sand and small organics	5Y 2/1	black	
87	silt with very fine sand and small organics	5Y 2/1	black	
88	silt with very fine sand and small organics	5Y 2/1	black	

GI12FP6C				Described 2/23/2015
Depth in Core (cm)	Texture	Munsell	Color	Features
1	sandy silt	2.5Y 5/1	grey	
2	sandy silt	2.5Y 5/1	grey	
3	sandy silt	2.5Y 5/1	grey	
4	silt with clay inclusions	2.5Y 5/1	grey / Gley 1 4/5gy	4-4.5 cm - green/grey clay
5	silt with clay inclusions	2.5Y 5/1	grey	
6	sandy silt with clay inclusions	2.5Y 5/1	grey / Gley 1 4/5gy	6-7 cm - green/grey clay
7	sandy silt	2.5Y 5/1	grey	
8	sandy silt	2.5Y 5/1	grey	8.0 cm - smear slide
9	sandy silt	2.5Y 5/1	grey	
10	sandy silt	2.5Y 5/1	grey	
11	sandy silt	2.5Y 4/1	dark grey	11.0 cm - visible sand grains
12	clayey silt with sand	2.5Y 4/1	dark grey	
13	sandy silt with clay	2.5Y 4/1	dark grey	
14	clayey silt with sand	2.5Y 4/1	dark grey	

15	clayey silt with sand	2.5Y 4/1	dark grey	
16	sandy silt	2.5Y 4/1	dark grey	
17	sandy silt	2.5Y 4/1	very dark grey	
18	sandy silt	2.5Y 4/1	very dark grey	18.5-20.0 cm - boundary
19	sandy silt	2.5Y 4/1	very dark grey	boundary - irregular
20	sandy silt	2.5Y 3/1	very dark grey	boundary - irregular
21	sandy silt	2.5Y 3/1	very dark grey	21.0 cm - visible sand grains
22	sandy silt	2.5Y 3/1	very dark grey	22.0 cm - visible sand grains
23	sandy silt	2.5Y 3/1	very dark grey	23.0-24.0 cm - organics (charcoal?)
24	sandy silt	2.5Y 3/1	very dark grey	
25	sandy silt	2.5Y 3/1	very dark grey	
26	sandy silt	2.5Y 3/1	very dark grey	
27	sandy silt	2.5Y 3/1	very dark grey	
28	sandy silt	2.5Y 3/1	very dark grey	
29	sandy silt with large organics	2.5Y 3/1	very dark grey	29.0 cm - large reddish organic piece
30	sandy silt	2.5Y 3/1	very dark grey	30.0 cm - smear slide (organics)
31	sandy silt	2.5Y 2.5/1	black	
32	sandy silt	2.5Y 2.5/1	black	

GI12FP7				Described 3/3/2015
Depth in Core (cm)	Texture	Munsell	Color	Features
1	silty clay	2.5Y 4/1	dark grey	
2	silty clay	2.5Y 4/1	dark grey	
3	silty clay	2.5Y 3/1	very dark grey	
4	clayey silt	2.5Y 4/1	dark grey	4.0 cm - boundary
5	clayey silt	5Y 4/1	dark grey	
6	silty clay	5Y 4/1	dark grey	
7	silty clay	5Y 4/1	dark grey	
8	clayey silt	5Y 4/1	dark grey	
9	clayey silt	5Y 4/1	dark grey	
10	silty clay	5Y 4/1	dark grey	

11	silty clay	5Y 4/1	dark grey	
12	sandy silt	5Y 4/1	dark grey	
13	sandy silt	5Y 3/1	very dark grey	
14	sandy silt	5Y 4/1	dark grey	14.0 cm - smear slide
15	sandy silt with some clay	5Y 4/1	dark grey	15.5 cm - boundary
16	sandy silt with some clay	5Y 4/1	dark grey	16.0 cm - small organics
17	sandy silt	5Y 4/1	dark grey	17.0 cm - small organics
18	sandy silt	5Y 4/1	dark grey	18.0 cm - small organics
19	silt with some sand	5Y 4/1	dark grey	19.0 cm - small organics
20	clayey silt with sand	5Y 4/1	dark grey	20.0 cm - small organics
21	silty clay	5Y 4/1	dark grey	21.0 cm - organics
22	silty clay	5Y 4/1	dark grey	22.0 cm - organics
23	sandy silt	5Y 4/1	dark grey	23.0 cm - organics
24	sandy silt	5Y 3/1	very dark grey	24.0 cm - organics
25	sandy silt	5Y 3/1	very dark grey	25.0 cm - organics
26	sandy silt	5Y 3/1	very dark grey	26.0 cm - organics
27	clayey silt with sand	5Y 4/1	dark grey	27.0 cm - small organics
28	sandy silt	5Y 4/1	dark grey	
29	clayey silt with sand	5Y 4/1	dark grey	
30	sandy clay	5Y 5/1	grey	30.0 cm - organics
31	silty clay	5Y 5/1	grey	31.0 cm - organics
32	silty clay	5Y 4/1	dark grey	
33	clay	5Y 4/1	dark grey	33.0 cm - organics
34	silty clay with sand	5Y 4/1	dark grey	34.0 cm - shell/claw
35	clayey silt	5Y 4/1	dark grey	35.0 cm - small organics
36	clayey silt	5Y 4/1	dark grey	
37	silt	5Y 4/1	dark grey	
38	silty clay with sand	5Y 4/1	dark grey	
39	silty clay	5Y 4/1	dark grey	
40	clayey silt	5Y 4/1	dark grey	
41	clayey silt	5Y 4/1	dark grey	41.0 cm - smear slide
42	silty clay	5Y 4/1	dark grey	42.0 cm - organics

43	clayey silt	5Y 4/1	dark grey	43.5 cm - boundary (color)
44	sandy silt	5Y 4/1	dark grey	
45	sandy silt	5Y 4/1	dark grey	
46	silty clay	5Y 3/1	very dark grey	46.0 cm - small organics
47	clayey silt with sand	5Y 3/1	very dark grey	47.0 cm - small organics
48	sandy silt	5Y 3/1	very dark grey	48.0 cm - organics; roots?
49	sandy silt	5Y 3/1	very dark grey	49.0 cm - organics; roots?
50	silty clay	5Y 3/1	very dark grey	50.0 cm - organics
51	sandy silt	5Y 3/1	very dark grey	51.0 cm - small organics
52	clayey silt with sand	5Y 3/1	very dark grey	
53	sandy silt	5Y 3/1	very dark grey	53.0 cm - small organics
54	silty clay with sand	5Y 3/1	very dark grey	
55	silty clay with some sand	5Y 3/1	very dark grey	
56	silty clay with some sand	5Y 3/1	very dark grey	
57	sandy silt	5Y 3/1	very dark grey	57.0 cm - small organics
58	sandy silt	5Y 3/1	very dark grey	58.0 cm - organics
59	sandy silt	5Y 2.5/1	black	59.0 cm - organics
60	silty clay with sand	5Y 2.5/1	black	60.0 cm - smear slide; organics
61	sandy clay	5Y 2.5/1	black	
62	firm clay with sand	5Y 3/1	very dark grey	
63	silty clay with sand	5Y 3/1	very dark grey	
64	clayey silt with sand	5Y 3/1	very dark grey	
65	silty clay with some sand	5Y 3/1	very dark grey	
66	sandy silt	5Y 3/1	very dark grey	
67	clayey silt with sand	5Y 3/1	very dark grey	67.0 cm - small organics
68	sandy silt	5Y 3/1	very dark grey	
69	silty clay with sand	5Y 2.5/1	black	
70	silty clay with sand	5Y 2.5/1	black	
71	clayey silt with some sand	5Y 3/1	very dark grey	
72	clayey silt with some sand	5Y 2.5/1	black	

73	clayey silt with sand	5Y 3/1	very dark grey	
74	clayey silt with sand	5Y 2.5/1	black	
75	sandy silt	5Y 2.5/1	black	
76	sandy silt	5Y 3/1	very dark grey	
77	clayey silt with sand	5Y 2.5/1	black	
78	silty clay with some sand	5Y 2.5/1	black	
79	clayey silt with sand	5Y 2.5/1	black	
80	silty clay with some sand	5Y 3/1	very dark grey	
81	sandy silt	5Y 2.5/1	black	
82	sandy silt	5Y 2.5/1	black	82.0 cm - smear slide
83	sandy clay	5Y 2.5/1	black	
84	sandy clay	5Y 3/1	very dark grey	
85	sandy clay	5Y 3/1	very dark grey	
86	sandy clay	5Y 3/1	very dark grey	
87	sandy clay	5Y 3/1	very dark grey	
88	sandy clay	5Y 3/1	very dark grey	

GI12FP8				Described 3/17/2015
Depth in Core (cm)	Texture	Munsell	Color	Features
1	yellow foam/part of sediment	2.5Y 4/2	dark greyish brown	
2	silt	2.5Y 4/2	dark greyish brown	
3	silt	2.5Y 4/2	dark greyish brown	3.5 cm - smear slide
4	silt	5Y 4/1	dark grey	
5	silt	5Y 4/1	dark grey	5.5-6.0 cm - boundary (color/comp.)
6	silt with fine sand	5Y 3/1	very dark grey	
7	silt with fine sand	5Y 3/1	very dark grey	
8	silt with medium sand	5Y 3/1	very dark grey	8.0 cm - organics
9	silt with fine sand	5Y 3/1	very dark grey	
10	silt with fine sand	5Y 3/1	very dark grey	10.0 cm - organics

11	silt with fine sand	5Y 3/1	very dark grey	
12	silt with very fine sand	5Y 4/1	dark grey	
13	silt with very fine sand	5Y 4/1	dark grey	
14	silt with fine sand	5Y 4/1	dark grey	
15	silt with very fine sand	5Y 4/1	dark grey	
16	silt with very fine sand	5Y 4/1	dark grey	
17	silt with fine sand	5Y 4/1	dark grey	
18	silt with fine sand	5Y 4/1	dark grey	18.0 cm - charcoal?
19	organics with silt	2.5Y 3/2	very dk greyish brown	19.0 cm - boundary (color/comp.)
20	organics with silt	2.5Y 3/2	very dk greyish brown	
21	silt with organics	2.5Y 3/2	very dk greyish brown	
22	silt with large organics	2.5Y 3/2	very dk greyish brown	
23	sandy silt with large organics	2.5Y 3/2	very dk greyish brown	
24	sandy silt with organics	2.5Y 3/2	very dk greyish brown	
25	sandy silt with large organics	2.5Y 3/2	very dk greyish brown	25.5 cm - smear slide
26	sandy silt with organics	2.5Y 3/2	very dk greyish brown	
27	medium sandy silt	2.5Y 4/1	dark grey	
28	medium sandy silt	2.5Y 4/1	dark grey	
29	medium sandy silt with organics	2.5Y 4/1	dark grey	
30	sandy silt with small organics	2.5Y 4/1	dark grey	
31	medium sandy silt with small organics	2.5Y 4/1	dark grey	
32	sandy silt with small organics	2.5Y 4/1	dark grey	
33	sandy silt with large organics	5Y 3/2	dark olive grey	
34	sandy silt with organics	5Y 3/2	dark olive grey	
35	sandy silt with small organics	5Y 3/2	dark olive grey	
36	sandy silt with small organics	5Y 3/2	dark olive grey	
37	sandy silt with small organics	5Y 3/2	dark olive grey	
38	sandy silt with large organics	5Y 3/2	dark olive grey	
39	clayey silt with large organics	5Y 3/2	dark olive grey	39.0 cm - no visible sand
40	medium sandy silt with organics	5Y 3/2	dark olive grey	
41	medium sandy silt with organics	5Y 3/2	dark olive grey	
42	silt	5Y 3/2	dark olive grey	42.0 cm - minimal sand

43	sandy silt	5Y 3/2	dark olive grey	
44	silt	5Y 3/2	dark olive grey	
45	sandy silt with organics	5Y 3/2	dark olive grey	
46	fine sandy silt with organics	5Y 3/2	dark olive grey	46.0 cm - minimal sand
47	fine sandy silt with organics	5Y 3/2	dark olive grey	47.0 cm - minimal sand
48	clayey silt	5Y 3/2	dark olive grey	
49	clayey silt	5Y 3/2	dark olive grey	
50	clayey silt with sand; shell	5Y 3/2	dark olive grey	
51	sandy silt; shell at depth	5Y 3/2	dark olive grey	51.0-52.0 cm - boundary (color/comp.)
52	silt	5Y 3/2	dark olive grey	52.0 cm - minimal sand
53	sandy silt	5Y 3/1	very dark grey	
54	sandy silt with organics	5Y 3/1	very dark grey	54.5 cm - smear slide
55	silt	5Y 3/1	very dark grey	
56	medium sandy silt	5Y 3/1	very dark grey	
57	medium sandy silt	5Y 3/1	very dark grey	
58	clayey silt with medium sand	5Y 3/1	very dark grey	
59	medium sandy silt	5Y 3/1	very dark grey	
60	medium sandy silt with organics	5Y 2.5/1	black	
61	medium sandy silt with organics	5Y 2.5/1	black	
62	medium sandy silt with organics	5Y 2.5/1	black	
63	medium sandy silt with organics	5Y 2.5/1	black	
64	medium sandy silt with organics	5Y 2.5/1	black	
65	medium sandy silt with organics	5Y 2.5/1	black	
66	medium sandy silt with organics	5Y 2.5/1	black	
67	medium sandy silt with large organics	5Y 2.5/1	black	
68	medium sandy silt with large organics	5Y 2.5/1	black	68.0 cm - spongy organics
69	medium sandy silt with large organics	5Y 2.5/1	black	69.5 cm - smear slide; spongy organics
70	medium sandy silt with large organics	5Y 2.5/1	black	70.0 cm - spongy organics
71	medium sandy silt with large organics	5Y 2.5/1	black	71.0 cm - spongy organics
72	medium sandy silt with organics	5Y 2.5/1	black	72.0 cm - spongy organics

GI12FP10				Described 3/19/2015
Depth in Core (cm)	Texture	Munsell	Color	Features
1	silty sand	10YR 4/1	dark grey	
2	silty fine angular sand	10YR 4/1	dark grey	2.0 cm - smear slide; microfossils
3	silty fine to medium angular sand	10YR 4/1	dark grey	3.0 cm - microfossils/forams
4	silty fine angular sand	10YR 4/1	dark grey	
5	silty fine angular sand	10YR 4/1	dark grey	
6	silty fine angular sand	10YR 4/1	dark grey	6.5-10.0 cm - boundary (color/comp.)
7	silty fine angular sand	10YR 4/1	dark grey	
8	silty fine angular sand	10YR 4/1	dark grey	8.0-9.0 cm - organics (sides)
9	silty fine angular sand	10YR 4/2	dark greyish brown	
10	fine to medium angular sandy silt	2.5Y 3/2	very dark greyish brown	10.0 cm - organics (center)
11	fine to medium angular sandy silt	2.5Y 3/2	very dark greyish brown	
12	fine to medium angular sandy silt	2.5Y 3/2	very dark greyish brown	12.0 cm - shell
13	fine to medium angular sandy silt	2.5Y 3/2	very dark greyish brown	13.0 cm - organics; shell fragment
14	fine to medium angular sandy silt	2.5Y 3/2	very dark greyish brown	cm - boundary (color/composition)
15	fine to medium angular sandy silt, small organics	2.5Y 3/2	very dark greyish brown	15.0 cm - boundary (color/comp.)
16	fine angular sandy silt	2.5Y 3/2	very dark greyish brown	16.0 cm - spongy organics
17	fine angular sandy silt	2.5Y 3/1	very dark grey	17.0 cm - spongy organics
18	fine angular sandy silt	2.5Y 3/1	very dark grey	18.0 cm - spongy organics
19	fine angular sandy silt	2.5Y 3/1	very dark grey	19.0 cm - smear slide; spongy organics
20	fine angular sandy silt	2.5Y 3/1	very dark grey	20.0 cm - spongy organics
21	fine angular sandy silt	2.5Y 2.5/1	black	21.0 cm - spongy organics
22	fine angular sandy silt	2.5Y 3/2	very dark greyish brown	22.0 cm - spongy organics
23	fine angular sandy silt	2.5Y 3/1	very dark grey	23.0 cm - spongy organics; shells
24	organics with fine sandy silt	2.5Y 2.5/1	black	24.0 cm - spongy organics
25	organics with fine sandy silt	2.5Y 3/1	very dark grey	25.0 cm - spongy organics
26	organics with fine sandy silt	2.5Y 3/2	very dark greyish brown	26.0 cm - spongy organics
27	organics with fine angular sand	10YR 2/1	black	27.0 cm - large organics
28	organics with fine angular sand	10YR 2/1	black	28.0 cm - large organics

29	organics with fine angular sand	2.5Y 3/1	very dark grey	29.0 cm - spongy organics
30	organics with fine angular sand	2.5Y 2.5/1	black	30.0 cm - large coral piece
31	organics with fine angular sand	2.5Y 3/1	very dark grey	31.0 cm - spongy organics
32	organics with fine angular sand	2.5Y 3/2	very dark greyish brown	32.0 cm - spongy organics
33	organics with fine angular sand	2.5Y 3/2	very dark greyish brown	33.0 cm - smear slide
34	fine angular sand with organics	2.5Y 3/2	very dark greyish brown	
35	fine angular sand with organics	2.5Y 3/2	very dark greyish brown	
36	fine angular sand with organics	2.5Y 3/2	very dark greyish brown	
37	fine angular sand with organics	2.5Y 3/2	very dark greyish brown	
38	fine angular sand with organics	2.5Y 3/1	very dark grey	

APPENDIX E

CORE IMAGES/ CORE CORRELATION

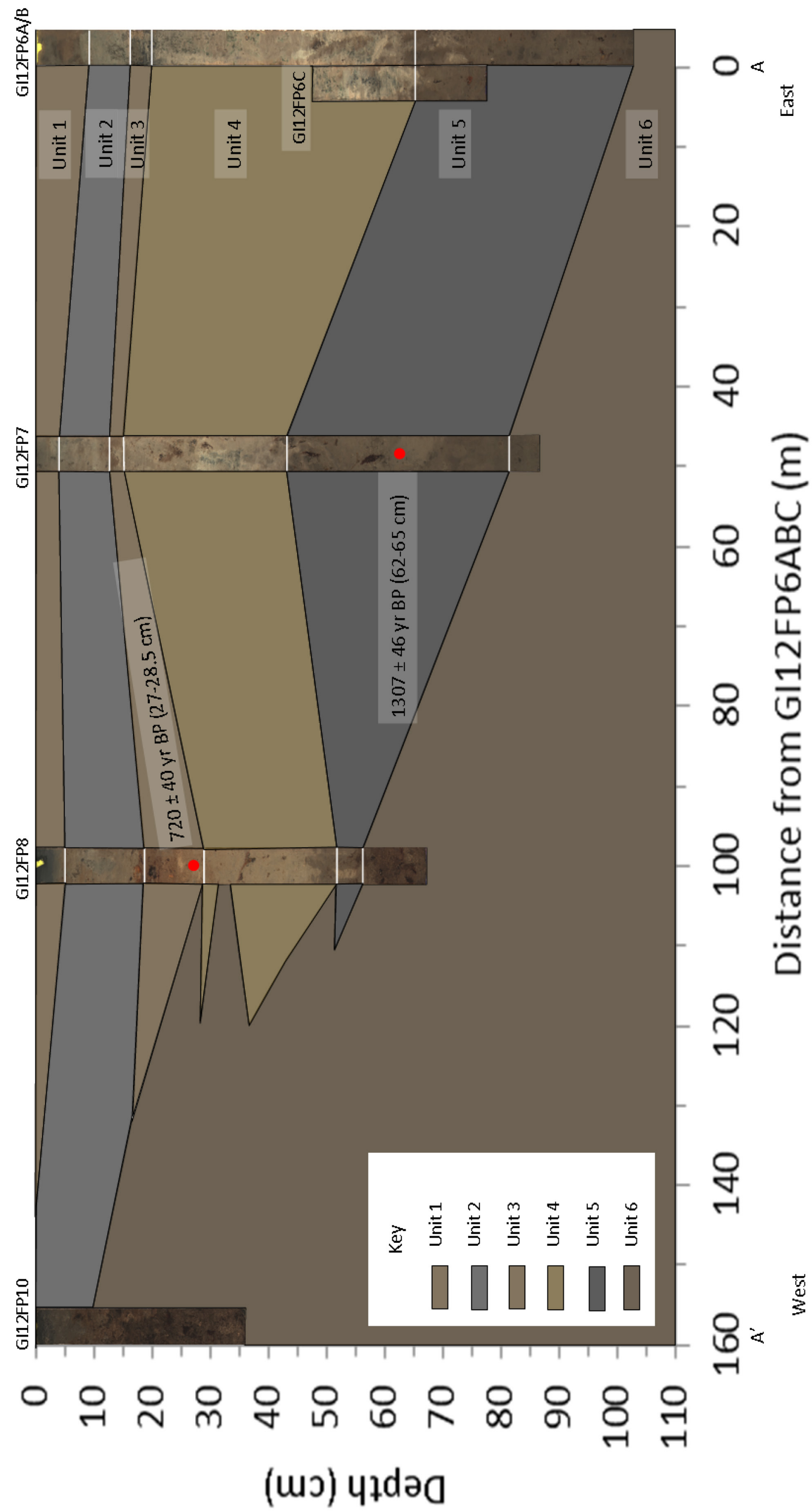

APPENDIX F
WEIGHT PERCENT DATA

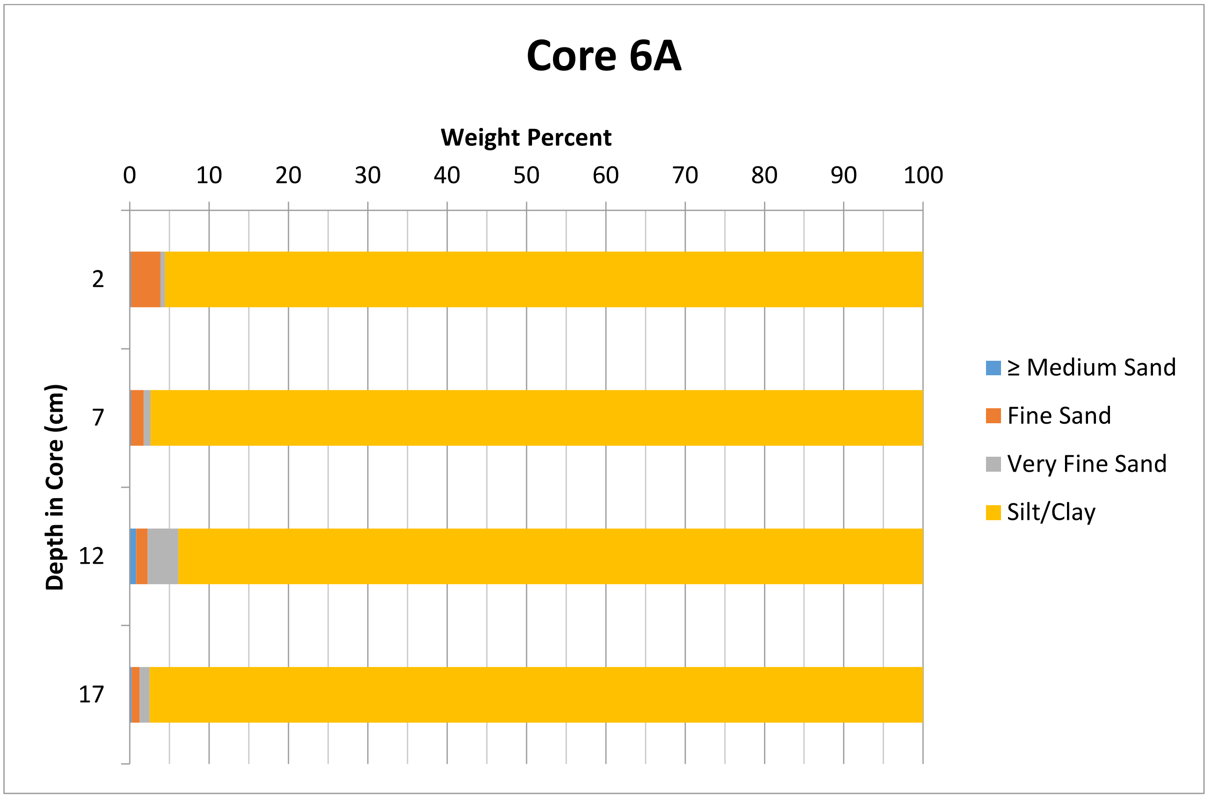

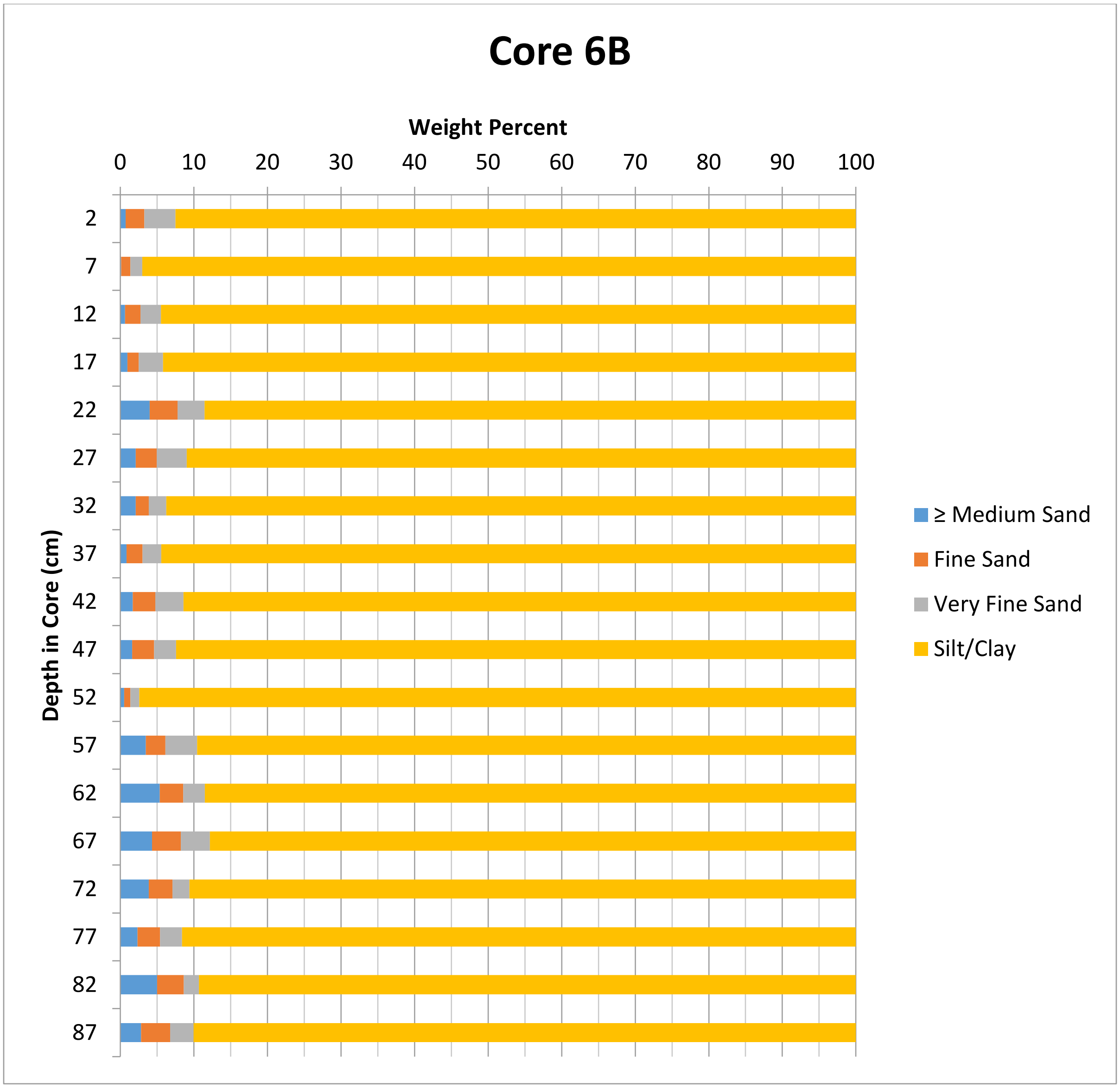

Core 6B
Weight Percent
0
10
20
30
40
50
60
70
80
90
100
Depth in Core (cm)
2
7
12
17
22
27
32
37
42
47
52
57
62
67
72
77
82
87
≥ Medium Sand
Fine Sand
Very Fine Sand
Silt/Clay

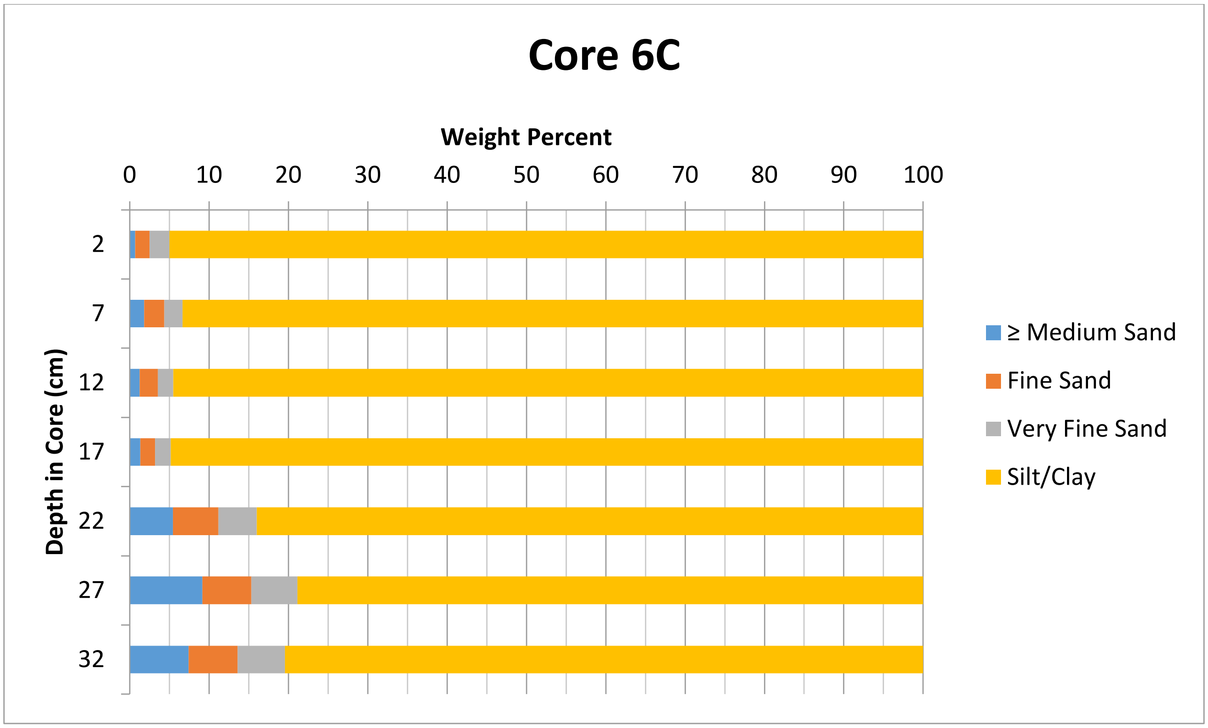

Core 6C
Weight Percent
0
10
20
30
40
50
60
70
80
90
100
Depth in Core (cm)
2
7
12
17
22
27
32
≥ Medium Sand
Fine Sand
Very Fine Sand
Silt/Clay

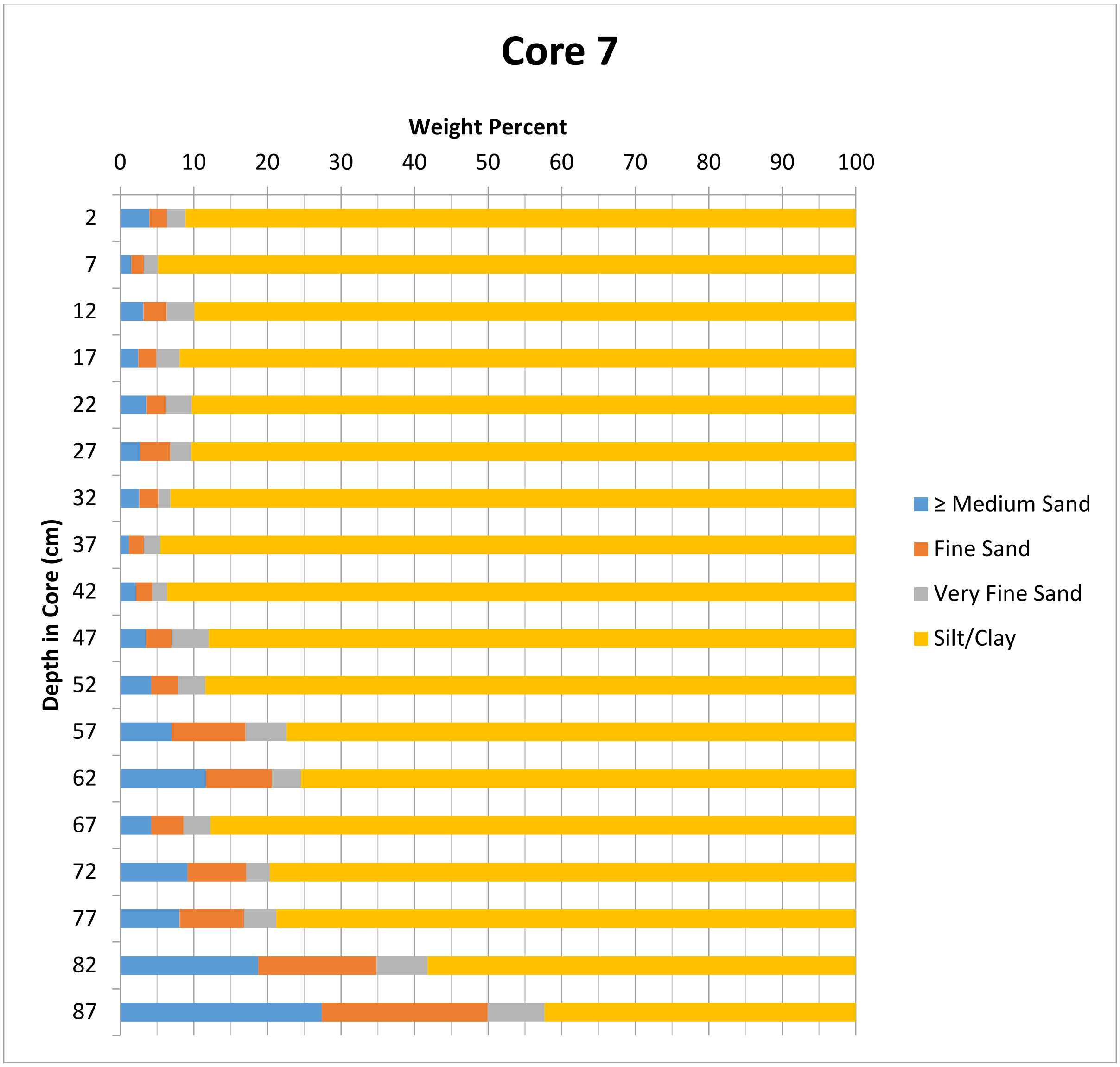
Core 7
Weight Percent
0
10
20
30
40
50
60
70
80
90
100
Depth in Core (cm)
2
7
12
17
22
27
32
37
42
47
52
57
62
67
72
77
82
87
≥ Medium Sand
Fine Sand
Very Fine Sand
Silt/Clay

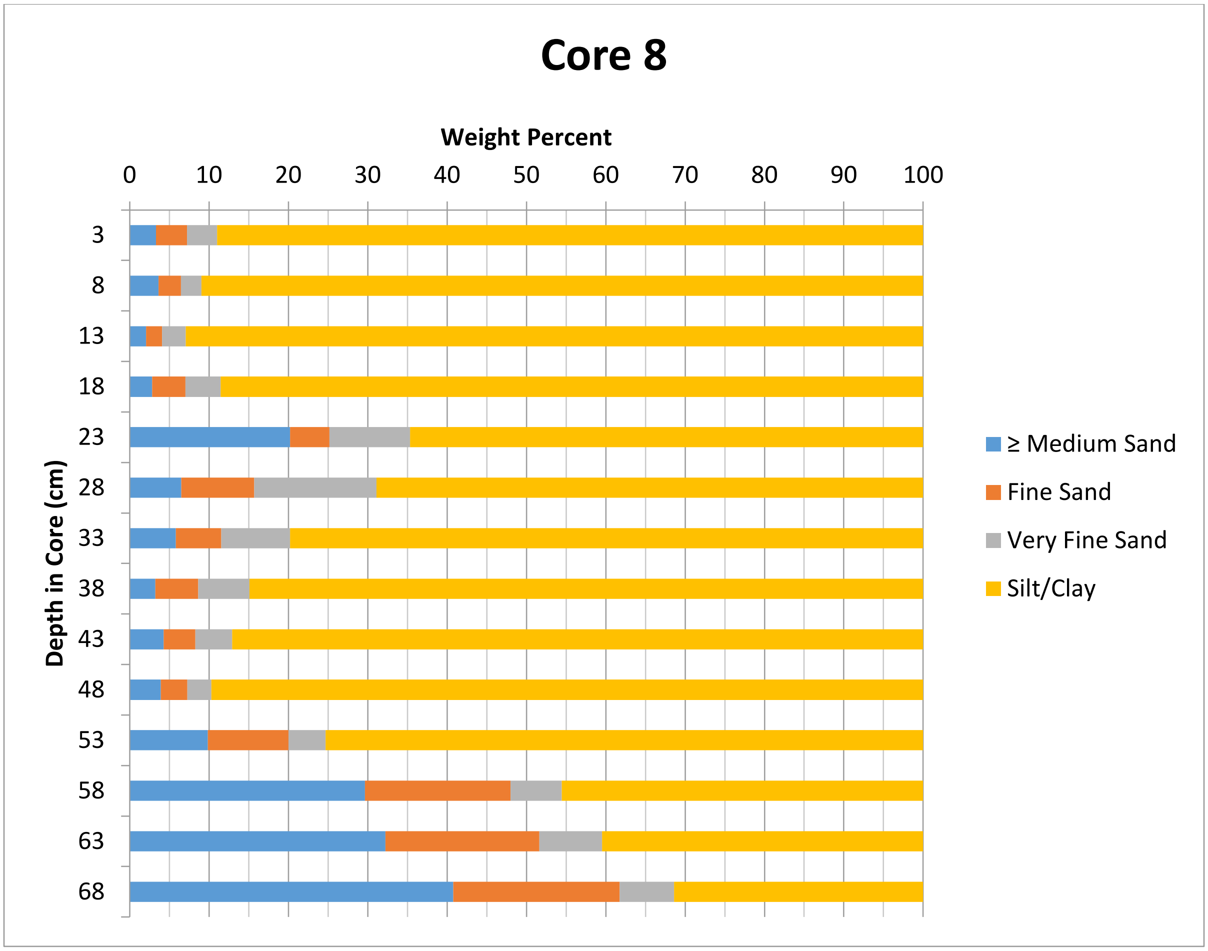
Core 8
Weight Percent
0
10
20
30
40
50
60
70
80
90
100
Depth in Core (cm)
3
8
13
18
23
28
33
38
43
48
53
58
63
68
≥ Medium Sand
Fine Sand
Very Fine Sand
Silt/Clay

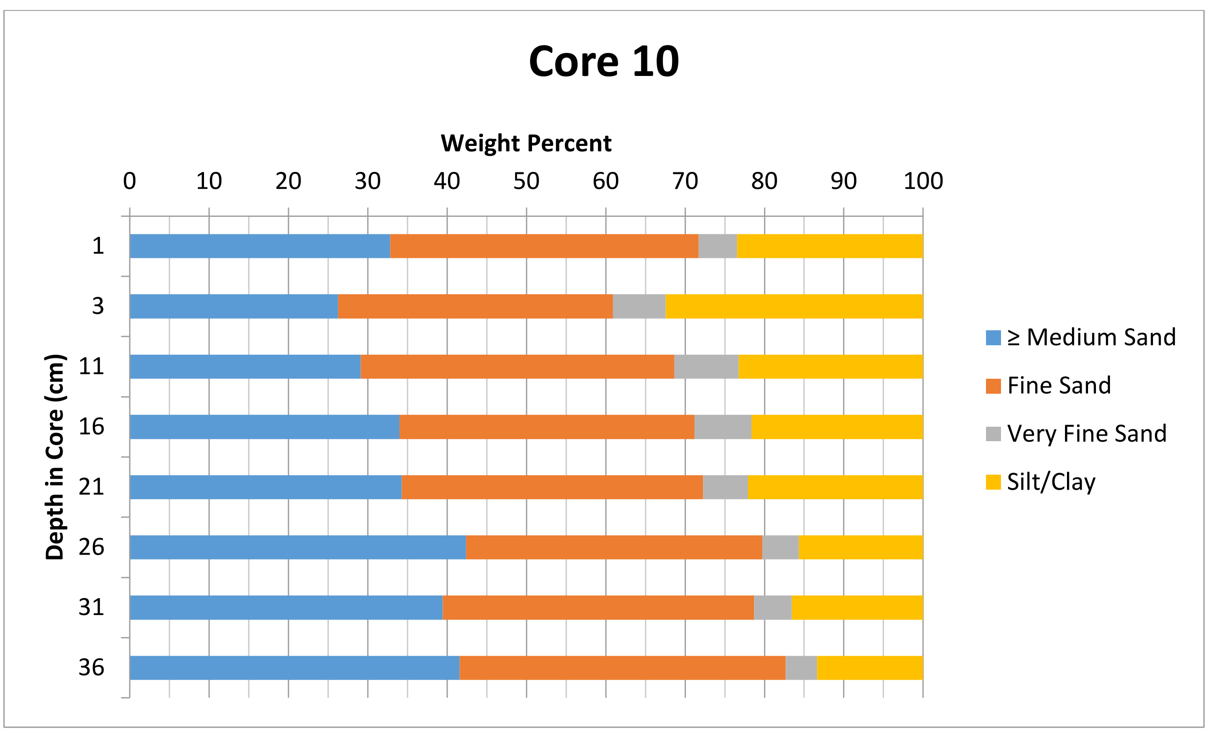
Core 10
Weight Percent
0
10
20
30
40
50
60
70
80
90
100
Depth in Core (cm)
1
3
11
16
21
26
31
36
≥ Medium Sand
Fine Sand
Very Fine Sand
Silt/Clay

GI12FP6A Grain Size Weight Percent Data				
Depth in Core (cm)	Medium Sand (≥ 250 micron)	Fine Sand (125 micron)	Very Fine Sand (63 micron)	Silt/Clay (<63 micron)
2	0.16	3.72	0.58	95.53
7	0.18	1.61	0.84	97.37
12	0.81	1.44	3.87	93.87
17	0.26	0.98	1.26	97.50

GI12FP6B Grain Size Weight Percent Data				
Depth in Core (cm)	Medium Sand (≥ 250 micron)	Fine Sand (125 micron)	Very Fine Sand (63 micron)	Silt/Clay (<63 micron)
2	0.75	2.52	4.25	92.48
7	0.12	1.28	1.59	97.00
12	0.68	2.08	2.77	94.48
17	0.97	1.53	3.32	94.19
22	4.02	3.79	3.65	88.54
27	2.13	2.83	4.09	90.95
32	2.09	1.81	2.36	93.73
37	0.86	2.19	2.53	94.43
42	1.70	3.08	3.80	91.41
47	1.63	2.98	2.98	92.41
52	0.54	0.84	1.22	97.41
57	3.47	2.66	4.32	89.55
62	5.38	3.18	2.95	88.49
67	4.35	3.89	3.94	87.82
72	3.87	3.24	2.31	90.58
77	2.34	3.06	3.01	91.59
82	5.02	3.61	2.07	89.30
87	2.83	3.97	3.20	90.01

GI12FP6C Grain Size Weight Percent Data				
Depth in Core (cm)	Medium Sand (≥ 250 micron)	Fine Sand (125 micron)	Very Fine Sand (63 micron)	Silt/Clay (<63 micron)
2	0.68	1.83	2.49	95.00
7	1.84	2.53	2.30	93.33
12	1.28	2.27	1.94	94.52
17	1.36	1.84	1.98	94.82
22	5.47	5.72	4.85	83.96
27	9.15	6.19	5.82	78.85
32	7.42	6.17	6.00	80.41

GI12FP7 Grain Size Weight Percent Data				
Depth in Core (cm)	Medium Sand (≥ 250 micron)	Fine Sand (125 micron)	Very Fine Sand (63 micron)	Silt/Clay (<63 micron)
2	3.96	2.38	2.53	91.13
7	1.50	1.70	1.93	94.87
12	3.17	3.15	3.78	89.90
17	2.49	2.41	3.16	91.94
22	3.60	2.62	3.50	90.28
27	2.71	4.08	2.86	90.35
32	2.59	2.57	1.66	93.18
37	1.19	2.01	2.25	94.55
42	2.15	2.19	2.05	93.61
47	3.51	3.49	5.01	87.99
52	4.21	3.64	3.72	88.42
57	7.01	10.01	5.64	77.35
62	11.66	8.97	3.96	75.41

67	4.22	4.37	3.68	87.73
72	9.16	7.94	3.23	79.67
77	8.10	8.72	4.41	78.78
82	18.75	16.08	6.94	58.22
87	27.38	22.58	7.72	42.33

GI12FP8 Grain Size Weight Percent Data				
Depth in Core (cm)	Medium Sand (≥ 250 micron)	Fine Sand (125 micron)	Very Fine Sand (63 micron)	Silt/Clay (<63 micron)
3	3.30	3.91	3.80	88.99
8	3.63	2.83	2.60	90.95
13	2.07	2.00	2.99	92.94
18	2.82	4.21	4.44	88.54
23	20.20	4.99	10.15	64.65
28	6.50	9.19	15.42	68.89
33	5.83	5.71	8.68	79.78
38	3.22	5.42	6.45	84.91
43	4.30	3.99	4.63	87.08
48	3.92	3.34	3.04	89.70
53	9.85	10.15	4.70	75.30
58	29.66	18.34	6.45	45.55
63	32.25	19.39	7.89	40.48
68	40.80	20.95	6.88	31.37

GI12FP10 Grain Size Weight Percent Data				
Depth in Core (cm)	Medium Sand (≥ 250 micron)	Fine Sand (125 micron)	Very Fine Sand (63 micron)	Silt/Clay (<63 micron)
1	32.83	38.90	4.81	23.45
6	26.27	34.63	6.66	32.43
11	29.12	39.54	8.08	23.25
16	34.02	37.16	7.18	21.63
21	34.27	38.02	5.65	22.06
26	42.40	37.35	4.57	15.68
31	39.47	39.22	4.75	16.56
36	41.58	41.09	3.96	13.37

APPENDIX G
XRF CHARTS AND DATA

Unit	Elemental Analysis	Depositional Environment
1	High Sr, Ti, Fe, Zr, Si, Ca; mid-range Cl	Fresh/marine mixed shallow water
2	High Sr, Ti, Fe, Ca; low Cl, Br	Fresh/ Brackish shallow water
3	Zr decreases with depth; high Cl, Br; low Ca, Sr but increases with depth	Marine shallow water
4	Low Cl, Br; High Ca, Sr, Si	Fresh shallow water; carbonate facies
5	Low Fe; mid-level Zr; pulses in Cl, Ca, Br, Sr, Si, Ti	Marine shallow water
6	Low Si, Ti, Fe; High Cl, Zr, Ca, Sr	Marine shallow water/ storm deposit

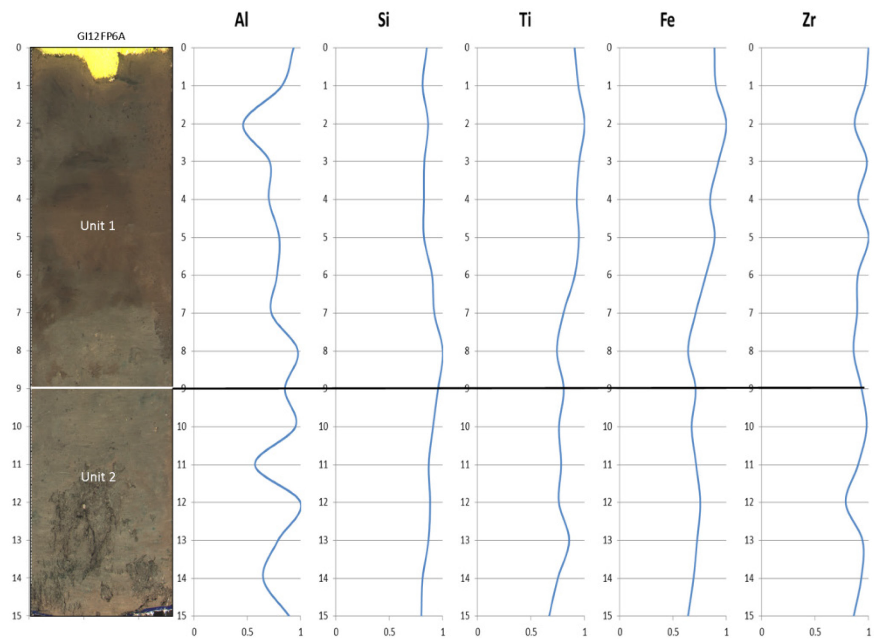

Core 6A Terrestrial Elemental Proxies

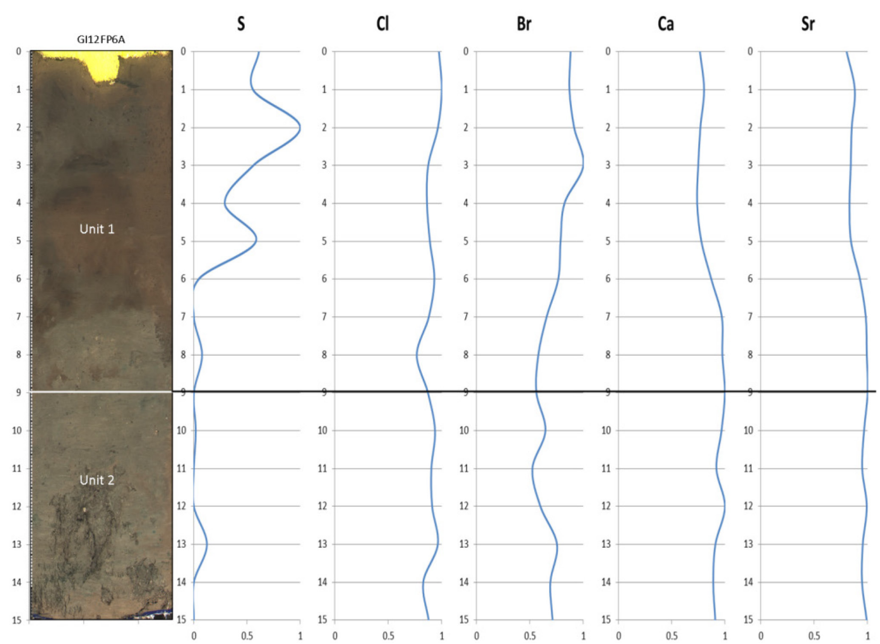

Core 6A Marine Elemental Proxies

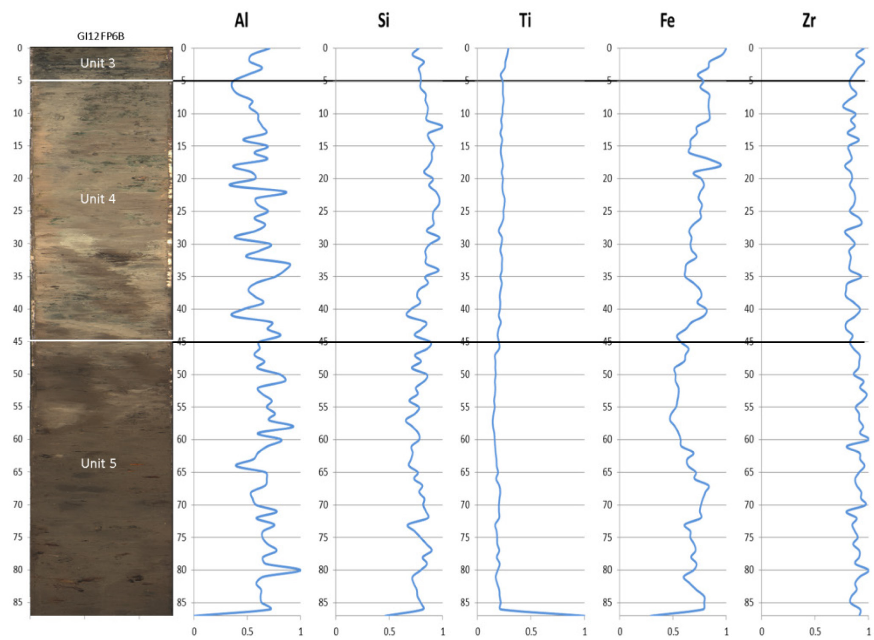

Core 6B Terrestrial Elemental Proxies

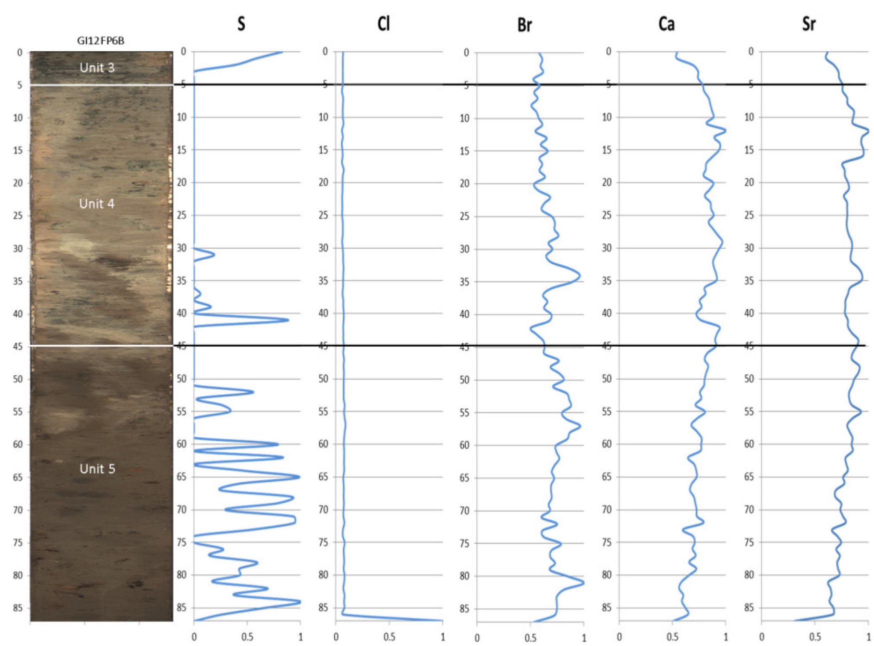

Core 6B Marine Elemental Proxies

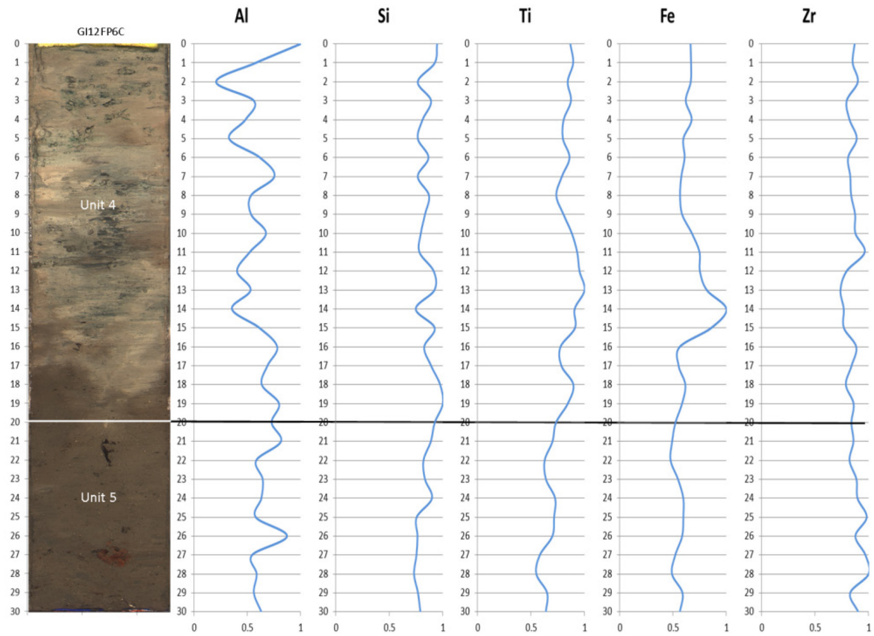

Core 6C Terrestrial Elemental Proxies

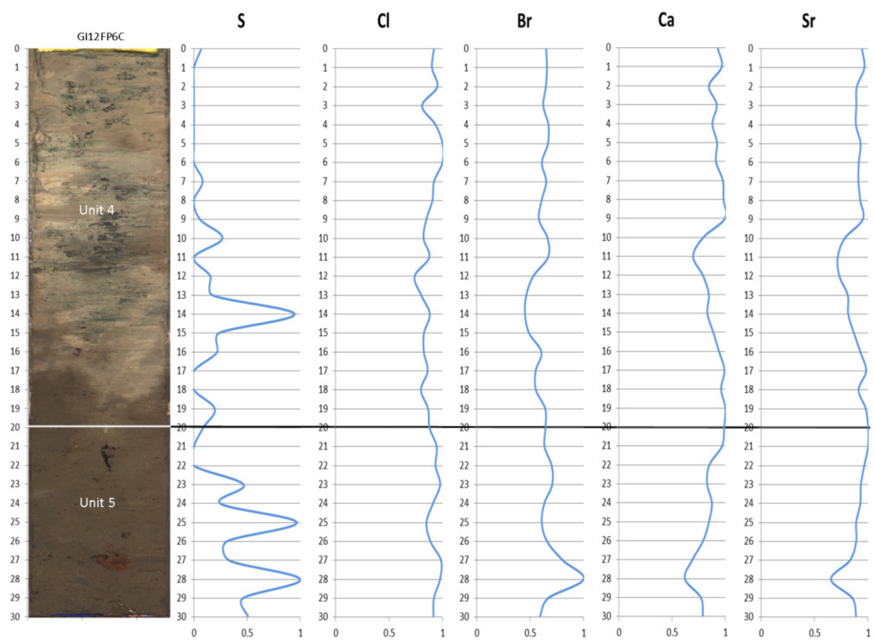

Core 6C Marine Elemental Proxies

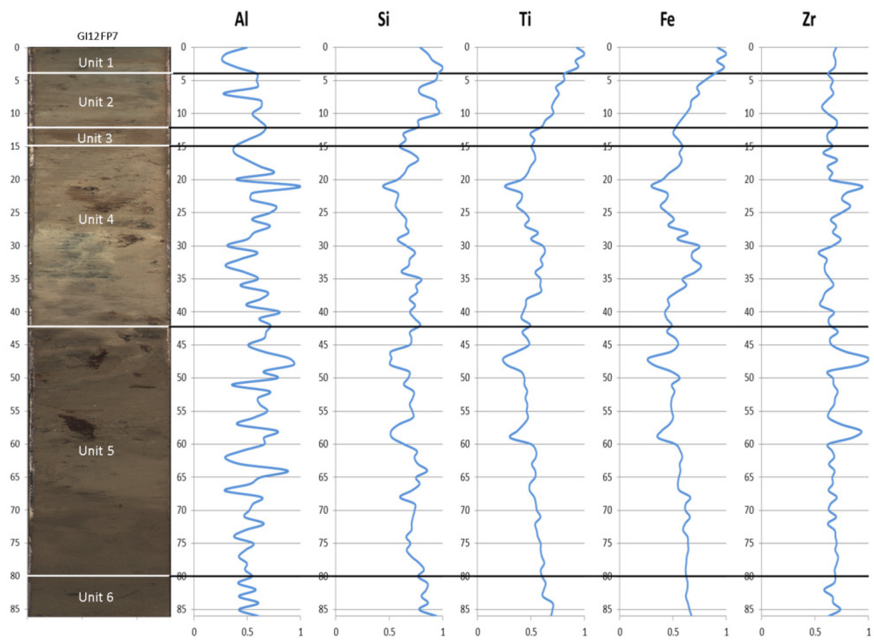

Core 7 Terrestrial Elemental Proxies

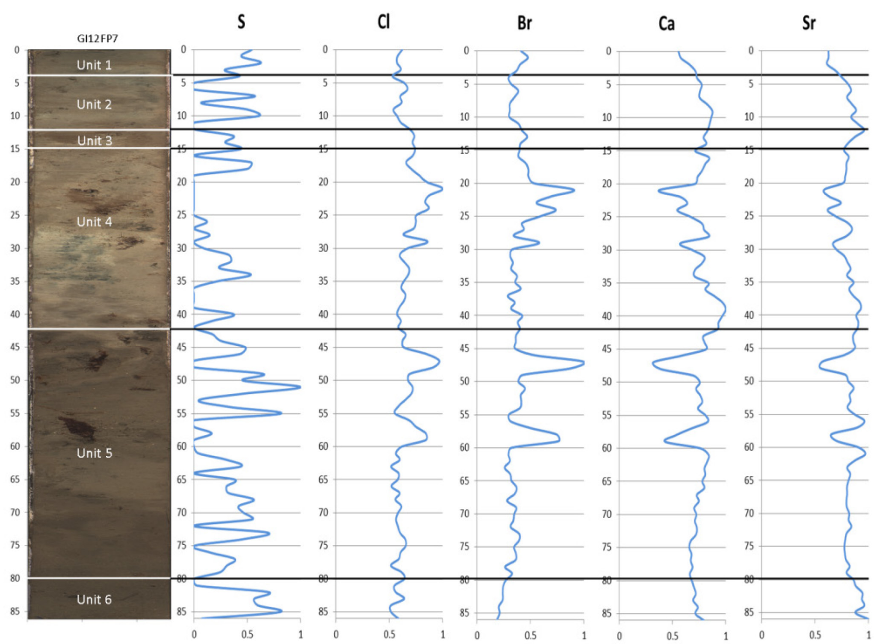

Core 7 Marine Elemental Proxies

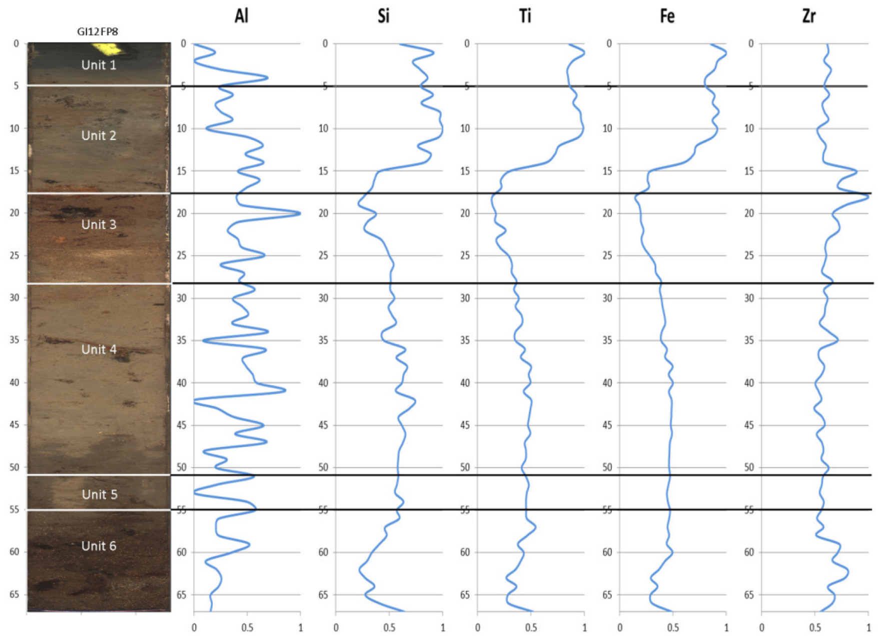

Core 8 Terrestrial Elemental Proxies

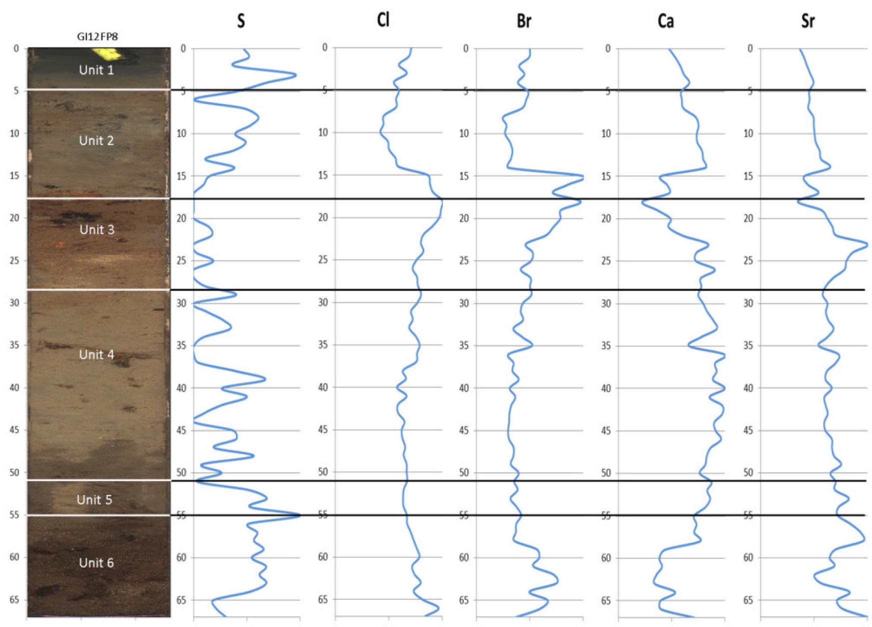

Core 8 Marine Elemental Proxies

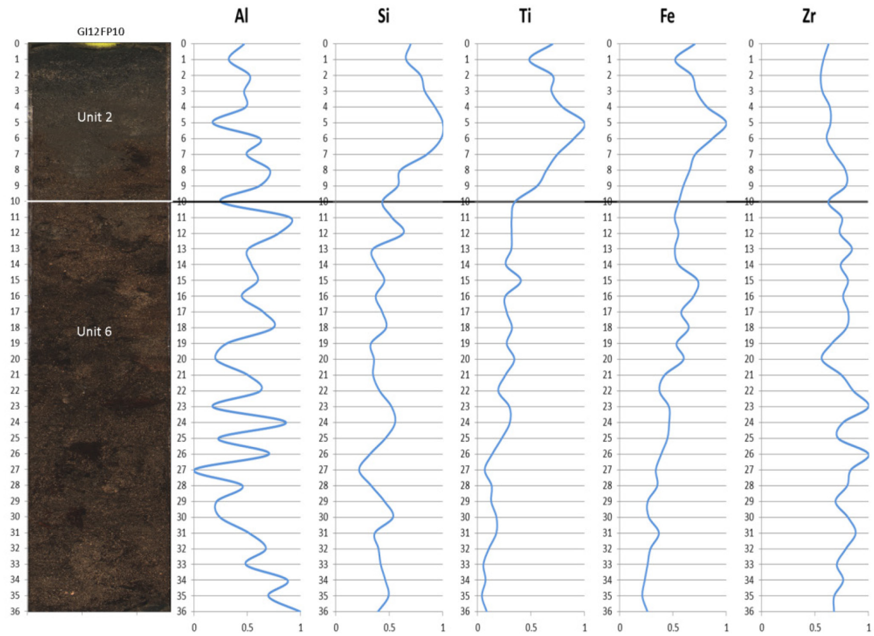

Core 10 Terrestrial Elemental Proxies

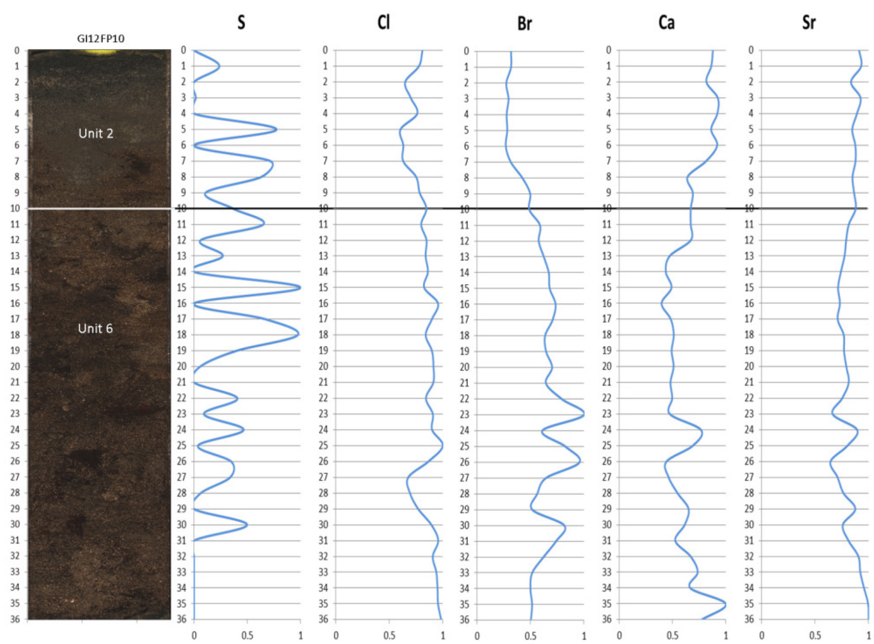

Core 10 Marine Elemental Proxies

Normalized XRF Data for GI12FP6A												
Depth in Core (cm)	Al	Si	Ti	Fe	Zr	S	Cl	Ca	Br	Sr	Mo inc	Mo coh
0	0.935	0.8499	0.9068	0.887836	0.9992	0.612	0.9739	0.764562	0.8807	0.80341	79666	29704
1	0.824	0.8118	0.9419	0.902031	0.9679	0.556	1.0000	0.803751	0.8701	0.87996	78973	30270
2	0.461	0.8629	1.0000	1.000000	0.8695	1.000	0.9647	0.768805	0.9140	0.85119	78952	30412
3	0.710	0.8266	0.9506	0.926082	0.9833	0.559	0.8732	0.748754	1.0000	0.84197	79690	30381
4	0.702	0.8234	0.9264	0.847662	0.9024	0.290	0.8620	0.738488	0.8236	0.83021	78909	30081
5	0.800	0.8234	0.9473	0.889904	1.0000	0.584	0.8889	0.777887	0.7869	0.84391	78681	30526
6	0.780	0.8991	0.9090	0.807443	0.8991	0.045	0.9309	0.871669	0.7652	0.92787	76435	29875
7	0.727	0.9204	0.8026	0.711543	0.8923	0.000	0.8792	0.970813	0.6560	0.98267	71657	29170
8	0.976	1.0000	0.7413	0.640262	0.8591	0.077	0.7663	0.975820	0.5785	0.99242	71591	29624
9	0.853	0.9554	0.8049	0.711505	0.9348	0.000	0.8707	0.999357	0.5609	1.00000	73146	29892
10	0.951	0.9082	0.7611	0.674148	0.9814	0.017	0.9371	0.967531	0.6450	0.96631	72559	29412
11	0.571	0.8687	0.7813	0.716408	0.9019	0.000	0.9028	0.919555	0.5229	0.94888	71290	29350
12	1.000	0.8816	0.7603	0.754857	0.7856	0.000	0.9100	1.000000	0.5982	0.99189	71805	29302
13	0.788	0.8661	0.8556	0.725755	0.9435	0.122	0.9635	0.910155	0.7536	0.95425	76312	30527
14	0.649	0.8111	0.7498	0.691350	0.9309	0.000	0.8267	0.890080	0.6911	0.94745	71116	28863
15	0.894	0.8001	0.6681	0.639543	0.8599	0.000	0.8775	0.908778	0.7116	0.99125	70874	28892

Normalized XRF Data for GI12FP6B												
Depth in Core (cm)	Al	Si	Ti	Fe	Zr	S	Cl	Ca	Br	Sr	Mo inc	Mo coh
0	0.708	0.7730	0.28593	1.000000	0.9550	0.828	0.06744	0.543390	0.5806	0.61678	86529	30752
1	0.539	0.7160	0.27584	0.957881	0.8840	0.586	0.06431	0.539678	0.6105	0.60092	85488	30764
2	0.523	0.8226	0.26026	0.844671	0.9586	0.382	0.06489	0.689033	0.5928	0.67478	81496	30773
3	0.640	0.7754	0.25408	0.828194	0.9022	0.000	0.06421	0.740145	0.6160	0.71686	82786	31322
4	0.506	0.7909	0.21551	0.732411	0.8594	0.000	0.06506	0.738925	0.5257	0.72471	79598	29651
5	0.367	0.7950	0.23329	0.785509	0.8237	0.000	0.06407	0.781982	0.5862	0.75612	79387	30685
6	0.357	0.7901	0.23562	0.756117	0.8369	0.000	0.05625	0.796229	0.5336	0.75676	76612	29739
7	0.412	0.8397	0.23535	0.837261	0.8866	0.000	0.06662	0.837279	0.5665	0.79834	78735	30510
8	0.545	0.8356	0.24379	0.834575	0.8066	0.000	0.06539	0.854480	0.5075	0.80482	78960	31079

9	0.519	0.8609	0.23349	0.832179	0.7631	0.000	0.06273	0.870548	0.5548	0.86177	77269	30630
10	0.597	0.8552	0.23157	0.840887	0.8774	0.000	0.06408	0.884434	0.5779	0.85615	79440	31030
11	0.604	0.8503	0.21894	0.834909	0.8334	0.000	0.07062	0.821473	0.6100	0.85541	76847	30324
12	0.643	1.0000	0.22677	0.724514	0.8724	0.000	0.05613	1.000000	0.5458	1.00000	75950	30187
13	0.675	0.8674	0.21229	0.723961	0.8026	0.000	0.06504	0.892605	0.6516	0.93996	77525	29611
14	0.461	0.8771	0.22910	0.666432	0.9096	0.000	0.05407	0.945024	0.5948	0.93194	76815	30136
15	0.692	0.9194	0.21867	0.664007	0.8123	0.000	0.06082	0.936800	0.6612	0.95200	77899	30576
16	0.565	0.8967	0.21585	0.652227	0.8260	0.000	0.06206	0.877680	0.5834	0.93911	74518	29747
17	0.685	0.8975	0.22636	0.841105	0.8405	0.000	0.05682	0.818491	0.6100	0.75842	74520	30098
18	0.367	0.8698	0.23562	0.944940	0.7785	0.000	0.07316	0.811527	0.5832	0.77504	77847	29842
19	0.542	0.8251	0.22388	0.696844	0.8331	0.000	0.06284	0.793825	0.6348	0.77936	78511	29733
20	0.571	0.9081	0.23596	0.764863	0.8457	0.000	0.06165	0.882239	0.5346	0.80741	78658	30283
21	0.338	0.8723	0.23047	0.790274	0.8241	0.000	0.06203	0.850429	0.5712	0.81537	80394	31292
22	0.864	0.9373	0.23432	0.755487	0.8620	0.000	0.05846	0.802603	0.6837	0.76810	82593	30774
23	0.581	0.9666	0.25278	0.739696	0.8743	0.000	0.05890	0.854853	0.6276	0.79790	81987	31138
24	0.601	0.9609	0.25079	0.771715	0.8601	0.000	0.05962	0.862219	0.6053	0.79860	81785	31461
25	0.695	0.9138	0.24049	0.753126	0.8246	0.000	0.05771	0.886488	0.6997	0.80088	82714	31062
26	0.565	0.9056	0.24214	0.759871	0.9115	0.000	0.06351	0.838055	0.7277	0.79491	85669	32104
27	0.669	0.9138	0.22059	0.689727	0.9283	0.000	0.06402	0.877342	0.7242	0.79837	84601	31720
28	0.575	0.8495	0.19746	0.650547	0.7806	0.000	0.06379	0.924678	0.7609	0.81555	81587	31263
29	0.380	0.9691	0.22711	0.673610	0.8272	0.000	0.05798	0.968453	0.6680	0.84241	80775	31635
30	0.718	0.8796	0.22155	0.663441	0.8708	0.000	0.06340	0.940979	0.7045	0.84478	82273	31470
31	0.617	0.8356	0.21181	0.676811	0.8180	0.191	0.06719	0.906362	0.6461	0.83288	83113	31779
32	0.497	0.8446	0.22780	0.719912	0.8341	0.000	0.06696	0.880540	0.6946	0.83704	85317	31920
33	0.896	0.8430	0.22622	0.629400	0.8241	0.000	0.07114	0.889792	0.8723	0.90212	87331	31473
34	0.854	0.9609	0.22594	0.615559	0.8260	0.000	0.06813	0.910810	0.9617	0.93753	90204	32176
35	0.760	0.8356	0.21201	0.615169	0.9318	0.000	0.06702	0.909029	0.8894	0.92991	85910	31631
36	0.578	0.8617	0.22512	0.694093	0.8045	0.000	0.06628	0.803105	0.6912	0.82998	84822	31612
37	0.510	0.7771	0.21462	0.752350	0.7901	0.061	0.06119	0.810127	0.6162	0.80718	84280	31021
38	0.568	0.7600	0.20611	0.765377	0.7877	0.000	0.06908	0.754649	0.6581	0.78345	85398	31539
39	0.649	0.7876	0.21153	0.729288	0.8649	0.159	0.06850	0.772731	0.6262	0.78213	87135	31736
40	0.461	0.7006	0.20769	0.812523	0.9198	0.000	0.07307	0.722594	0.6957	0.77887	88991	32149

41	0.360	0.6672	0.19774	0.789276	0.8786	0.885	0.07158	0.764671	0.6699	0.80591	87007	32045
42	0.731	0.8413	0.21613	0.673966	0.7948	0.000	0.06788	0.937723	0.5027	0.80744	82712	31427
43	0.688	0.8039	0.19629	0.620559	0.7889	0.000	0.06946	0.918888	0.5563	0.84520	84197	31513
44	0.812	0.7380	0.18710	0.538708	0.8499	0.000	0.06874	0.899171	0.6203	0.90301	89475	32746
45	0.610	0.8836	0.19870	0.572338	0.8246	0.000	0.07385	0.907827	0.6310	0.88870	86260	31619
46	0.617	0.8592	0.20240	0.644012	0.8573	0.000	0.06804	0.829779	0.6302	0.85183	87788	32028
47	0.565	0.7396	0.16198	0.615846	0.9153	0.000	0.07577	0.801360	0.7652	0.84399	92262	32352
48	0.662	0.7974	0.16651	0.603012	0.9117	0.000	0.07114	0.834863	0.6865	0.91225	88205	32474
49	0.594	0.7095	0.16520	0.513297	0.9051	0.000	0.07486	0.817020	0.7714	0.90552	91322	32177
50	0.808	0.8503	0.16870	0.524601	0.8613	0.000	0.07281	0.801197	0.8096	0.86657	96976	33486
51	0.854	0.8267	0.16115	0.523234	0.9529	0.000	0.07182	0.795728	0.7102	0.84662	95498	33393
52	0.604	0.7486	0.16479	0.550428	0.9191	0.557	0.07235	0.756832	0.8372	0.81863	97518	33580
53	0.643	0.7648	0.16163	0.550574	0.9822	0.029	0.07182	0.769381	0.8623	0.81879	100228	33716
54	0.731	0.6867	0.15319	0.540504	0.9434	0.264	0.08214	0.714831	0.8765	0.84375	97330	33200
55	0.682	0.7762	0.15896	0.527524	0.8791	0.334	0.07568	0.805726	0.7937	0.92919	94689	33305
56	0.760	0.7396	0.14811	0.483151	0.9110	0.000	0.08175	0.732674	0.8394	0.85058	100843	34028
57	0.705	0.6526	0.14063	0.471936	0.9122	0.000	0.08960	0.676040	0.9655	0.80075	104639	33785
58	0.932	0.7168	0.14310	0.519099	0.9491	0.000	0.08270	0.727479	0.8689	0.82069	102438	34290
59	0.597	0.7714	0.15504	0.551834	0.9200	0.000	0.07642	0.772241	0.8428	0.84968	97073	33066
60	0.821	0.7771	0.15841	0.570731	0.9993	0.790	0.07385	0.768108	0.7386	0.84020	95403	33722
61	0.688	0.7071	0.16321	0.578569	0.7950	0.000	0.07722	0.760602	0.7430	0.85016	94674	32873
62	0.601	0.7177	0.16788	0.691042	0.9134	0.838	0.07664	0.645310	0.7698	0.78511	93176	32485
63	0.555	0.7022	0.17536	0.631448	0.9207	0.000	0.07587	0.701874	0.7261	0.79129	93502	32395
64	0.393	0.6843	0.17804	0.641660	0.9617	0.459	0.07731	0.723113	0.6981	0.80562	91302	32454
65	0.672	0.7665	0.19087	0.714504	0.9112	0.990	0.06865	0.726423	0.7213	0.76120	91691	32333
66	0.682	0.7315	0.17344	0.702218	0.8743	0.424	0.07122	0.680675	0.6940	0.77239	92416	32706
67	0.669	0.8096	0.20206	0.832278	0.8883	0.248	0.07340	0.663614	0.6920	0.69335	91750	31983
68	0.539	0.7779	0.21126	0.804004	0.9307	0.917	0.07144	0.699877	0.6979	0.68843	90906	32081
69	0.549	0.8267	0.20377	0.780461	0.9290	0.780	0.07491	0.714306	0.6689	0.74409	91335	32567
70	0.584	0.8169	0.19918	0.761161	0.9704	0.293	0.07054	0.726621	0.6807	0.73472	91482	32351
71	0.779	0.8421	0.19959	0.750358	0.7924	0.933	0.06968	0.729487	0.6020	0.76036	90510	31958
72	0.584	0.8609	0.20075	0.760419	0.8880	0.943	0.07911	0.788683	0.7499	0.78310	94157	33039

73	0.753	0.6737	0.16397	0.609015	0.8473	0.557	0.06545	0.597123	0.6100	0.65854	86205	30676
74	0.649	0.7356	0.17701	0.662216	0.8708	0.000	0.06391	0.690749	0.6258	0.70624	84333	30541
75	0.643	0.7925	0.18270	0.661684	0.8982	0.000	0.08178	0.707757	0.7841	0.74342	93690	32773
76	0.692	0.8478	0.18421	0.696776	0.8551	0.274	0.07269	0.686973	0.6964	0.69689	91815	32046
77	0.776	0.8959	0.20206	0.710981	0.9131	0.146	0.07485	0.717744	0.6839	0.73082	92672	32745
78	0.646	0.8120	0.17914	0.669201	0.9112	0.589	0.07697	0.655227	0.7298	0.70601	97451	32562
79	0.672	0.8519	0.20570	0.720306	0.8753	0.424	0.07184	0.724181	0.6806	0.71407	90506	31644
80	1.000	0.7925	0.18771	0.690952	1.0000	0.430	0.08061	0.654427	0.8490	0.72588	99127	33472
81	0.649	0.7168	0.16884	0.599142	0.9172	0.172	0.07691	0.584206	1.0000	0.62277	103674	33028
82	0.584	0.7274	0.18222	0.656178	0.8738	0.691	0.06915	0.561577	0.8159	0.64318	91230	30719
83	0.630	0.7567	0.20144	0.718892	0.8885	0.373	0.07999	0.600385	0.7476	0.65246	95553	32223
84	0.623	0.7632	0.20563	0.791568	0.8398	1.000	0.07594	0.587976	0.7453	0.63377	94280	32353
85	0.636	0.7941	0.21572	0.791723	0.8317	0.656	0.07914	0.621672	0.7465	0.67118	94260	32207
86	0.714	0.8145	0.21544	0.781957	0.9209	0.261	0.06614	0.644225	0.7194	0.66547	93419	32531
87	0.000	0.4605	1.00000	0.290759	0.9131	0.000	1.00000	0.507319	0.5296	0.30803	101561	25832

Normalized XRF Data for GI12FP6C

Depth in Core (cm)	Al	Si	Ti	Fe	Zr	S	Cl	Ca	Br	Sr	Mo inc	Mo coh
0	1.000	0.9467	0.8664	0.663794	0.8687	0.068	0.9191	0.927180	0.6486	0.94318	85703	31415
1	0.579	0.9248	0.8934	0.668405	0.8509	0.000	0.9010	0.966046	0.6568	0.96427	80819	30796
2	0.206	0.7659	0.8421	0.665589	0.8984	0.000	0.9504	0.845839	0.6460	0.89431	80882	30432
3	0.561	0.8896	0.8728	0.618834	0.7950	0.000	0.8084	0.918617	0.6224	0.88961	81472	30302
4	0.482	0.8107	0.8047	0.673697	0.8216	0.000	0.9340	0.878286	0.6703	0.88536	80684	29682
5	0.329	0.7659	0.7975	0.596470	0.8884	0.000	1.0000	0.921501	0.6656	0.92907	80043	30142
6	0.618	0.8658	0.8591	0.607654	0.8082	0.000	0.9984	0.911859	0.6095	0.91248	83943	30800
7	0.754	0.7659	0.7880	0.576954	0.8283	0.081	0.9204	0.976489	0.6491	0.90945	83665	30571
8	0.535	0.8706	0.7356	0.565453	0.8365	0.000	0.9051	0.982854	0.6065	0.92646	81498	30666
9	0.535	0.8335	0.8025	0.584385	0.8730	0.056	0.8480	0.996451	0.5813	0.95005	83842	31463
10	0.675	0.7945	0.8806	0.675848	0.8761	0.267	0.8223	0.792513	0.6627	0.78062	87973	31074
11	0.522	0.7812	0.9311	0.747690	0.9630	0.000	0.8757	0.696861	0.6664	0.71509	91387	31458
12	0.404	0.9144	0.9529	0.751264	0.7945	0.154	0.7388	0.789025	0.5281	0.73089	82081	28988

13	0.531	0.9220	1.0000	0.816084	0.7366	0.173	0.8003	0.844108	0.4632	0.80951	78125	29758
14	0.355	0.7469	0.9074	1.000000	0.7671	0.945	0.8807	0.830762	0.4503	0.81354	76868	29567
15	0.614	0.9239	0.9107	0.858351	0.7683	0.235	0.8260	0.886109	0.4887	0.86722	80166	29683
16	0.781	0.8259	0.7749	0.562316	0.8838	0.218	0.8245	0.939631	0.6042	0.92747	86136	31052
17	0.689	0.8906	0.7830	0.551526	0.8403	0.000	0.8604	0.991301	0.5506	0.98099	84303	30682
18	0.636	0.9753	0.8954	0.614672	0.7870	0.000	0.7980	0.960347	0.5528	0.91074	83003	30442
19	0.798	1.0000	0.8430	0.584080	0.8595	0.196	0.8648	1.000000	0.6406	0.97796	88445	31753
20	0.728	0.9248	0.7331	0.521878	0.8389	0.087	0.8780	0.989116	0.6423	1.00000	89657	31499
21	0.816	0.8877	0.7001	0.490636	0.8576	0.000	0.9454	0.969412	0.6338	0.99989	91232	31385
22	0.583	0.8192	0.6268	0.476304	0.8216	0.000	0.9344	0.849129	0.7009	0.96386	91605	30681
23	0.645	0.8335	0.6391	0.546226	0.8862	0.467	0.9771	0.828109	0.7055	0.93190	90082	31501
24	0.632	0.8982	0.7244	0.595577	0.8960	0.249	0.9100	0.873570	0.6314	0.92723	88452	31444
25	0.579	0.7555	0.7152	0.595960	0.9818	0.966	0.8497	0.845927	0.6078	0.88794	88221	31078
26	0.873	0.7631	0.6990	0.585089	0.8764	0.307	0.8863	0.791427	0.6579	0.88836	88969	30740
27	0.544	0.7536	0.5813	0.520106	0.9705	0.330	0.9859	0.690191	0.8056	0.82980	99522	32341
28	0.588	0.7307	0.5490	0.489271	1.0000	1.000	0.9761	0.619224	1.0000	0.65251	113429	33165
29	0.561	0.7678	0.6499	0.588126	0.8274	0.460	0.9187	0.770380	0.6676	0.85337	88699	30749
30	0.632	0.7897	0.6379	0.563929	0.9023	0.510	0.9156	0.789657	0.5883	0.88842	89434	31218

Normalized XRF Data for GI12FP7												
Depth in Core (cm)	Al	Si	Ti	Fe	Zr	S	Cl	Ca	Br	Sr	Mo inc	Mo coh
0	0.496	0.7875	0.9261	0.917299	0.6989	0.542	0.6203	0.556003	0.4105	0.62405	87407	31285
1	0.297	0.8618	1.0000	1.000000	0.6729	0.443	0.5750	0.579670	0.4747	0.62538	91135	31321
2	0.264	0.9070	0.9161	0.912182	0.6903	0.627	0.5721	0.661785	0.4050	0.61212	89909	31060
3	0.399	1.0000	0.9391	0.979650	0.6814	0.289	0.6078	0.715947	0.3685	0.69166	85419	31228
4	0.591	0.9539	0.8105	0.887342	0.6208	0.424	0.5291	0.730655	0.2938	0.74967	79035	29949
5	0.587	0.9300	0.8095	0.796842	0.6651	0.000	0.6378	0.774600	0.3201	0.80738	79464	30167
6	0.594	0.7892	0.7328	0.725043	0.6444	0.000	0.6695	0.757705	0.3854	0.83565	83415	30889
7	0.275	0.7892	0.7592	0.744401	0.6695	0.574	0.6022	0.755345	0.3479	0.79807	82172	30068
8	0.623	0.9283	0.7202	0.673380	0.6106	0.064	0.6147	0.826632	0.3064	0.84112	81516	30549
9	0.630	0.9403	0.6939	0.662072	0.5629	0.493	0.5381	0.874879	0.3061	0.88298	81851	30509

10	0.547	0.9616	0.7073	0.622070	0.6163	0.606	0.5716	0.863304	0.3020	0.83623	84479	31007
11	0.609	0.7730	0.6354	0.572894	0.6979	0.000	0.6074	0.847182	0.3869	0.89626	84972	31784
12	0.674	0.7713	0.5988	0.528985	0.6934	0.000	0.6904	0.827055	0.4184	0.95823	87370	31030
13	0.634	0.6340	0.4936	0.500952	0.6197	0.368	0.7333	0.791850	0.4691	0.87282	88130	30970
14	0.500	0.6544	0.5325	0.550816	0.6180	0.291	0.7163	0.815893	0.4066	0.80597	84034	30740
15	0.380	0.5956	0.5030	0.588023	0.6594	0.439	0.7411	0.710878	0.3980	0.76897	88377	31092
16	0.380	0.7108	0.5302	0.558611	0.5762	0.000	0.7184	0.842279	0.3882	0.81356	84100	30714
17	0.493	0.7705	0.5379	0.581711	0.7057	0.533	0.6566	0.807341	0.4567	0.79261	90114	31640
18	0.620	0.6783	0.4950	0.548949	0.6157	0.501	0.7041	0.777398	0.4799	0.79181	89960	31702
19	0.746	0.6416	0.4671	0.463790	0.6620	0.000	0.7795	0.734221	0.4800	0.78036	97448	32056
20	0.399	0.5751	0.4107	0.399467	0.6389	0.000	0.8518	0.712648	0.5308	0.76115	95027	31607
21	1.000	0.4394	0.2544	0.295123	0.9415	0.000	1.0000	0.369154	0.9073	0.58386	128231	36317
22	0.551	0.5759	0.4056	0.442989	0.7912	0.000	0.8747	0.576610	0.6919	0.62796	111408	32904
23	0.533	0.5725	0.4081	0.435825	0.7508	0.000	0.8332	0.638265	0.5556	0.74110	99161	32861
24	0.768	0.5589	0.3672	0.381705	0.8294	0.000	0.8685	0.545305	0.7368	0.61680	118643	34653
25	0.714	0.6041	0.4397	0.445240	0.7451	0.000	0.7531	0.671099	0.5908	0.68929	103996	32951
26	0.543	0.6578	0.4810	0.508041	0.6455	0.122	0.7485	0.775999	0.4224	0.80292	91056	31889
27	0.714	0.6519	0.4449	0.457107	0.6981	0.000	0.7286	0.797666	0.4375	0.84503	89797	31561
28	0.565	0.6783	0.5647	0.636549	0.6655	0.148	0.6343	0.838734	0.3444	0.79399	82312	30634
29	0.500	0.5776	0.4992	0.541469	0.7390	0.000	0.8596	0.572282	0.5825	0.67067	100477	32861
30	0.312	0.6578	0.6098	0.744323	0.6630	0.090	0.6723	0.685238	0.3297	0.69631	83818	30475
31	0.594	0.7406	0.6286	0.680811	0.5315	0.325	0.5969	0.798032	0.3106	0.77023	81658	30338
32	0.438	0.6911	0.5903	0.683350	0.6079	0.347	0.6344	0.777022	0.3345	0.80264	83776	30691
33	0.293	0.6800	0.6056	0.763798	0.5885	0.236	0.6842	0.711431	0.3197	0.83148	84285	30708
34	0.478	0.6160	0.5391	0.705113	0.5956	0.535	0.6774	0.707025	0.3735	0.79822	85877	30610
35	0.601	0.7961	0.5879	0.589052	0.6387	0.218	0.6344	0.838097	0.3562	0.85968	84014	30901
36	0.435	0.7491	0.5845	0.623708	0.6704	0.000	0.6120	0.808625	0.4064	0.81825	86857	31473
37	0.688	0.7602	0.5895	0.533152	0.5975	0.000	0.6494	0.894850	0.2861	0.85389	85169	31469
38	0.630	0.6894	0.4629	0.451923	0.5703	0.000	0.6341	0.973018	0.3516	0.91604	82887	31809
39	0.493	0.7406	0.4507	0.463265	0.5486	0.000	0.5908	1.000000	0.3195	0.92737	83131	31102
40	0.804	0.6928	0.4257	0.423725	0.6746	0.375	0.5718	0.966805	0.4210	0.88476	94487	32287
41	0.612	0.7372	0.4111	0.439965	0.6280	0.169	0.6085	0.931459	0.3810	0.90336	87953	32119

42	0.717	0.7884	0.4924	0.486602	0.6377	0.000	0.5830	0.922651	0.4011	0.89531	89137	31814
43	0.678	0.6945	0.4183	0.442163	0.7124	0.171	0.6519	0.791970	0.3638	0.85561	91460	31976
44	0.656	0.7065	0.4613	0.522719	0.6408	0.251	0.6233	0.800564	0.3620	0.85762	85934	31488
45	0.507	0.6894	0.4786	0.545669	0.6563	0.484	0.6355	0.816916	0.3559	0.86989	88116	31493
46	0.652	0.5137	0.3654	0.480309	0.7832	0.430	0.8483	0.580119	0.5371	0.77531	103603	33848
47	0.891	0.5205	0.2396	0.265956	1.0000	0.000	0.9665	0.317248	1.0000	0.56904	143751	37440
48	0.935	0.5102	0.2724	0.316601	0.9193	0.000	0.9121	0.387005	0.8728	0.54934	135747	35472
49	0.652	0.6834	0.4042	0.482251	0.6189	0.649	0.6908	0.696552	0.4233	0.78082	93047	31258
50	0.783	0.6766	0.4377	0.561462	0.6655	0.458	0.6764	0.756541	0.3866	0.80886	91483	31478
51	0.355	0.6357	0.4371	0.487695	0.6733	1.000	0.7170	0.721189	0.4489	0.86007	94807	31921
52	0.710	0.7261	0.4637	0.512895	0.7107	0.456	0.7046	0.760080	0.4086	0.82272	96054	32536
53	0.601	0.7184	0.4467	0.488810	0.6864	0.041	0.6438	0.779314	0.4129	0.83079	97112	33038
54	0.620	0.6911	0.4647	0.480065	0.6774	0.334	0.5784	0.739666	0.3995	0.80264	92599	31637
55	0.688	0.7150	0.4579	0.486887	0.6351	0.816	0.5537	0.809627	0.2961	0.86868	86128	30475
56	0.558	0.7193	0.4710	0.499825	0.6258	0.000	0.6835	0.829347	0.3146	0.96164	84314	30897
57	0.406	0.5887	0.4289	0.463528	0.7439	0.000	0.7497	0.675631	0.4961	0.89263	103237	33114
58	0.783	0.5171	0.3700	0.389921	0.9310	0.165	0.8409	0.532472	0.7464	0.65206	135101	36430
59	0.656	0.5256	0.3033	0.357681	0.8497	0.000	0.8406	0.431524	0.7624	0.69753	123944	34543
60	0.659	0.6382	0.5010	0.522407	0.6201	0.000	0.6158	0.763422	0.3202	0.90661	80813	29641
61	0.449	0.7568	0.5461	0.567060	0.6581	0.039	0.5608	0.838954	0.2926	0.96999	80633	30133
62	0.290	0.7346	0.5435	0.585438	0.6776	0.308	0.5962	0.826021	0.3066	0.87003	85115	31450
63	0.435	0.7688	0.5066	0.561628	0.6282	0.439	0.5154	0.800334	0.2592	0.80014	84713	30405
64	0.880	0.8541	0.5381	0.568544	0.6812	0.000	0.5848	0.807027	0.3107	0.82826	84907	30657
65	0.623	0.7500	0.5379	0.553926	0.6598	0.385	0.5768	0.779377	0.3228	0.81178	86403	31482
66	0.525	0.7824	0.4894	0.544516	0.6645	0.304	0.5184	0.798951	0.3692	0.79731	90426	31917
67	0.286	0.7090	0.4868	0.560027	0.6254	0.321	0.5955	0.729402	0.3495	0.79890	85769	30586
68	0.634	0.5990	0.5292	0.661171	0.7029	0.561	0.5565	0.747336	0.2798	0.79244	83900	30560
69	0.554	0.7355	0.5447	0.619057	0.6448	0.418	0.6130	0.702613	0.3650	0.79506	87094	30604
70	0.518	0.7363	0.5541	0.615387	0.6292	0.465	0.5806	0.723909	0.3470	0.81861	87240	30731
71	0.475	0.7201	0.5873	0.657940	0.6964	0.544	0.5622	0.709071	0.3391	0.81308	85484	30519
72	0.656	0.7082	0.5387	0.612817	0.6180	0.000	0.5783	0.729110	0.3152	0.83841	84054	30612
73	0.478	0.7065	0.5513	0.593759	0.6822	0.692	0.5989	0.721262	0.3936	0.79391	89721	31345

74	0.377	0.6578	0.5633	0.635812	0.6898	0.458	0.6480	0.671183	0.3932	0.78079	89783	31187
75	0.558	0.6971	0.5893	0.639130	0.7008	0.000	0.6526	0.657488	0.3456	0.77336	89131	31612
76	0.482	0.6621	0.5887	0.642864	0.6879	0.150	0.6051	0.678544	0.3631	0.77745	88336	30806
77	0.420	0.7082	0.6012	0.628021	0.7141	0.383	0.5866	0.670969	0.3578	0.78807	86096	31036
78	0.496	0.7816	0.6228	0.623306	0.7025	0.306	0.5140	0.687796	0.2621	0.82256	84859	30427
79	0.478	0.8234	0.5903	0.617727	0.6818	0.242	0.6162	0.662605	0.3276	0.79362	87097	30533
80	0.543	0.7679	0.6026	0.623678	0.6892	0.000	0.6390	0.681066	0.2703	0.85651	81132	30478
81	0.413	0.8558	0.6358	0.636639	0.6755	0.026	0.5486	0.700770	0.2432	0.88108	80045	30143
82	0.580	0.8447	0.6192	0.632161	0.5838	0.700	0.5596	0.718407	0.2398	0.94170	75014	28907
83	0.420	0.8003	0.6100	0.619606	0.6615	0.563	0.6376	0.693388	0.2388	0.93738	75131	29630
84	0.605	0.8618	0.7013	0.638818	0.6695	0.600	0.5143	0.738272	0.2037	0.95834	75619	29215
85	0.420	0.7799	0.6997	0.654217	0.7350	0.805	0.5156	0.714679	0.2110	0.87552	78552	29979
86	0.605	0.9437	0.6865	0.673252	0.6252	0.073	0.5846	0.794126	0.1871	1.00000	76321	30181

Normalized XRF Data for GI12FP8												
Depth in Core (cm)	Al	Si	Ti	Fe	Zr	S	Cl	Ca	Br	Sr	Mo inc	Mo coh
0	0.000	0.598	0.8544	0.853949	0.6128	0.469	0.7092	0.475642	0.4997	0.36502	93378	30289
1	0.199	0.914	1.0000	1.000000	0.6237	0.517	0.6874	0.532985	0.4921	0.40432	93950	31386
2	0.000	0.723	0.8911	0.919198	0.5836	0.376	0.5932	0.580246	0.3987	0.43241	88222	30047
3	0.244	0.788	0.8399	0.889159	0.6487	0.954	0.6678	0.613987	0.4485	0.46499	92065	31224
4	0.692	0.858	0.8473	0.805809	0.6114	0.677	0.5475	0.665271	0.3872	0.49357	85080	30814
5	0.244	0.793	0.8627	0.806630	0.5852	0.406	0.5943	0.589924	0.4825	0.45226	94844	31276
6	0.365	0.909	0.9257	0.888005	0.6312	0.000	0.5668	0.595229	0.4648	0.45669	92642	31366
7	0.205	0.800	0.8939	0.871192	0.5685	0.468	0.5673	0.610513	0.4257	0.44388	85775	29498
8	0.250	0.971	0.9578	0.929721	0.5857	0.607	0.4525	0.722204	0.2512	0.49159	79109	30043
9	0.359	0.971	0.9679	0.869444	0.6231	0.534	0.4489	0.751982	0.2807	0.49613	78677	29545
10	0.115	1.000	0.9889	0.916051	0.5231	0.387	0.4204	0.735229	0.2668	0.50261	77837	29514
11	0.506	0.962	0.9430	0.870765	0.5450	0.489	0.4891	0.740177	0.3132	0.51444	78681	28875
12	0.647	0.766	0.7660	0.721636	0.6006	0.370	0.5024	0.784103	0.3359	0.55044	79650	28864
13	0.481	0.890	0.7236	0.694452	0.5773	0.105	0.5623	0.795249	0.3215	0.56371	82888	29993
14	0.654	0.823	0.6394	0.598342	0.5909	0.382	0.5898	0.815614	0.2977	0.64660	82233	30133

15	0.410	0.412	0.3023	0.287244	0.8860	0.147	0.8645	0.395546	1.0000	0.40859	148918	37209
16	0.615	0.361	0.2183	0.259945	0.7476	0.092	0.8838	0.455917	0.8565	0.44008	132611	34626
17	0.487	0.335	0.2201	0.269146	0.7195	0.000	0.9128	0.475043	0.7151	0.53908	123398	34011
18	0.397	0.262	0.1373	0.145319	1.0000	0.000	1.0000	0.222416	0.9759	0.34454	165484	38883
19	0.442	0.214	0.1389	0.180571	0.7875	0.000	0.9884	0.364307	0.7897	0.56643	133227	34902
20	1.000	0.375	0.1710	0.195806	0.6633	0.000	0.9717	0.488836	0.7859	0.62371	126399	33912
21	0.417	0.294	0.1657	0.198066	0.7143	0.143	0.9090	0.470392	0.7198	0.67164	123327	34047
22	0.314	0.271	0.2628	0.222348	0.7216	0.166	0.8235	0.603886	0.6475	0.70575	116060	32852
23	0.410	0.415	0.1756	0.202384	0.6211	0.000	0.7995	0.843525	0.4614	0.99889	96763	30828
24	0.449	0.468	0.2086	0.225300	0.5935	0.019	0.8225	0.731544	0.5259	0.86148	104698	32168
25	0.660	0.501	0.2898	0.281645	0.6041	0.183	0.7587	0.729115	0.5100	0.80181	99939	31700
26	0.250	0.540	0.3212	0.329988	0.5839	0.000	0.7217	0.905756	0.4128	0.78338	93365	31198
27	0.468	0.512	0.3189	0.338681	0.5661	0.000	0.7631	0.773482	0.5062	0.67861	98174	31801
28	0.423	0.513	0.3643	0.387919	0.6636	0.111	0.7709	0.778315	0.5006	0.60724	102315	33172
29	0.571	0.508	0.3401	0.374412	0.5815	0.399	0.8016	0.749160	0.5140	0.57903	101970	32279
30	0.365	0.547	0.3856	0.390192	0.6164	0.000	0.7681	0.795974	0.4334	0.62362	98775	32694
31	0.455	0.492	0.3544	0.400800	0.5951	0.124	0.7077	0.835611	0.4137	0.60920	94127	31397
32	0.506	0.524	0.4096	0.417328	0.5847	0.279	0.7232	0.891620	0.4346	0.63230	91536	31573
33	0.359	0.561	0.4158	0.425757	0.5424	0.342	0.6903	0.921252	0.3437	0.68095	87282	31130
34	0.692	0.434	0.3523	0.392697	0.6323	0.088	0.7525	0.768293	0.4308	0.62178	97656	32601
35	0.083	0.451	0.3537	0.387249	0.7107	0.000	0.7876	0.664347	0.5187	0.54168	107428	33320
36	0.667	0.649	0.4425	0.441764	0.5489	0.000	0.7631	0.996865	0.2991	0.72668	86790	31260
37	0.462	0.565	0.4040	0.425456	0.5338	0.042	0.7549	0.907538	0.3464	0.70254	86943	30934
38	0.487	0.666	0.4986	0.495503	0.5852	0.399	0.6319	0.921675	0.3372	0.61877	88685	31781
39	0.551	0.633	0.4772	0.458369	0.5604	0.672	0.6594	0.888436	0.3952	0.60609	92715	30871
40	0.590	0.618	0.4931	0.497959	0.5021	0.263	0.5756	1.000000	0.3103	0.66401	83842	30196
41	0.840	0.563	0.4303	0.460508	0.5325	0.500	0.6658	0.854218	0.3633	0.59625	93307	31256
42	0.000	0.738	0.5014	0.485708	0.5580	0.261	0.5857	0.974711	0.3261	0.60603	87988	30780
43	0.218	0.688	0.4947	0.485497	0.4901	0.090	0.5856	0.974596	0.3081	0.62649	86786	30709
44	0.372	0.586	0.4815	0.483212	0.5648	0.000	0.6454	0.899630	0.3049	0.59429	88357	30912
45	0.654	0.617	0.4707	0.477825	0.5883	0.372	0.6194	0.914021	0.2956	0.60457	86011	31165
46	0.385	0.650	0.4922	0.489766	0.5146	0.399	0.6267	0.963571	0.3041	0.66481	84568	30666

47	0.679	0.628	0.4414	0.470075	0.5615	0.187	0.6519	0.864410	0.3471	0.66657	88013	31583
48	0.096	0.591	0.4522	0.465444	0.5779	0.563	0.6381	0.828597	0.3449	0.68507	88840	31156
49	0.308	0.583	0.4488	0.462236	0.5593	0.073	0.6656	0.814527	0.3217	0.75277	87078	30318
50	0.205	0.577	0.4114	0.462159	0.6268	0.261	0.6658	0.762505	0.3948	0.65192	91711	30693
51	0.564	0.584	0.4499	0.471213	0.5739	0.029	0.6707	0.873369	0.3529	0.69990	90880	31253
52	0.212	0.570	0.4783	0.455812	0.5619	0.515	0.6393	0.833098	0.3844	0.69366	91832	30699
53	0.000	0.555	0.4587	0.442016	0.5432	0.687	0.6325	0.860972	0.3175	0.82401	87538	30728
54	0.494	0.632	0.4525	0.450266	0.5807	0.527	0.6363	0.814334	0.3760	0.72916	91512	30754
55	0.577	0.570	0.4539	0.470681	0.5578	1.000	0.6672	0.709034	0.4175	0.71996	98068	32171
56	0.231	0.592	0.4603	0.462533	0.5175	0.511	0.6694	0.732565	0.3723	0.83981	90202	30885
57	0.205	0.461	0.5427	0.447001	0.5786	0.597	0.7027	0.711596	0.3683	0.93461	89216	30787
58	0.231	0.475	0.4633	0.462545	0.5119	0.565	0.7313	0.765297	0.3535	0.96031	86376	29992
59	0.519	0.407	0.3754	0.440211	0.7256	0.656	0.7621	0.435177	0.5643	0.70192	114846	33503
60	0.353	0.336	0.4315	0.494901	0.7117	0.544	0.7858	0.383754	0.5869	0.64417	115875	33302
61	0.109	0.292	0.4029	0.424435	0.6627	0.679	0.7191	0.408221	0.5317	0.68668	112456	32348
62	0.212	0.219	0.3539	0.367171	0.8024	0.616	0.7385	0.353759	0.7258	0.50261	135271	34555
63	0.256	0.274	0.2681	0.290082	0.7782	0.681	0.7983	0.339272	0.7492	0.56544	139790	35653
64	0.231	0.361	0.3632	0.354250	0.6198	0.527	0.7312	0.532720	0.4948	0.83057	108992	32384
65	0.154	0.274	0.2822	0.287069	0.6815	0.181	0.8164	0.393764	0.6658	0.71328	127728	34858
66	0.167	0.408	0.2880	0.303690	0.6601	0.212	0.9659	0.399304	0.5962	0.76352	107267	31722
67	0.154	0.642	0.5192	0.488534	0.5487	0.303	0.8337	0.711819	0.3710	1.00000	84069	30010

Normalized XRF Data for GI12FP10

Depth in Core (cm)	Al	Si	Ti	Fe	Zr	S	Cl	Ca	Br	Sr	Mo inc	Mo coh
0	0.470	0.699	0.7002	0.702554	0.6254	0.000	0.80960	0.878855	0.3174	0.911760	63209	26348
1	0.326	0.657	0.4824	0.519040	0.5776	0.238	0.77675	0.863784	0.3175	0.930355	61038	25244
2	0.523	0.793	0.7011	0.676351	0.5520	0.000	0.64771	0.818344	0.2731	0.835039	56857	24111
3	0.470	0.832	0.6902	0.717922	0.5670	0.016	0.69993	0.925091	0.2941	0.924295	60366	25716
4	0.485	0.927	0.7936	0.818946	0.6372	0.000	0.76046	0.920399	0.2762	0.890829	60738	25715
5	0.174	1.000	1.0000	1.000000	0.6439	0.775	0.60381	0.862984	0.2823	0.847132	61218	25876

6	0.621	0.984	0.8993	0.868893	0.6083	0.000	0.63025	0.919167	0.2682	0.875870	60539	26002
7	0.492	0.851	0.7451	0.707386	0.6840	0.717	0.62884	0.815579	0.3155	0.877581	63657	25648
8	0.712	0.604	0.6439	0.656001	0.7823	0.632	0.75056	0.641506	0.4232	0.849240	71275	26659
9	0.614	0.579	0.5561	0.595976	0.7867	0.107	0.78307	0.690453	0.4969	0.863688	75308	27589
10	0.250	0.434	0.3497	0.553831	0.6235	0.365	0.84610	0.671053	0.4882	0.879260	75609	27012
11	0.902	0.524	0.3181	0.514958	0.7495	0.651	0.79779	0.670711	0.5888	0.814765	81399	28072
12	0.795	0.631	0.3176	0.549617	0.7307	0.062	0.84734	0.671701	0.5767	0.789946	80161	28562
13	0.508	0.346	0.3153	0.516421	0.8446	0.270	0.83895	0.473809	0.6244	0.774760	82232	28352
14	0.538	0.377	0.2641	0.551557	0.7387	0.000	0.86065	0.436368	0.6710	0.740480	84933	27392
15	0.598	0.453	0.4046	0.731623	0.8071	1.000	0.82581	0.490218	0.6793	0.714494	87636	28380
16	0.447	0.372	0.2581	0.691604	0.7614	0.000	0.95518	0.396978	0.7343	0.731183	90634	28938
17	0.652	0.434	0.2719	0.576226	0.8102	0.671	0.89765	0.483731	0.7058	0.710170	93889	29598
18	0.742	0.469	0.3213	0.646532	0.7924	0.974	0.83978	0.511130	0.6356	0.767344	87490	28604
19	0.303	0.327	0.2719	0.531921	0.6540	0.397	0.89840	0.491451	0.6462	0.769692	84467	28211
20	0.205	0.356	0.3432	0.597651	0.5626	0.055	0.91303	0.509703	0.7019	0.790988	90890	29384
21	0.508	0.348	0.2586	0.418766	0.7480	0.000	0.91128	0.480634	0.6441	0.813887	82953	27669
22	0.621	0.409	0.1931	0.372292	0.8580	0.407	0.84219	0.496890	0.7934	0.752694	95052	29863
23	0.174	0.521	0.2966	0.461034	0.9992	0.091	0.90721	0.474957	1.0000	0.663305	112737	31908
24	0.864	0.553	0.3011	0.462665	0.7609	0.466	0.89998	0.767269	0.6099	0.892963	84178	29577
25	0.227	0.463	0.2252	0.446495	0.7157	0.036	1.00000	0.690306	0.8249	0.802053	104440	31830
26	0.705	0.319	0.1355	0.388207	1.0000	0.349	0.86480	0.443351	0.9581	0.643668	114088	32360
27	0.000	0.217	0.0659	0.337651	0.8335	0.339	0.67623	0.463241	0.6433	0.709640	84047	27561
28	0.455	0.330	0.1304	0.351537	0.8002	0.062	0.69261	0.547228	0.5624	0.764642	74326	26226
29	0.212	0.455	0.1268	0.261385	0.6902	0.000	0.76977	0.650584	0.5161	0.875264	71484	26543
30	0.242	0.534	0.1757	0.271224	0.8058	0.498	0.89299	0.614201	0.8161	0.758450	102811	30692
31	0.515	0.364	0.1744	0.366385	0.8792	0.000	0.95676	0.525590	0.7385	0.811520	89979	29114
32	0.674	0.398	0.1043	0.287024	0.7870	0.000	0.90604	0.669658	0.6211	0.904350	84180	28986
33	0.485	0.419	0.0540	0.260195	0.7026	0.000	0.93955	0.736083	0.5154	0.921770	77381	27304
34	0.879	0.463	0.0732	0.233030	0.7622	0.000	0.95028	0.666788	0.4990	0.956789	74242	27408
35	0.697	0.492	0.0398	0.210820	0.6778	0.000	0.95527	1.000000	0.5146	0.995310	75599	27544
36	1.000	0.392	0.0851	0.259480	0.6762	0.000	0.98445	0.775078	0.5030	1.000000	78837	28746

APPENDIX H
SEM IMAGES

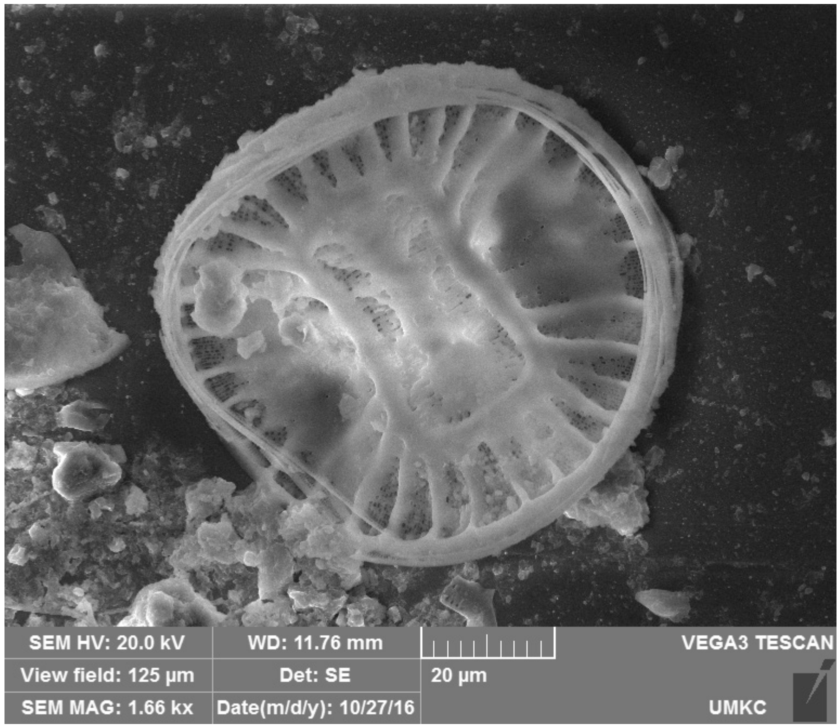

Campylodiscus clypeus, Core GI12FP7, Unit 5

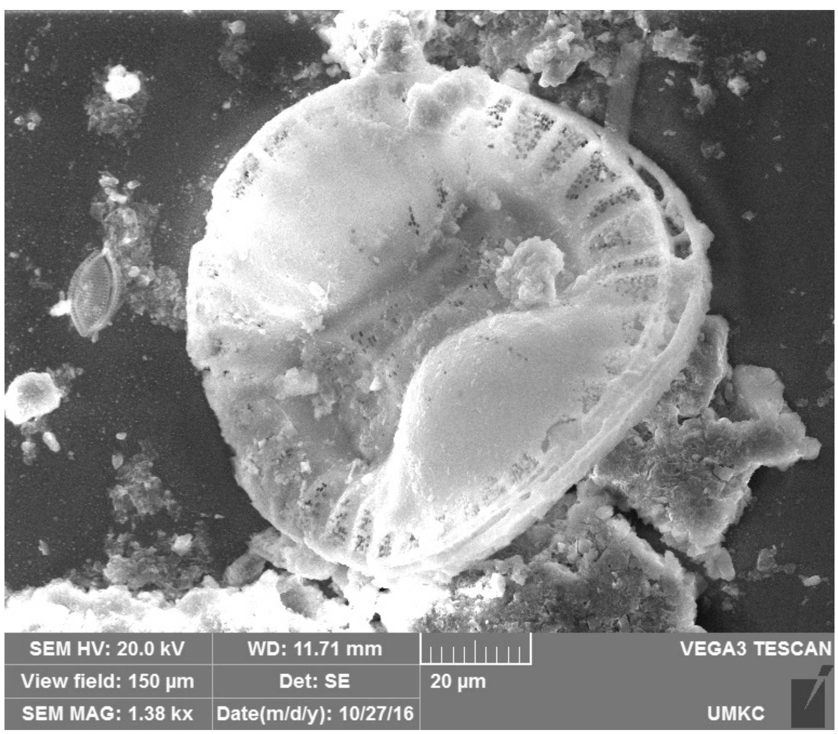

Campylodiscus clypeus, Core GI12FP7, Unit 5

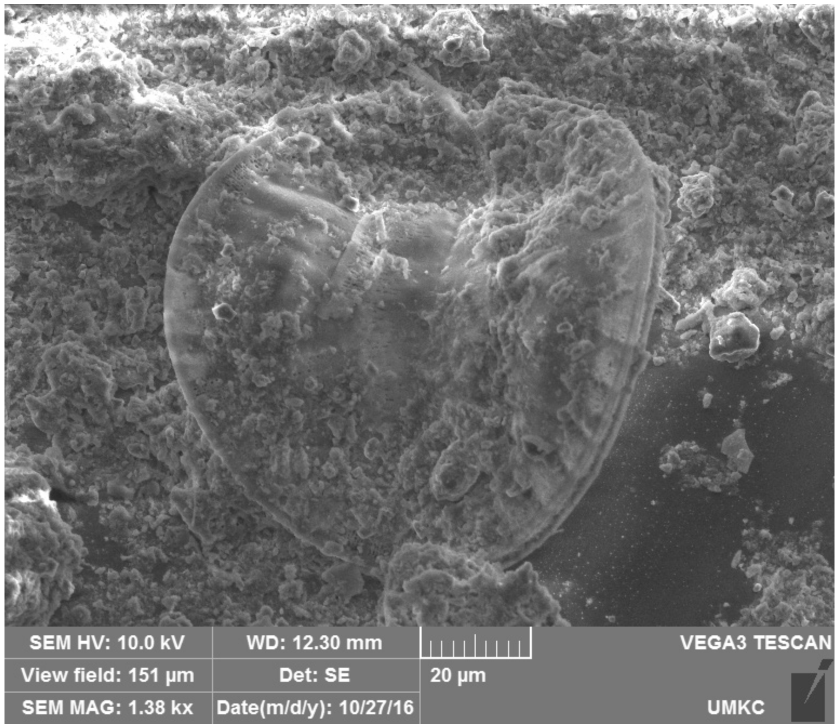

Campylodiscus clypeus, Core GI12FP7, Unit 5

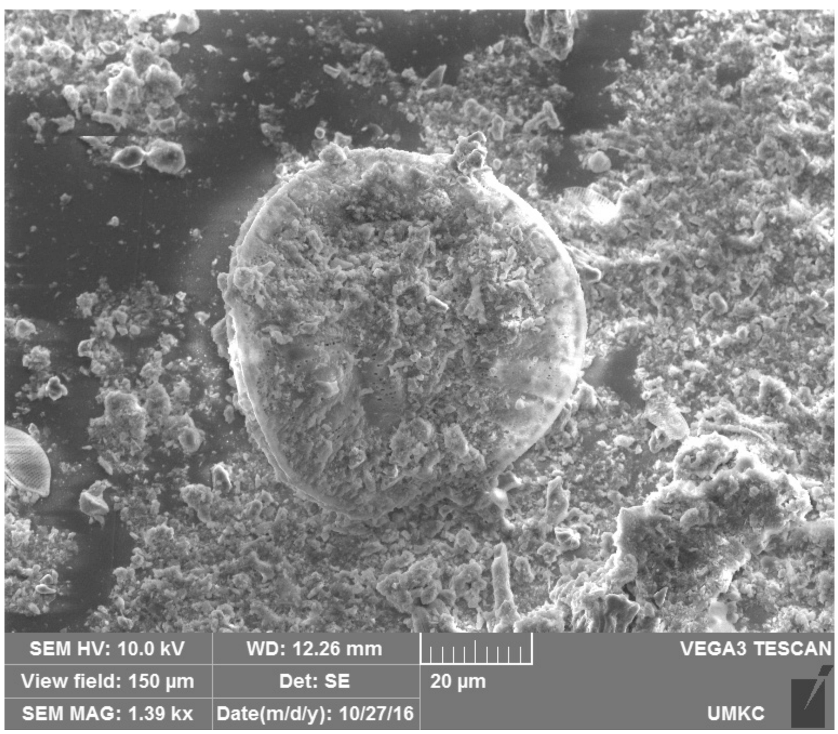

Campylodiscus clypeus, Core GI12FP7, Unit 5

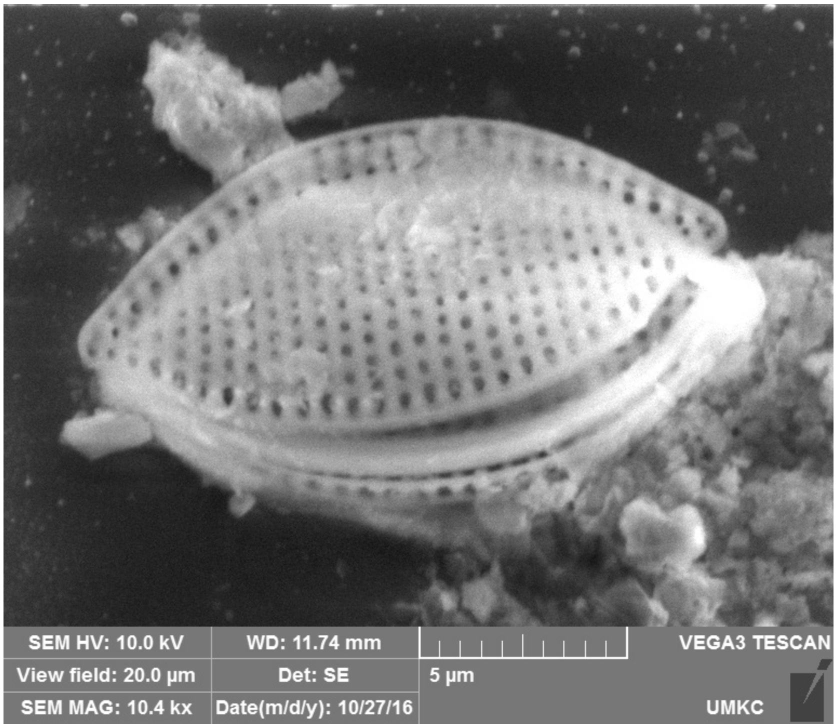

Tryblionella compressa, Core GI12FP7, Unit 5

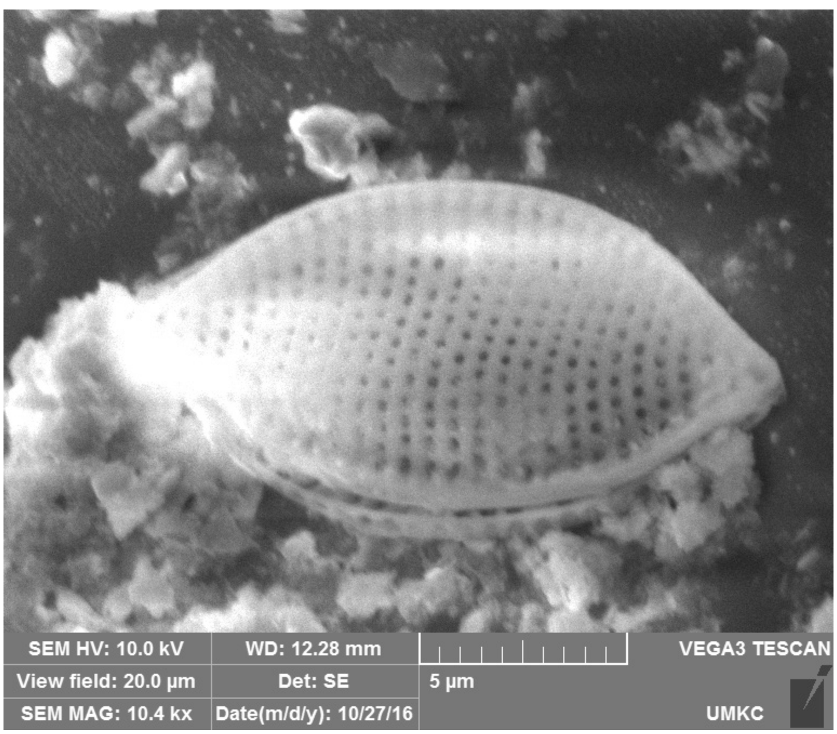

Tryblionella compressa, Core GI12FP7, Unit 5

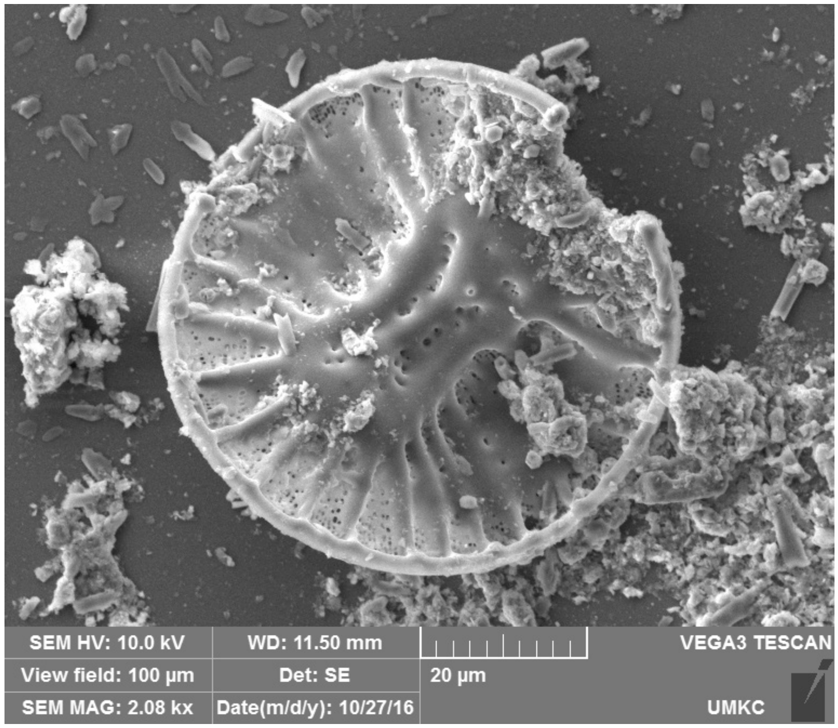

Campylodiscus clypeus, Core GI12FP8, Unit 5

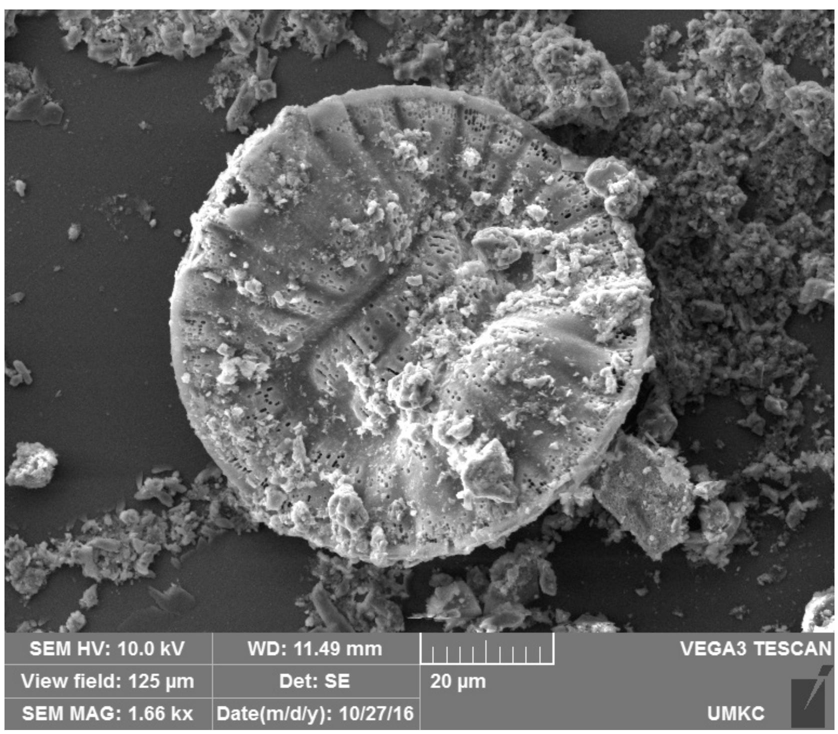

Campylodiscus clypeus, Core GI12FP8, Unit 5

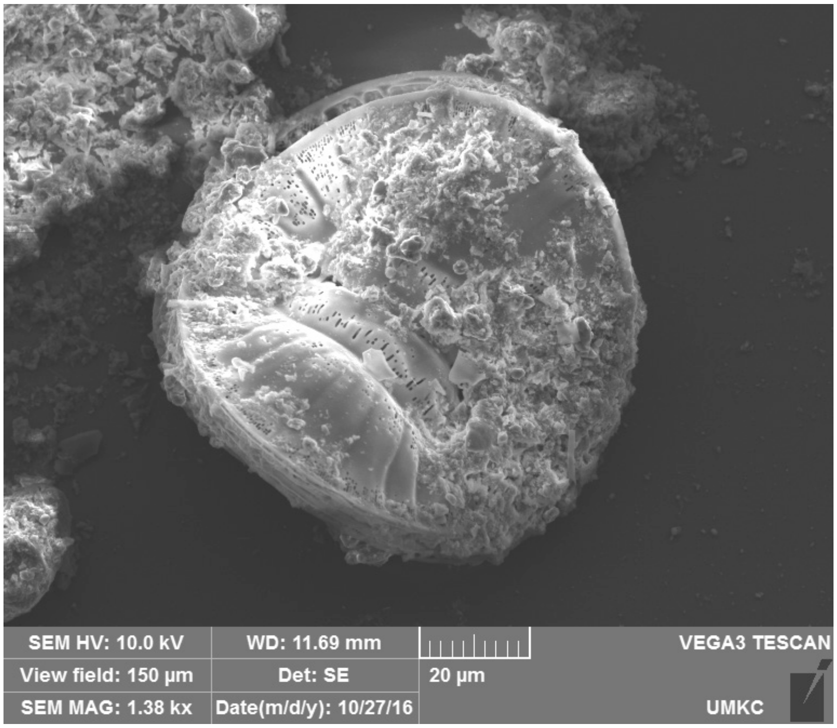

Campylodiscus clypeus, Core GI12FP8, Unit 3

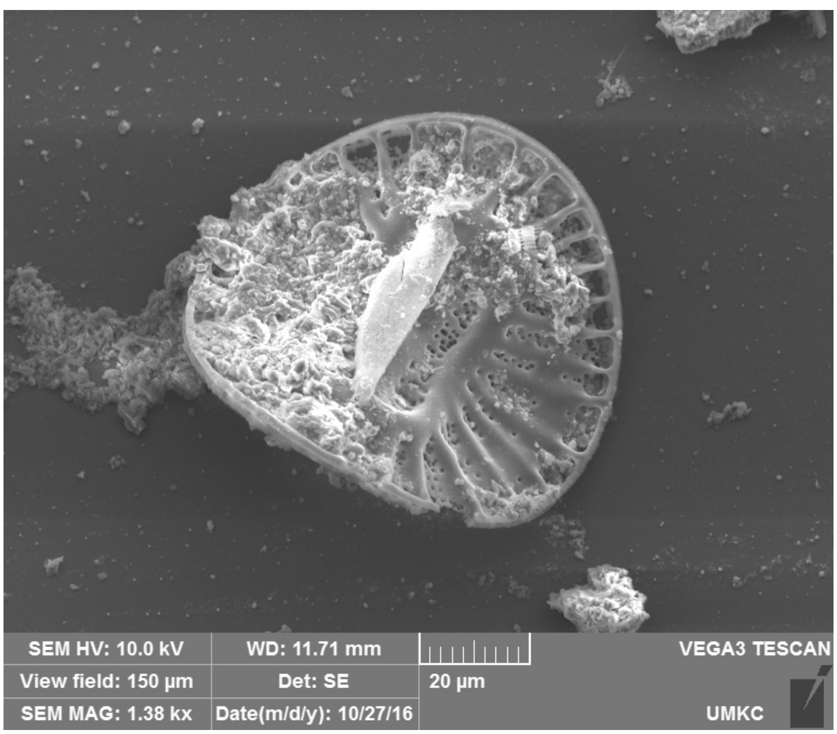

Campylodiscus clypeus, Core GI12FP8, Unit 3

APPENDIX I

MICROFOSSIL ASSEMBLAGES AND PHOTO PLATES

Unit	Core	Name	Photo #	Environment
1	GI12FP6A	*Pyrgophorus parvulus*	1	marine
	GI12FP6A	*Cyprodeis sp.*	2	marine
	GI12FP6A	*Cyprodeis sp.*	3	marine
	GI12FP7	*Pyrgophorus parvulus*	4	marine
	GI12FP7	*Pyrgophorus parvulus*	5	marine
	GI12FP7	*Pyrgophorus parvulus*	6	marine
	GI12FP7	*Pyrgophorus parvulus*	7	marine
	GI12FP7	*Cyprodeis sp.*	8	marine
	GI12FP7	*Cyprodeis sp.*	9	marine
	GI12FP8	*Chara fibrosa*	10	freshwater
	GI12FP8	*Chara fibrosa*	11	freshwater
	GI12FP8	*Pyrgophorus parvulus*	12	marine
	GI12GP8	*Cyprodeis sp.*	13	brackish/marine
	GI12FP8	*Cyprodeis sp.*	14	brackish/marine
2	GI12FP6A	*Chara fibrosa*	15	freshwater
	GI12FP6A	*Pyrgophorus platyrachis*	16	brackish/fresh
	GI12FP6A	*Pyrgophorus platyrachis*	17	brackish/fresh
	GI12FP6A	*Cyprodeis sp.*	18	brackish/marine
	GI12FP6A	*Cyprodeis sp.*	19	brackish/marine
	GI12FP6A	*Cyprodeis sp.*	20	brackish/marine
	GI12FP7	*Chara fibrosa*	21	freshwater
	GI12FP7	*Chara fibrosa*	22	freshwater
	GI12FP7	*Pyrgophorus platyrachis*	23	brackish/fresh
	GI12FP7	*Pyrgophorus platyrachis*	24	brackish/fresh
	GI12FP7	*Cyprodeis sp.*	25	brackish/marine
	GI12FP7	*Cyprodeis sp.*	26	brackish/marine
	GI12FP8	*Chara fibrosa*	27	freshwater
	GI12FP8	*Chara fibrosa*	28	freshwater
	GI12FP8	*Chara fibrosa*	29	freshwater
	GI12FP8	*Chara fibrosa*	30	freshwater
	GI12FP8	*Pyrgophorus platyrachis*	31	brackish/fresh
	GI12FP8	*Pyrgophorus platyrachis*	32	brackish/fresh
	GI12FP8	*Pyrgophorus platyrachis*	33	brackish/fresh
	GI12FP8	*Pyrgophorus platyrachis*	34	brackish/fresh
	GI12FP8	*Cyprodeis sp.*	35	brackish/marine

	GI12FP8	*Cyprodeis sp.*	36	brackish/marine
	GI12FP8	*Cyprodeis sp.*	37	brackish/marine
	GI12FP8	*Cyprodeis sp.*	38	brackish/marine
	GI12FP10	*Cerithideopsis costata*	39	brackish
	GI12FP10	*Chara fibrosa*	40	freshwater
	GI12FP10	*Chara fibrosa*	41	freshwater
	GI12FP10	*Chara fibrosa*	42	freshwater
	GI12FP10	*Chara fibrosa*	43	freshwater
	GI12FP10	*Pyrgophorus platyrachis*	44	brackish/fresh
	GI12FP10	*Pyrgophorus platyrachis*	45	brackish/fresh
	GI12FP10	*Pyrgophorus platyrachis*	46	brackish/fresh
	GI12FP10	*Pyrgophorus platyrachis*	47	brackish/fresh
	GI12FP10	*Pyrgophorus platyrachis*	48	brackish/fresh
	GI12FP10	*Pyrgophorus platyrachis*	49	brackish/fresh
	GI12FP10	*Pyrgophorus platyrachis*	50	brackish/fresh
	GI12FP10	*Cyprodeis sp.*	51	brackish/marine
	GI12FP10	*Cyprodeis sp.*	52	brackish/marine
3	GI12FP6B	*Chara fibrosa*	53	freshwater
	GI12FP6B	*Cyprodeis sp.*	54	brackish/marine
	GI12FP6B	*Cyprodeis sp.*	55	brackish/marine
	GI12FP8	*Pyrgophorus parvulus*	56	freshwater
	GI12FP8	*Cyprodeis sp.*	57	brackish/marine
	GI12FP8	*Cyprodeis sp.*	58	brackish/marine
	GI12FP10	*Chara fibrosa*	59	freshwater
	GI12FP10	*Pyrgophorus parvulus*	60	marine
	GI12FP10	*Pyrgophorus parvulus*	61	marine
	GI12FP10	*Pyrgophorus parvulus*	62	marine
	GI12FP10	*Cyprodeis sp.*	63	brackish/marine
4	GI12FP6B	*Chara fibrosa*	64	freshwater
	GI12FP6B	*Chara fibrosa*	65	freshwater
	GI12FP6B	*Chara fibrosa*	66	freshwater
	GI12FP6B	*Chara fibrosa*	67	freshwater
	GI12FP6B	*Chara fibrosa*	68	freshwater
	GI12FP6B	*Chara fibrosa*	69	freshwater
	GI12FP6B	*Pyrgophorus platyrachis*	70	brackish/fresh
	GI12FP6B	*Pyrgophorus platyrachis*	71	brackish/fresh
	GI12FP6B	*Pyrgophorus platyrachis*	72	brackish/fresh
	GI12FP6B	*Pyrgophorus platyrachis*	73	brackish/fresh
	GI12FP6B	*Pyrgophorus platyrachis*	74	brackish/fresh
	GI12FP6B	*Pyrgophorus platyrachis*	75	brackish/fresh
	GI12FP6B	*Pyrgophorus platyrachis*	76	brackish/fresh

	GI12FP6B	*Cyprodeis sp.*	77	brackish/marine
	GI12FP6B	*Cyprodeis sp.*	78	brackish/marine
	GI12FP6B	*Cyprodeis sp.*	79	brackish/marine
	GI12FP6B	*Cyprodeis sp.*	80	brackish/marine
	GI12FP6B	*Cyprodeis sp.*	81	brackish/marine
	GI12FP6B	*Cyprodeis sp.*	82	brackish/marine
	GI12FP6B	*Cyprodeis sp.*	83	brackish/marine
	GI12FP6B	*Cyprodeis sp.*	84	brackish/marine
	GI12FP6C	*Chara fibrosa*	85	freshwater
	GI12FP6C	*Chara fibrosa*	86	freshwater
	GI12FP6C	*Chara fibrosa*	87	freshwater
	GI12FP6C	*Chara fibrosa*	88	freshwater
	GI12FP6C	*Pyrgophorus platyrachis*	89	brackish/fresh
	GI12FP6C	*Pyrgophorus platyrachis*	90	brackish/fresh
	GI12FP6C	*Pyrgophorus platyrachis*	91	brackish/fresh
	GI12FP6C	*Cyprodeis sp.*	92	brackish/marine
	GI12FP6C	*Cyprodeis sp.*	93	brackish/marine
	GI12FP6C	*Cyprodeis sp.*	94	brackish/marine
	GI12FP6C	*Cyprodeis sp.*	95	brackish/marine
	GI12FP6C	*Cyprodeis sp.*	96	brackish/marine
	GI12FP6C	*Cyprodeis sp.*	97	brackish/marine
	GI12FP7	*Chara fibrosa*	98	freshwater
	GI12FP7	*Pyrgophorus platyrachis*	99	brackish/fresh
	GI12FP7	*Pyrgophorus platyrachis*	100	brackish/fresh
	GI12FP7	*Cyprodeis sp.*	101	brackish/marine
	GI12FP7	*Cyprodeis sp.*	102	brackish/marine
	GI12FP7	*Cyprodeis sp.*	103	brackish/marine
	GI12FP7	*Cyprodeis sp.*	104	brackish/marine
	GI12FP7	*Cyprodeis sp.*	105	brackish/marine
	GI12FP8	*Chara fibrosa*	106	freshwater
	GI12FP8	*Chara fibrosa*	107	freshwater
	GI12FP8	*Chara fibrosa*	108	freshwater
	GI12FP8	*Chara fibrosa*	109	freshwater
	GI12FP8	*Chara fibrosa*	110	freshwater
	GI12FP8	*Chara fibrosa*	111	freshwater
	GI12FP8	*Chara fibrosa*	112	freshwater
	GI12FP8	*Chara fibrosa*	113	freshwater
	GI12FP8	*Chara fibrosa*	114	freshwater
	GI12FP8	*Pyrgophorus platyrachis*	115	brackish/fresh
	GI12FP8	*Pyrgophorus platyrachis*	116	brackish/fresh
	GI12FP8	*Pyrgophorus platyrachis*	117	brackish/fresh

	GI12FP8	*Pyrgophorus platyrachis*	118	brackish/fresh
	GI12FP8	*Pyrgophorus platyrachis*	119	brackish/fresh
	GI12FP8	*Pyrgophorus platyrachis*	120	brackish/fresh
	GI12FP8	*Cyprodeis sp.*	121	brackish/marine
	GI12FP8	*Cyprodeis sp.*	122	brackish/marine
	GI12FP8	*Cyprodeis sp.*	123	brackish/marine
	GI12FP8	*Cyprodeis sp.*	124	brackish/marine
	GI12FP8	*Cyprodeis sp.*	125	brackish/marine
	GI12FP8	*Cyprodeis sp.*	126	brackish/marine
	GI12FP8	*Cyprodeis sp.*	127	brackish/marine
	GI12FP8	*Cyprodeis sp.*	128	brackish/marine
	GI12FP8	*Cyprodeis sp.*	129	brackish/marine
	GI12FP10	*Pyrgophorus platyrachis*	130	brackish/fresh
	GI12FP10	*Pyrgophorus platyrachis*	131	brackish/fresh
	GI12FP10	*Pyrgophorus platyrachis*	132	brackish/fresh
	GI12FP10	*Pyrgophorus platyrachis*	133	brackish/fresh
	GI12FP10	*Cyprodeis sp.*	134	brackish/marine
5	GI12FP6B	*Chara fibrosa*	135	freshwater
	GI12FP6B	*Pyrgophorus parvulus*	136	marine
	GI12FP6B	*Pyrgophorus parvulus*	137	marine
	GI12FP6B	*Cyprodeis sp.*	138	brackish/marine
	GI12FP6B	*Cyprodeis sp.*	139	brackish/marine
	GI12FP6B	*Cyprodeis sp.*	140	brackish/marine
	GI12FP6B	*Cyprodeis sp.*	141	brackish/marine
	GI12FP6B	*Cyprodeis sp.*	142	brackish/marine
	GI12FP6B	*Cyprodeis sp.*	143	brackish/marine
	GI12FP6B	*Cyprodeis sp.*	144	brackish/marine
	GI12FP6B	*Cyprodeis sp.*	145	brackish/marine
	GI12FP6B	*Cyprodeis sp.*	146	brackish/marine
	GI12FP6B	*Cyprodeis sp.*	147	brackish/marine
	GI12FP6B	*Cyprodeis sp.*	148	brackish/marine
	GI12FP6B	*Cyprodeis sp.*	149	brackish/marine
	GI12FP6C	*Chara fibrosa*	150	freshwater
	GI12FP6C	*Pyrgophorus parvulus*	151	marine
	GI12FP6C	*Pyrgophorus parvulus*	152	marine
	GI12FP6C	*Cyprodeis sp.*	153	brackish/marine
	GI12FP6C	*Cyprodeis sp.*	154	brackish/marine
	GI12FP6C	*Cyprodeis sp.*	155	brackish/marine
	GI12FP6C	*Cyprodeis sp.*	156	brackish/marine
	GI12FP6C	*Cyprodeis sp.*	157	brackish/marine
	GI12FP7	*Chara fibrosa*	158	freshwater

	GI12FP7	*Pyrgophorus parvulus*	159	marine
	GI12FP7	*Cerithium lutosum*	160	marine
	GI12FP7	*Cyprodeis sp.*	161	brackish/marine
	GI12FP7	*Cyprodeis sp.*	162	brackish/marine
	GI12FP7	*Cyprodeis sp.*	163	brackish/marine
	GI12FP7	*Cyprodeis sp.*	164	brackish/marine
	GI12FP7	*Cyprodeis sp.*	165	brackish/marine
	GI12FP7	*Cyprodeis sp.*	166	brackish/marine
	GI12FP7	*Cyprodeis sp.*	167	brackish/marine
	GI12FP8	*Chara fibrosa*	168	freshwater
	GI12FP8	*Pyrgophorus parvulus*	169	marine
	GI12FP8	*Pyrgophorus parvulus*	170	marine
	GI12FP8	*Pyrgophorus parvulus*	171	marine
	GI12FP8	*Pyrgophorus parvulus*	172	marine
	GI12FP8	*Cyprodeis sp.*	173	brackish/marine
	GI12FP8	*Cyprodeis sp.*	174	brackish/marine
	GI12FP8	*Cyprodeis sp.*	175	brackish/marine
	GI12FP8	*Cyprodeis sp.*	176	brackish/marine
	GI12FP8	*Cyprodeis sp.*	177	brackish/marine
	GI12FP8	*Cyprodeis sp.*	178	brackish/marine
6	GI12FP10	*Cerithium lutosum*	179	marine

Microfossil Plate 1

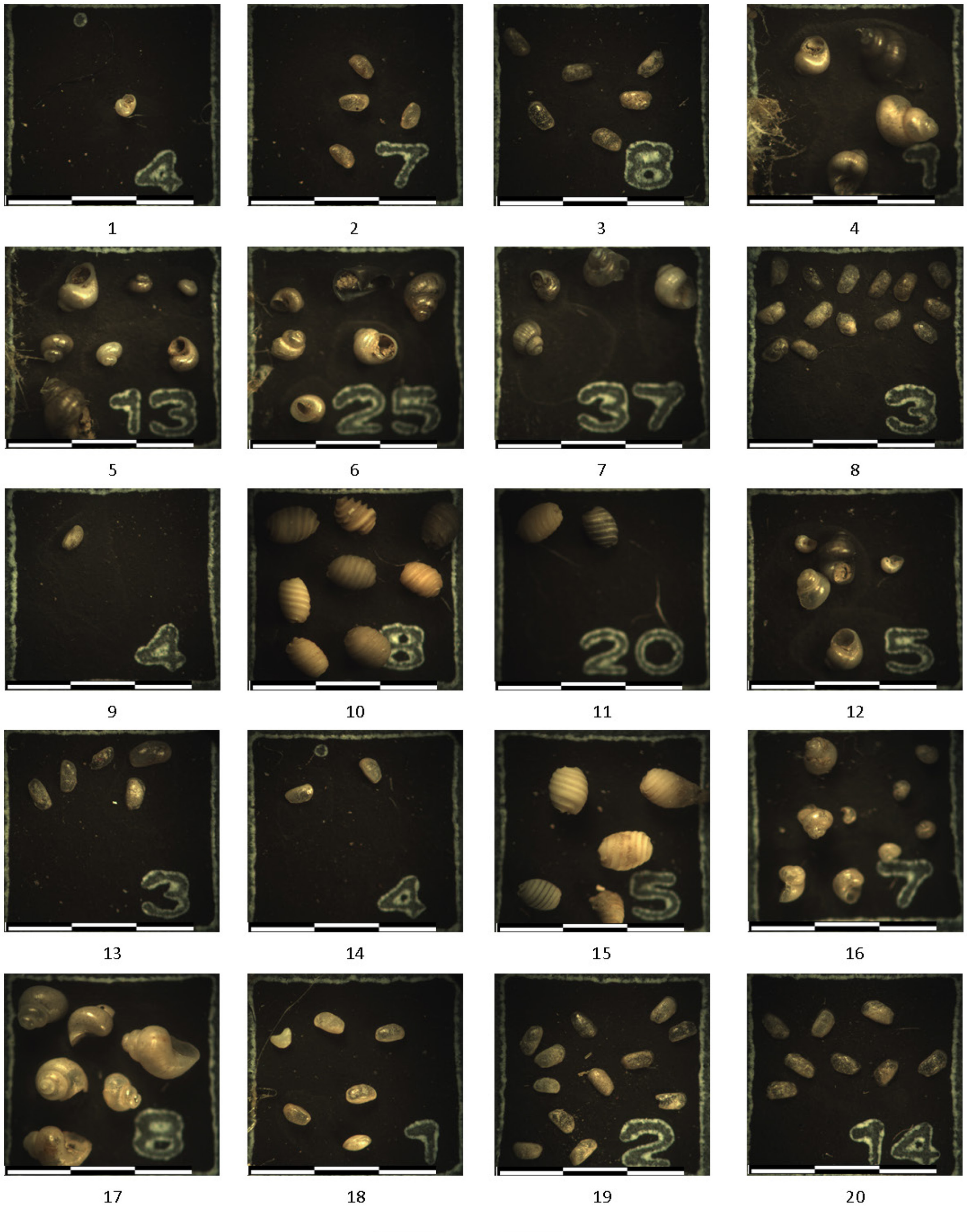

3.0mm

Microfossil Plate 2

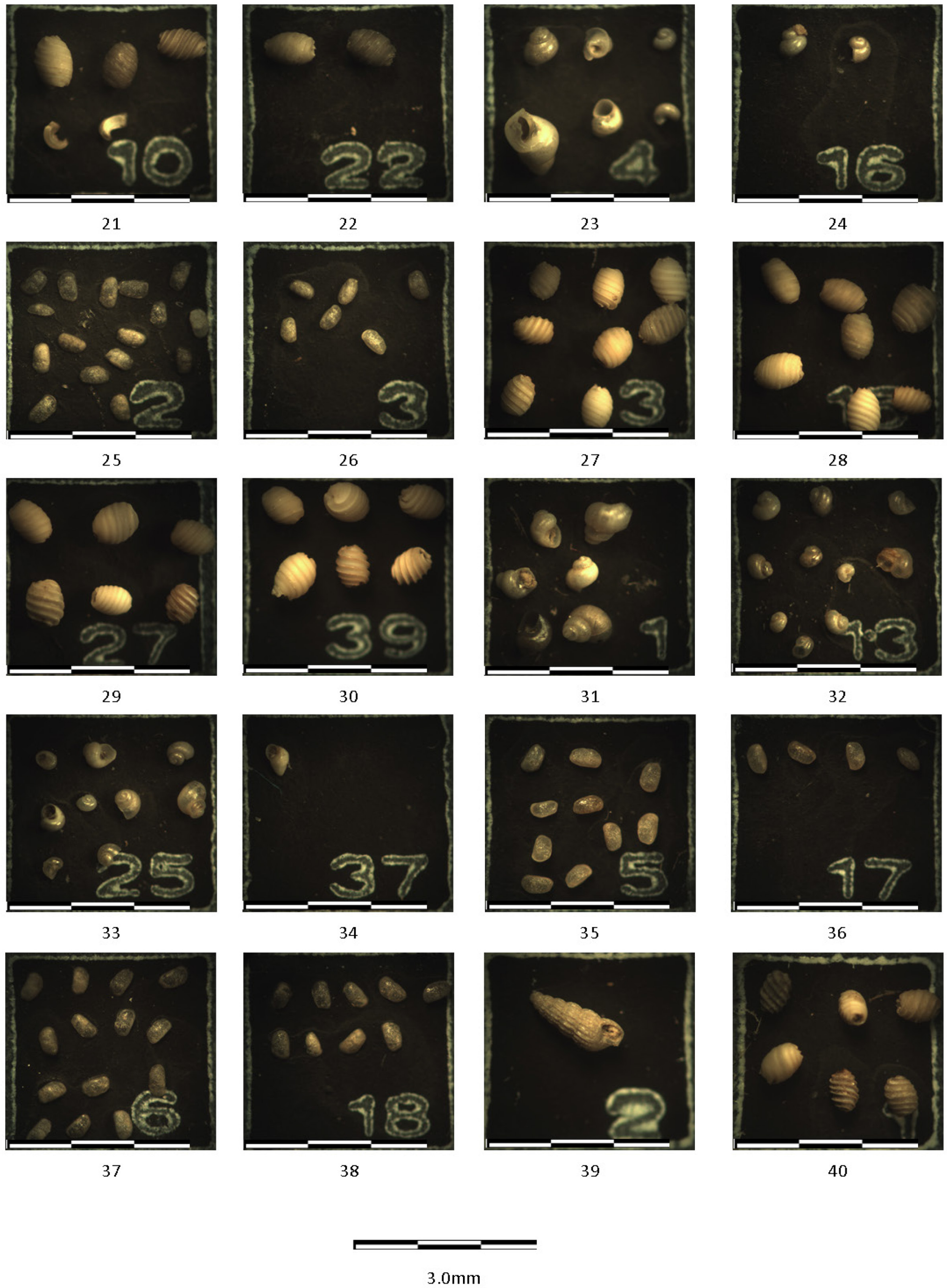

Microfossil Plate 3

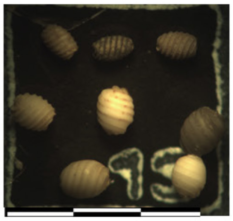
41


42


43

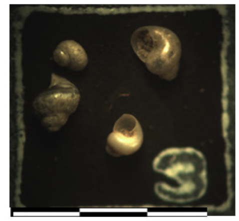
44

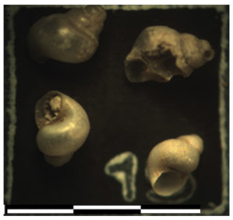
45

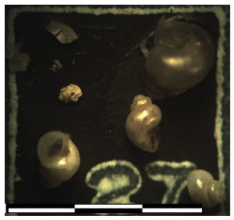
46

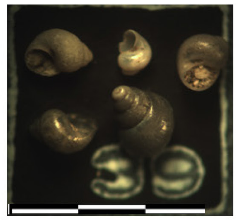
47

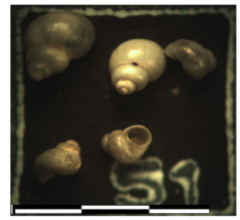
48

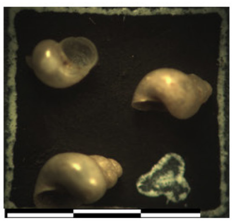
49

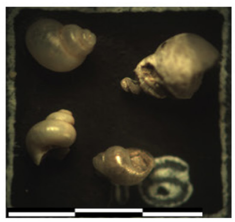
50

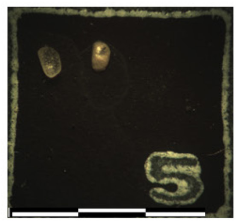
51

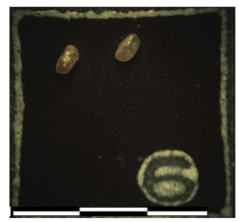
52


53

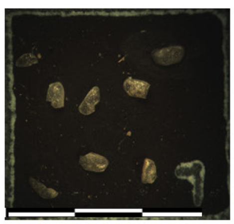
54

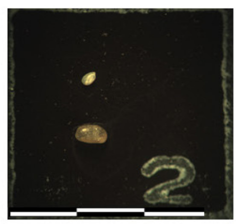
55

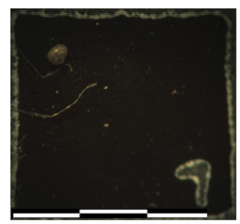
56

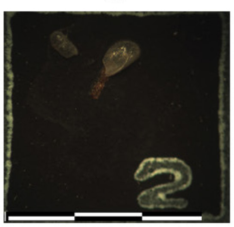
57

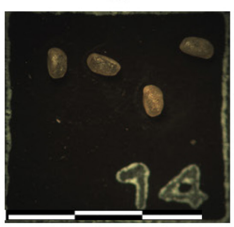
58

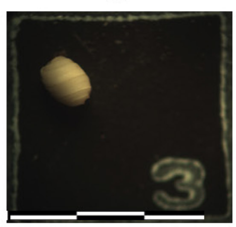
59

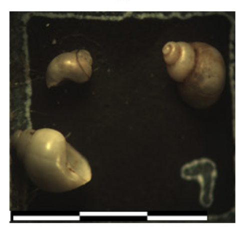
60

3.0mm

Microfossil Plate 4

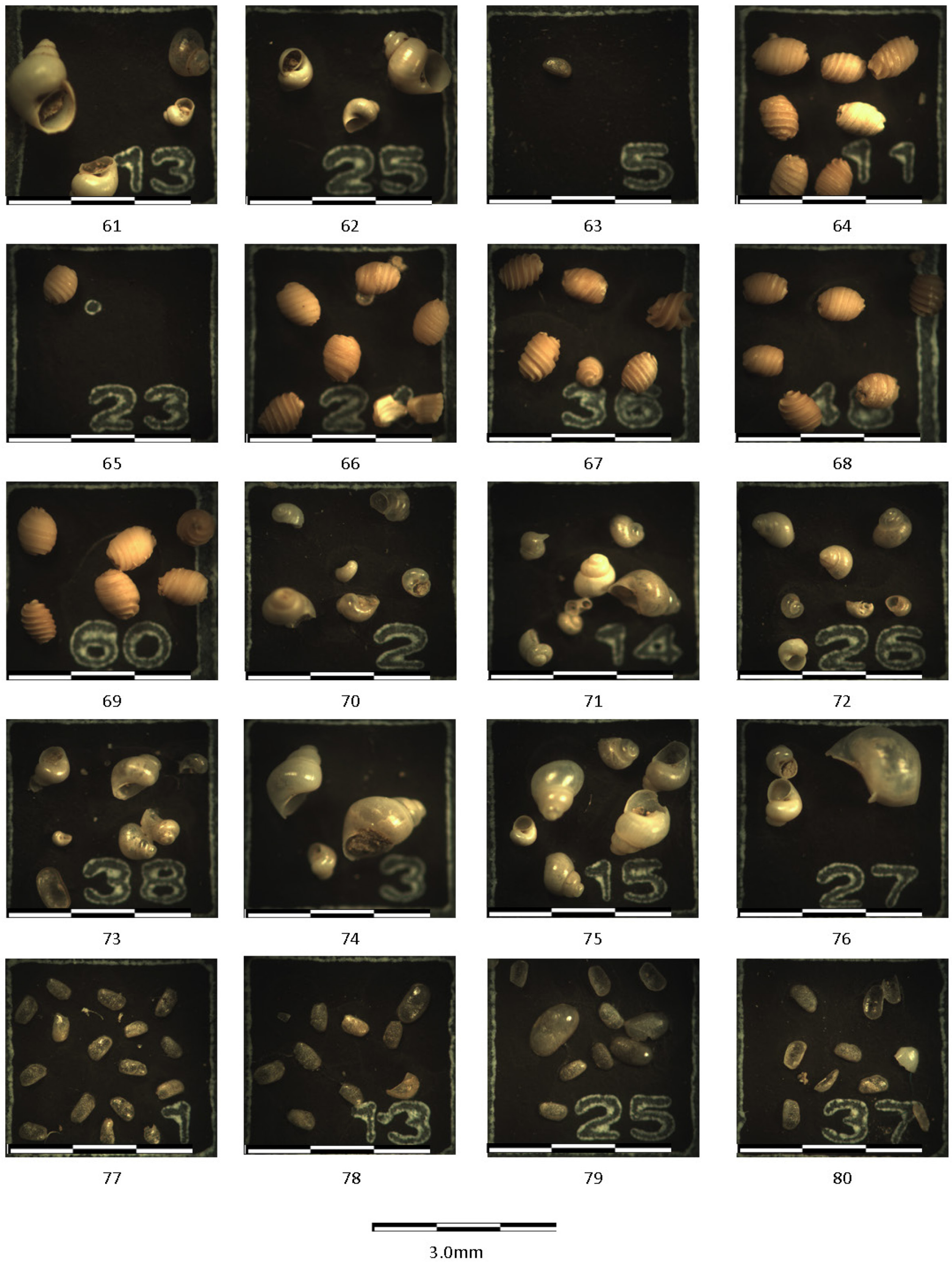

Microfossil Plate 5

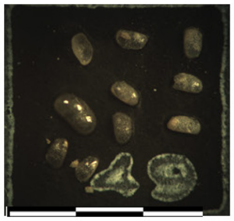

81

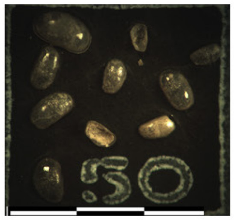

82

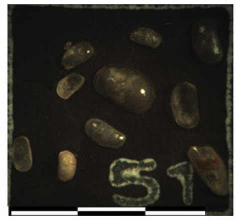

83

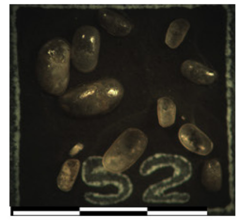

84

85

86

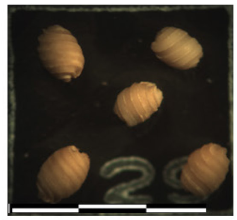

87

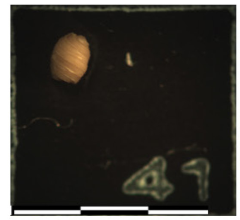

88

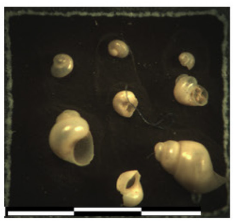

89

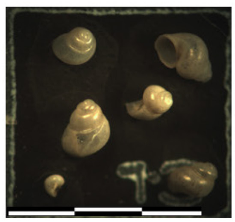

90

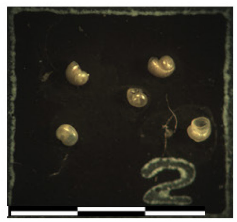

91

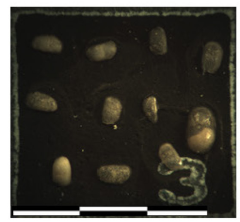

92

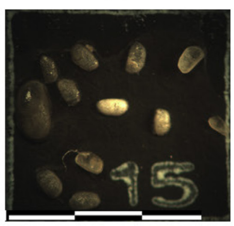

93

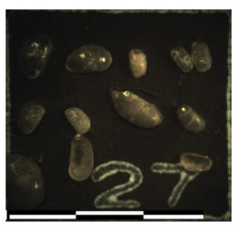

94

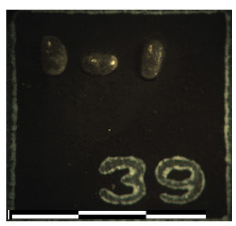

95

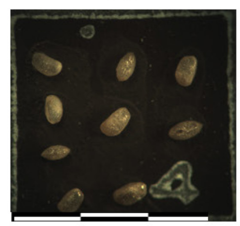

96

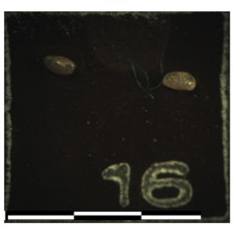

97

98

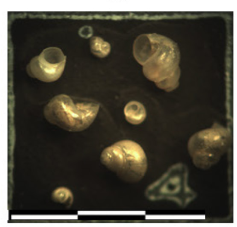

99

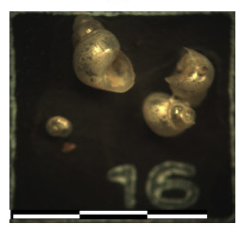

100

3.0mm

Microfossil Plate 6

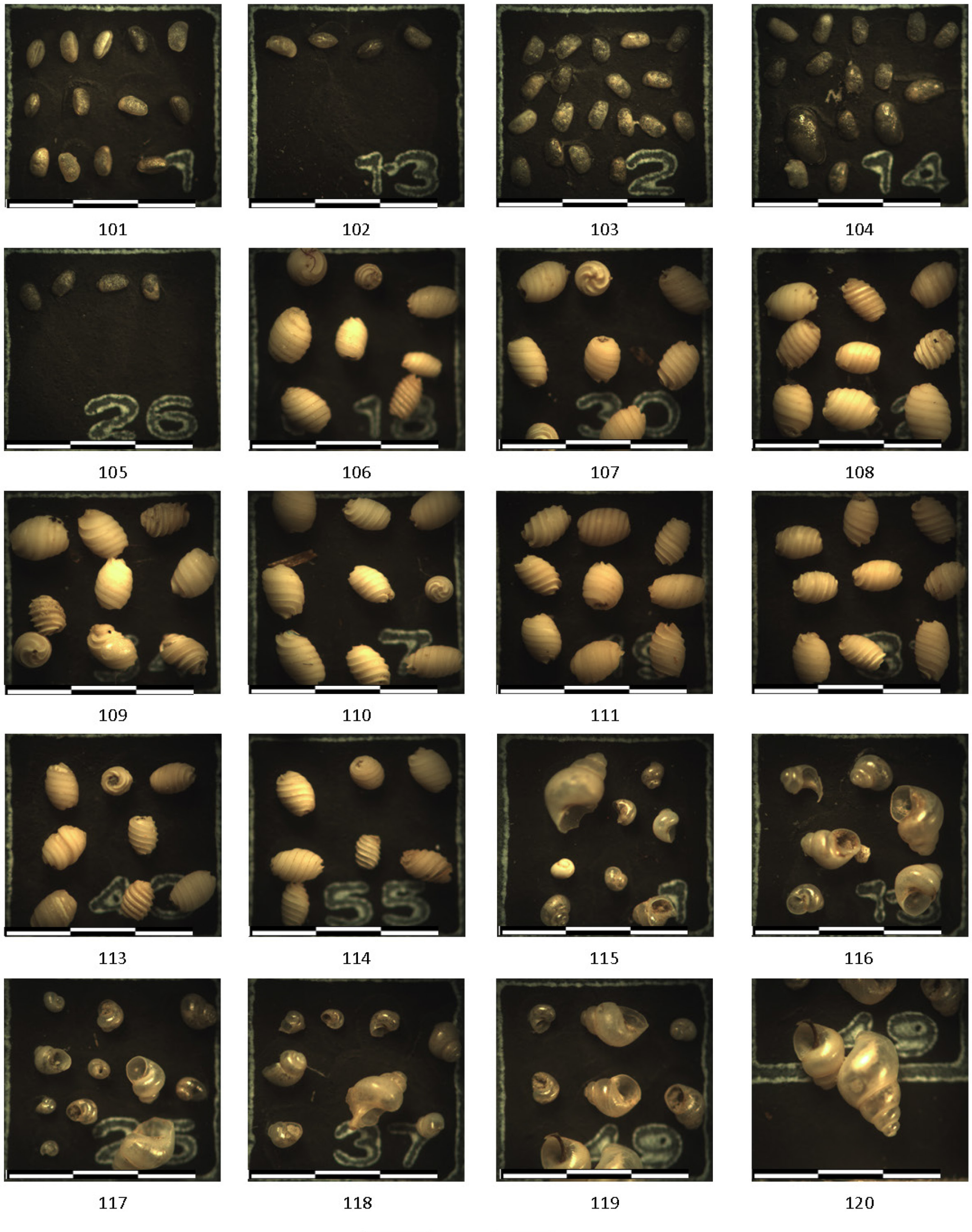

3.0mm

Microfossil Plate 7

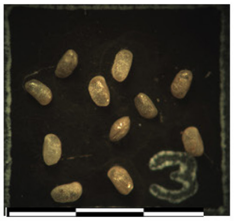

121

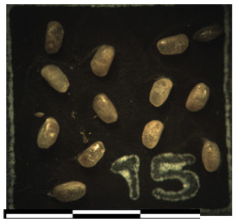

122

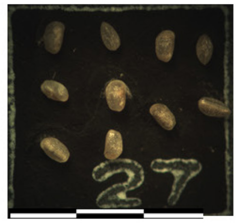

123

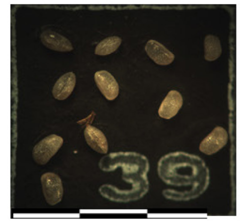

124

125

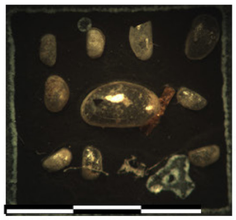
126

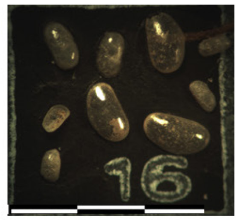

127

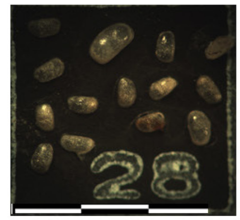

128

129

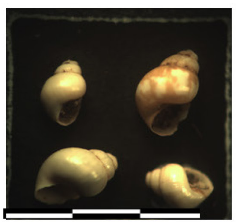
130

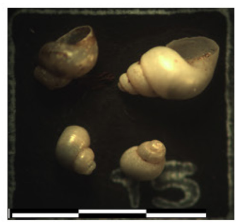
131

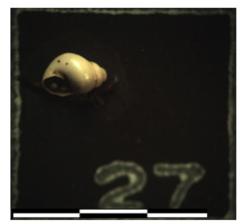

132

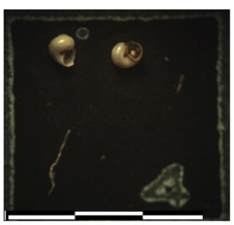

133

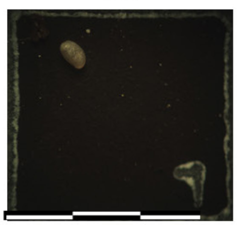
134

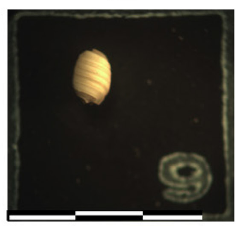

135

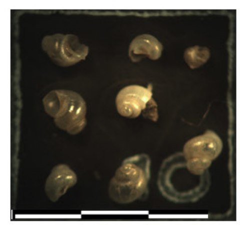
136

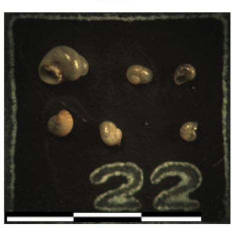

137

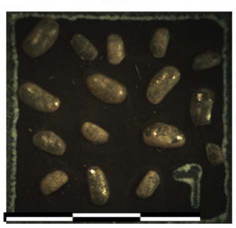
138

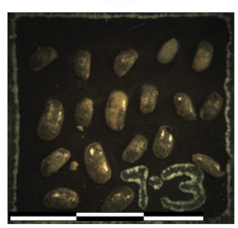

139

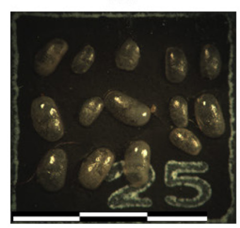

140

3.0mm

Microfossil Plate 8

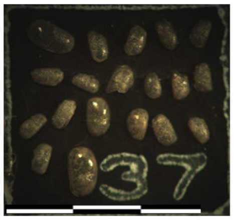

141

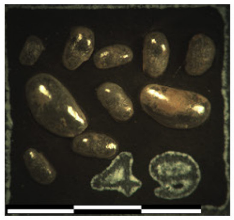

142

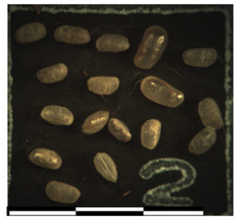

143

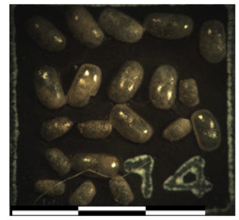

144

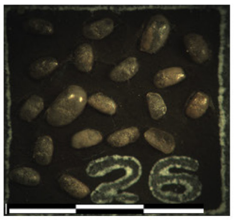

145

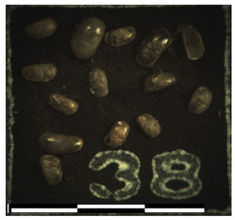

146

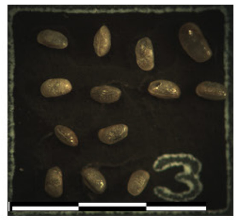

147

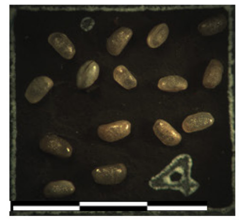

148

149

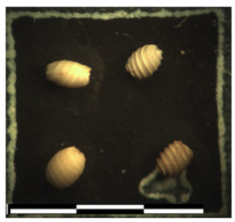
150

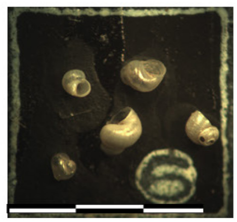

151

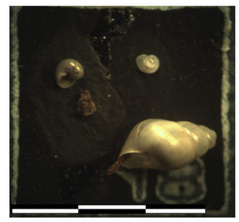
152

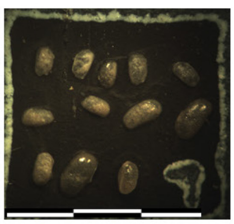
153

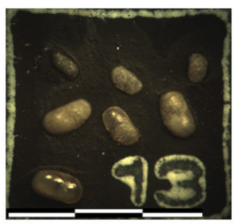

154

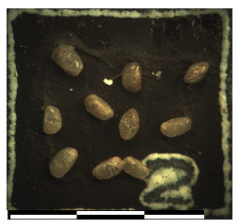

155

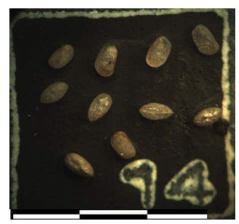

156

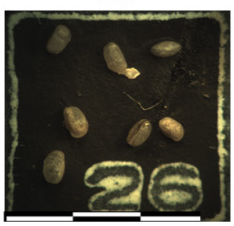

157

158

159

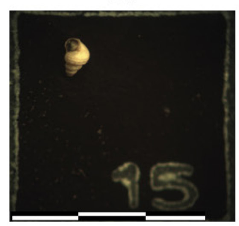

160

3.0mm

Microfossil Plate 9

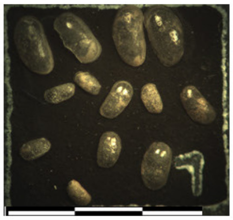
161

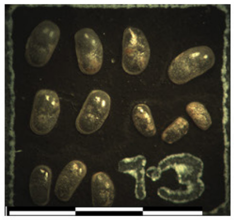

162

163

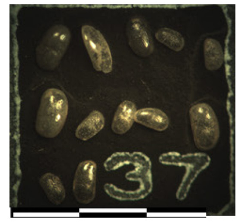

164

165

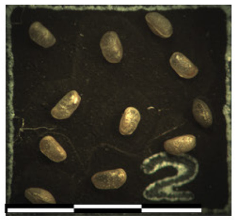

166

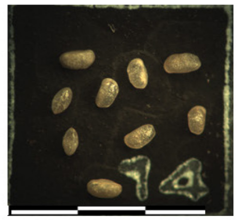

167

168

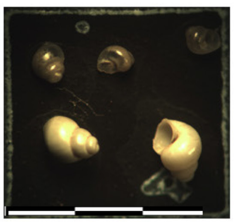
169

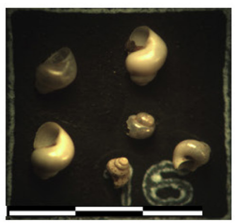

170

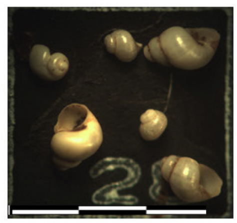
171

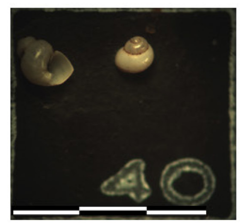

172

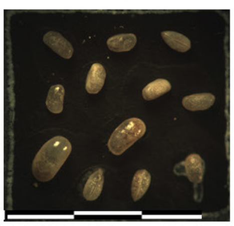
173

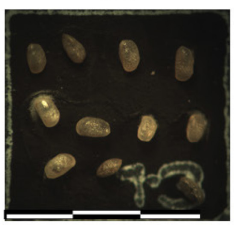

174

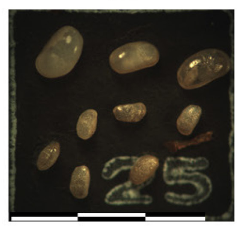

175

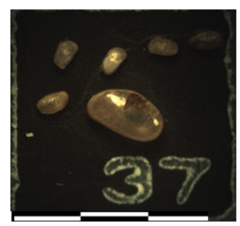

176

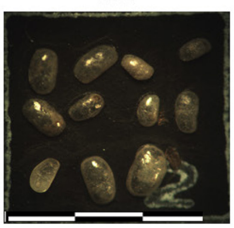
177

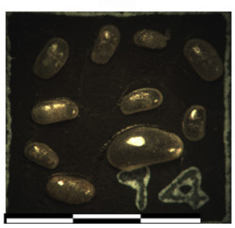

178

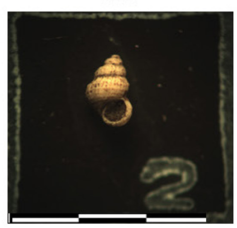

179

3.0mm

APPENDIX J
RADIOCARBON DATA

2 RADIOCARBON CALIBRATION PROGRAM*
CALIB REV7.1.0
Copyright 1986-2016 M Stuiver and PJ Reimer
*To be used in conjunction with:
Stuiver, M., and Reimer, P.J., 1993, Radiocarbon, 35, 215-230.

FP7 62-65
Lab Code
Sample Description
Radiocarbon Age BP 1380 +/- 35
Calibration data set: intcal13.14c # Reimer et al. 2013

% area enclosed	cal BP age ranges	relative area under probability distribution
68.3 (1 sigma)	cal BP 1280 - 1317	1.000
95.4 (2 sigma)	cal BP 1194 - 1196	0.002
	1261 - 1353	0.998

Median Probability: 1300

FP8 27-28.5
Lab Code
Sample Description
Radiocarbon Age BP 830 +/- 30
Calibration data set: intcal13.14c # Reimer et al. 2013

% area enclosed	cal BP age ranges	relative area under probability distribution
68.3 (1 sigma)	cal BP 700 - 761	1.000
95.4 (2 sigma)	cal BP 688 - 789	1.000

Median Probability: 737

References for calibration datasets:
Reimer PJ, Bard E, Bayliss A, Beck JW, Blackwell PG, Bronk Ramsey C, Buck CE Cheng H, Edwards RL, Friedrich M, Grootes PM, Guilderson TP, Haflidason H, Hajdas I, Hatté C, Heaton TJ, Hogg AG, Hughen KA, Kaiser KF, Kromer B, Manning SW, Niu M, Reimer RW, Richards DA, Scott EM, Southon JR, Turney CSM, van der Plicht J.
IntCal13 and MARINE13 radiocarbon age calibration curves 0-50000 years calBP Radiocarbon 55(4). DOI: 10.2458/azu_js_rc.55.16947

Comments:
* This standard deviation (error) includes a lab error multiplier.

** 1 sigma = square root of (sample std. dev.^2 + curve std. dev.^2)
** 2 sigma = 2 x square root of (sample std. dev.^2 + curve std. dev.^2)
where ^2 = quantity squared.
[ ] = calibrated range impinges on end of calibration data set
0* represents a "negative" age BP
1955* or 1960* denote influence of nuclear testing C-14

NOTE: Cal ages and ranges are rounded to the nearest year which may be too precise in many instances. Users are advised to round results to the nearest 10 yr for samples with standard deviation in the radiocarbon age greater than 50 yr.

REFERENCES CITED

AlgaeBase, 2016. http://www.algaebase.org/search/species/detail/?species_id=27154; http://www.algaebase.org/search/species/detail/?species_id=33256; http://www.algaebase.org/search/species/detail/?species_id=84144. Last accessed 1-3-17.

Bouysse, P., Westercamp, D., Andreieff, P. 1990. The Lesser Antilles Island Arc. Proceedings of the Ocean Drilling Program, Scientific Results. Vol. 110.

Brenner, M., Binford, M. 1988. A Sedimentary Record of Human Disturbance from Lake Miragoane, Haiti. Journal of Paleolimnology 1, p. 85-97.

Brink, U., Danforth, W., Polloni, C. 2004. New Seafloor Map of the Puerto Rico Trench Helps Assess Earthquake and Tsunami Hazards. EOS, Transactions, American Geophysical Union, Vol. 85, No. 37, p. 349-360.

Chenoweth, J. 2014. Practicing and Preaching Quakerism: Creating a Religion of Peace on a Slavery-Era Plantation. American Anthropologist, Vol. 116, No. 1, p 94-109.

Davis, D. 2011. Out of the Shadows: A review of the archaeological evidence for the isolation, interaction, and abandonment of the British Virgin Islands in the pre-Columbian Caribbean. Master's Thesis, January 2011.

Dellwig, O., Watermann, F., Brumsack, H.J., Gerdes, G., Krumbein, W.E. 2001. Sulphur and iron geochemistry of Holocene coastal peats (NW Germany): a tool for palaeoenvironmental reconstruction. Palaeogeography, Palaeoclimatology, Palaeoecology, Vol 167, p. 359-379.

Encyclopædia Britannica, Inc. http://www.britannica.com/place/Virgin-Islands; http://www.britannica.com/place/British-Virgin-Islands. Last accessed 1-3-17.

Figueredo, A. The Virgin Islands as an Historical Frontier Between the Taínos and the Caribs. The Journal of Caribbean Amerindian History and Anthropology. December 2006.

Gischler, E. and Storz, D. 2009. High-Resolution windows into Holocene climate using proxy data from Belize Corals (Central America). Paleobiology, Paleoenvironment, Vol. 89, p. 211-221.

Google Earth, 2016. https://www.google.com/earth. Last accessed 1-3-17.

Goldstein, J., Newbury, D., Joy, D., Lyman, C., Echlin, P., Lifshin, E., Sawyer, L., and Michael, J. 2003. Scanning Electron Microscopy and X-Ray Microanalysis. New York: Springer Science Publishing.

Guana Island. www.guanaisland.com. Last accessed 1-3-17.

Haug, G., Hughen, K., Sigman, D., Peterson, L., Rohl, U. 2001. Southward Migration of the Intertropical Convergence Zone Through the Holocene. Science. Vol. 293, Issue 5533, p. 1304-1308.

Helsley, C. 1960. Geology of the British Virgin Islands. Princeton University Doctoral Dissertation, May 1960.

Hodell, D., Curtis, J., Jones, G., Higuera-Gundy, A., Brenner, M., Binford, M., Dorsey, K. 1991. Reconstruction of Caribbean climate change over the past 10,500 years. Nature, Vol. 352, p. 790-793.

Island Resources Foundation and Jost Van Dykes (BVI) Preservation Society. An Environmental Profile of the Islands of Jost Van Dyke, British Virgin Islands, including Little Jost Van Dyke, Sandy Cay, Green Cay, and Sandy Spit. JVDPS. Jost Van Dyke, British Virgin Islands. 2009.

Jarecki, L. 2003. Salt ponds of the British Virgin Islands: Investigations in an unexplored ecosystem. University of Kent at Canterbury Doctoral Dissertation, 19 August 2003.

Jenkins, C. 1923. Tortola: A Quaker Experiment of Long Ago in the Tropics. London: Friends Bookshop.

LacCore: National Lacustrine Core Facility http://lrc.geo.umn.edu/laccore/index.html; http://lrc.geo.umn.edu/laccore/procedures.html. Last accessed 1-3-17.

Large Lakes Observatory. http://scse.d.umn.edu/large-lakes-observatory/vessels-facilities/analytical-facilities/itrax-xrf. Last accessed 1-3-17.

Lawrence Livermore National Laboratory. https://str.llnl.gov/str/Holloway.html. Last accessed 1-3-17.

Malaizé, R., Bertran, P., Carbonel, P., Bonnissent, D., Charlier, K., Galop, D., Imbert, D., Serrand, N., Stouvenot, Ch., Pujol, C. 2011. Hurricanes and climate in the Caribbean during the past 3700 years BP. The Holocene, Vol. 21, No. 6, p. 911-924.

Mangini A., Blumbach, P., Verdes, P., Spötl, C., Scholz, D., Machel, S. Mahon, S. 2007. Combined records from a stalagmite from Barbados and from lake sediments in Haiti reveal variable seasonality in the Caribbean between 6.7 and 3ka BP. Quaternary Science Reviews, Vol. 26, Issues 9-10, p. 1332-1343.

Mann, C. 1493: Uncovering the New World Columbus Created. Random House, Inc. New York, New York. 2011.

Marshall, M., Scholaut, G., Nakagawa, T., Lamb, H., Brauer, A., Staff, R., Ramsey, C., Tarasov, P., Gotanda,K., Haraguchi, T., Tokoyama, Y., Yonenobu, H., Tada, R. 2012. A novel approach to varve counting using µXRF and Z-radiography in combination with thin-section microscopy, applied tp the Late Glacial chronology from Lake Suigetsu, Japan. Quaternary Geochronology, Vol. 13, p. 70-80.

Nealon, J. and Dillon, W. 2001. Earthquakes and Tsunamis in Puerto Rico and the U.S. Virgin Islands. USGS Fact Sheet FS-141-00.

Nearing, M., Jetten, V., Baffaut,C., Cerdan, O., Couturier, A., Hernandez, M., LeBissonnais, Y., Nichols, M.H., Nunes, J.P., Renschler, C.S., Souchére, V., van Oost, K. 2005. Modeling response of soil erosion and runoff to changes in precipitation and cover. Catena 61, p. 131-154.

Oldfield, F., Wake, R., Boyle, J., Jones, R., Nolan, S., Gibbs, Z., Appleby, P., Fisher, E., and Wolff, G., 2003. The late-Holocene history of Gromire Lake (NE England) and its catchment: a multiproxy reconstruction of past human impact. The Holocene, Vol. 13, No. 5, p. 667-690.

Pindell, J., Barrett, S. 1990. Geological evolution of the Caribbean region; A plate-tectonic perspective. The Geology of North America, Vol. H, The Caribbean Region. The Geological Society of America.

Reimer, P.J., Brown, T.A., Reimer, R.W. 2004b. Discussion: Reporting and calibration of Post-Bomb 14C Data. Radiocarbon 46, p. 1299-1304.

Reinhardt, E.G., Stanley, D.J., Patterson, R.T. 1998. Strontium isotopic-paleontological method as a high-resolution paleosalinity tool for lagoonal environments. Geology, Vol. 26, No. 11, p. 1003-1006.

Righter, E. Guana Island Archaeology Report 2008. Science Report, compiled by Dr. James D. Lazell of the Conservation Agency. 2008

Rimbu, N., et al. Arctic/North Atlantic Oscillation signature in Holocene sea surface temperature trends as obtained from alkenone data. Geophysics Research Letters, Vol. 30, No. 6, 1280.

Rogoziński, J. A Brief History of the Caribbean: From the Arawak and Carib to the Present. Facts on File, Inc. New York, New York. 1999.

Saunders, N. The peoples of the Caribbean. ABC-CLIO. 2005

Shamberger, E. and Foos, A. 2004. Depositional history of a coastal saline Salt Pond, San Salvador, Bahamas. Lewis, R.D. and Panuska, B.C. eds. Proceedings of the Eleventh Symposium on the Geology of the Bahamas and other Carbonate Regions: San Salvador, Bahamas, Gerace Research Center, p. 179-186.

Song, Y., Müller, G. 1993. Freshwater Sediments: Sinks and Sources of Bromine. Naturwissenschaften 80, p. 558-560.

Stuiver, M., and Reimer, P.J. 1993. Radiocarbon Calibration Program. Radiocarbon 35, p. 215-230.

Tedesco, K., and Thunell, R. 2003. High resolution tropical climate record for the last 6,000 years. Geophysical Research Letters, Vol. 30, No. 17, 1891, p. 2-1 – 2-4.

Thompson, L., Mosley-Thompson, E., Davis, M., Henderson, K., Brecher, H., Zagorodnov, V., Mashiotta, T., Lin, P., Mikhalenko, V., Hardy, D., Beer, J. 2002. Kilimanjaro Ice Core Records: Evidence of Holocene Climate Change in Tropical Africa. Science, Vol. 298, Issue 5593, p. 589-593.

United States National Park Service. Prehistory of the Caribbean Culture Area. https://www.nps.gov/history/seac/research/fp/fp00012/caribpre.htm. Last accessed 1-3-17.

Whitaker, F.F. and Smart, P.L. 2007. Geochemistry of meteoric diagenesis in carbonate islands of the northern Bahamas: 1. Evidence from field studies. Hydrological Processes, Vol. 21, p. 949-966.

Wooller, M., Behling, H., Guerrero, J., Jantz, N., Zweigert, M. 2009. Late Holocene hydrologic and vegetation changes at Turneffe atoll, Belize, compared with records from mainland Central America and Mexico. Palaios, Vol. 24, p. 650-656.

World Register of Marine Species. http://www.marinespecies.org/aphia.php?p=taxdetails&id=533366; http://www.marinespecies.org/aphia.php?p=taxdetails&id=758590; http://www.marinespecies.org/aphia.php?p=taxdetails&id=127986; http://www.marinespecies.org/aphia.php?p=taxdetails&id=419610. Last accessed 1-3-17.

VITA

Theresa Lynne Goyette was born in Glendale, California on July 7, 1989. She grew up in a suburb of Los Angeles and greatly enjoyed watching meteor showers and learning all she could about earthquakes and the San Andreas Fault. After moving to Lee's Summit, Missouri in 2005, she attended and graduated from Lee's Summit North High School in 2007.

Miss Goyette enrolled at the University of Missouri – Kansas City in 2007 and majored in Political Science, planning on attending law school after graduation. Two years into a Political Science program, and after working at a law firm for multiple years, she determined that she no longer wanted to be a lawyer. In 2009 she added a degree in Geology, and graduated with a B.S. in Geology and a B.A. in Political Science in December 2011. She began pursuing her M.S. in Environmental and Urban Geosciences, with an emphasis in Environmental Geology at the University of Missouri – Kansas City in 2012.